THERMOELECTRIC POWER OF DILUTE ALLOYS OF TRANSITION METAL ATOMS IN NOBLE METALS AND THE EFFECTS ON THEM OF MAGNETIC FIELDS

by

Charles William Eden Walker

B.A., Cambridge University, 1937

M.A , Cambridge University, 1941

A DISSERTATION SUBMITTED IN PARTIAL FULFILMENT

OF THE REQUIREMENTS FOR THE DEGREE OF

DOCTOR OF PHILOSOPHY

in the Department

of

Physics

SIMON FRASER UNIVERSITY

April 1971

APPROVAL

Name: Charles William Eden Walker

Degree: Doctor of Philosophy

Title of Thesis: Thermoelectric Power of Dilute Alloys of Transition Metal Atoms in Noble Metals and the Effects on Them of Magnetic Fields

Examining Committee:

Chairman: K.E. Rieckhoff

D.J. Huntley
Senior Supervisor

J.F. Cochran

K.S. Viswanathan

S. Gygax

A.V Gold
External Examiner
Professor
University of British Columbia, Canada

Date Approved: April 26, 1971

ABSTRACT

Thermoelectric power measurements have been made over the temperature range 1.2K to 7K in applied magnetic fields up to 50 KOe on dilute alloys of Fe in Au, Cu and Rh and of Ce in Au. Alloy concentrations were in the range .06 to 250 p.p.m. atomic.

It has been shown that the observed results on alloys of Fe in Au can be explained qualitatively as arising from Fe-Fe interactions, and the internal fields predicted by a simple pair interaction are seen to be of the same order of magnitude as found from Mössbauer experiments. The magnetothermopower results show that the interactions extend to tens of lattice spacings.

A theoretical model for the distribution function describing the internal fields proposed by Klein, based on a Ruderman-Kittel-Yosida interaction, is shown not to fit the Mössbauer results of Window, nor explain the observed magnetothermopower results in Au Fe.

It is shown that at extreme dilution of less than 1 p.p.m. and in high fields, the Au Fe alloy results agree with predictions of theory proposed by Weiner and Béal-Monod.

A correlation is noted between the existence of strong internal fields as reported by Window and T/T_K; this is further illustrated by the magnetothermopower results in Au Fe and Cu Fe alloys which show the existence of Fe-Fe interactions in Au, but not in Cu. Since the long-range interaction exists via the intermediary action of the conduction electrons it is easily broken up by lattice vibrations above temperatures of the order of 10 to 30K; it is also progressively screened out as the temperature is lowered below the Kondo temperature T_K by formation of the Nagaoka bound state between the conduction electrons and the d electrons of the localised moments. In Au Fe alloys with $T_K \approx 1K$, this leaves a temperature range from about 30K to below 1K for strong interaction to exist, but for Cu Fe alloys with $T_K \approx 18K$, the interaction begins to be screened out as the temperature is lowered, before the decrease in lattice vibrations has allowed it to form.

A method for producing very high purity Au containing less than 0.1 p.p.m. atomic Fe was developed as a means for producing the dilute alloys required for this investigation.

Anomalies in the Au Fe and Cu Fe alloy data have been interpreted as due to superconducting transitions occurring in Pb impurities present to the extent of only a few parts per million and believed to be separated in submicroscopic occlusions throughout the alloy.

The measurements made on Rh Fe and Au Ce alloys are reported without comment because they appear to represent quite different systems from Au Fe and Cu Fe, thus requiring quite different theoretical interpretation, and because the work done here has shown the need for extensive further work on alloy preparation in order to produce meaningful results.

ACKNOWLEDGEMENTS

I should like to express my thanks to:

Dr. R. Haering, for extending to me the facilities of the Physics Department at Simon Fraser University.

Dr. D.J. Huntley, my tutor, for accepting me, albeit "with trepidation", and for bearing with me with much patience. His guidance was a great help and comfort.

Dr. D.S. Russell and Dr. T. Tymchuk of the National Research Council in Ottawa, who performed analyses of the Au wire specimen, and the staff of the Mineral Sciences Division, Department of Energy, Mines and Resources in Ottawa who analyzed the Rh wire specimens.

Dr. J. Kopp, for performing the resistivity measurements vs. temperature on the Rh wire specimens to determine their Fe concentrations, and for stimulating and helpful discussions.

Mr. J. Mercier, who performed the electron beam vacuum evaporations for me, and all the members of the Physics Department staff, who assisted me in so many ways.

The research was largely supported by grants from the National Research Council, Ottawa.

CONTENTS

CONTENTS (cont'd)

CONTENTS (cont'd)

LIST OF TABLES

LIST OF FIGURES

THERMOELECTRIC POWER OF DILUTE ALLOYS OF TRANSITION METAL ATOMS IN NOBLE METALS AND THE EFFECTS ON THEM OF MAGNETIC FIELDS

CHAPTER 1

INTRODUCTION

Alloys consisting of very small amounts of transition elements as impurities in noble metals have shown anomalous behaviour at low temperatures, all the electronic properties of the metals being strongly affected. The experimental and theoretical evidence has pointed to these effects having a magnetic origin and being concerned with the scattering of the conduction electrons in the metal at isolated magnetic impurity sites. It therefore appeared that useful information could be obtained about these scattering centers by studying the effect of strong external magnetic fields, particularly on the anomalous thermoelectric powers which theory indicates are proportional not to the scattering cross sections but to the rate of change of the scattering cross sections with electron energy in the neighbourhood of the Fermi surface. Thus the information so obtained should be significantly different from that obtained from resistivity or specific heat measurements, and could be expected to throw new light on the subject.

Previous measurements on gold-iron alloys had shown marked field dependence with the thermoelectric power increasing when an external field was applied. It was accordingly decided to study this Au-Fe system further, both by applying larger external fields and by preparing more dilute alloys, for reasons which are discussed in more detail below. Several other alloys were studied by the same techniques, chosen in each case because they had already been shown to exhibit giant thermoelectric power in the liquid helium temperature range. In addition, something was either known already about the field dependence as in the cases of Au-Fe and Cu-Fe, or they represented a significantly different system as in the case of Rh-Fe, in which the Rh as well as the Fe has an unfilled d electron shell and as in the case of Au-Ce, in which Ce is a rare earth with unfilled f electron shell.

Localised Moments

The problem of localised moments is well documented in the literature with a recent review article by Daybell and Steyert (1968) covering most of the recent experimental work done up to that time and including the theoretical work done on the subject. In brief outline the experimental work had shown departures from a Curie law for the susceptibility

below some critical temperature, a minimum in the electrical resistivity, a maximum in the specific heat and a giant negative thermoelectric power with a maximum at some critical temperature T_c. The first major theoretical success was achieved by Kondo (1964) in explaining the resistance minimum. A critical Kondo temperature T_k was defined in relation to the resistivity phenomenon as a parameter of each noble metal and it appears on both theoretical and experimental grounds that the maximum of the characteristic thermoelectric power occurs at $T \simeq 4\ T_k$. Subsequent theoretical work, however, has produced divers definitions of T_k and the matter is therefore somewhat imprecise.

Subsequent to Kondo's initial work, a number of workers (Nagaoka 1965, Suhl 1965, Abrikosov 1965) pointed out that his perturbation treatment breaks down below T_k due to the formation of what has been termed a quasi-bound state in which the transition metal spins are compensated or screened out by a cloud of conduction electrons. This produces departures from a Curie law in the magnetic susceptibility and this in turn should be reflected in the effect of external magnetic fields on the thermopower. More will be said on this below in connection with the interpretation of our experimental results.

Several attempts have been made to provide a theory covering the whole range above and below T_k and more recently this has been achieved by Rivier and Zuckermann (1968) in terms of localised spin fluctuations which involve a continuous formation and breakdown of the quasi-bound state following a more or less random pattern with a resulting statistically probable life time for the bound state.

Specific attempts to deal theoretically with the giant thermoelectric powers have been made by Kondo (1965), by Suhl and Wong (1967), by Fischer (1968) and by Maki (1969); these will be discussed further below.

A useful review of the whole field with emphasis on the effects of magnetic fields and on thermoelectric power data is given by Kopp (1969).

Thermoelectric Powers

The thermoelectric power S of a material is defined as the voltage gradient produced in the material by a temperature gradient under conditions of zero current flow

$$S = \frac{\partial V / \partial x}{\partial T / \partial x} \qquad (1.1)$$

Calculation of the transport properties for the electrons in a metal leads to an expression (Ziman, 1964, chapter 7)

$$S = \frac{\pi^2 k^2 T}{3e} \left\{ \frac{d \ \ln \sigma(E)}{dE} \right\}_{E=E_F} \qquad (1.2)$$

where $\sigma(E)$ is the electrical conductivity due to electrons of energy E which is proportional to their mean scattering life time. Since the derivative is evaluated at the Fermi energy E_F, this expression shows that the thermoelectric power is a function of the energy dependence of the electron scattering in the neighbourhood of the Fermi surface.

It often happens that more than one scattering process is involved, affecting the conductivity σ, but in general each process will have a different energy dependence at the Fermi surface and so their contributions to the total thermoelectric power will be very different and may even be of opposite sign. If S_i is the thermoelectric power which scattering process i would produce if it acted alone or was strong enough to completely dominate the electron scattering, and if ρ_i is the contribution that this scattering process makes to the electrical resistivity of the metal, then the Nordheim-Gorter rule, which can be derived from (1.2), shows

that for n different scattering processes

$$S = \sum_{i=1}^{n} S_i \rho_i \; / \; \sum_{i=1}^{n} \rho_i \qquad (1.3)$$

This relation is important when we wish to analyse the thermoelectric power due to one particular scattering process. In our case it can be greatly simplified, because the magnitude of the thermopower produced by the localised moments is so large that all the other S_i can be neglected, in comparison.

Kondo (1965), using a perturbation calculation, following essentially the same principles which he had used successfully to calculate the resistivity anomaly, derived a formula for the thermoelectric power of the localised magnetic moments,

$$S = A \frac{k}{e} \int_0^{\infty} p(2\mu_B H) \quad Q_s\left(\frac{2\mu_B H}{kT}\right) d(2\mu_B H) \qquad (1.4)$$

in which H is the resultant magnetic field at the site of a transition impurity atom and $p(2\mu_B H)$ is its distribution function for which a form must be found or assumed. $Q_s\ (2\mu_B H/KT)$ is a function of the impurity spin as well as H and has an explicit form given by Kondo. This equation is discussed in a published paper by Huntley and Walker (1969) where it is shown to provide a reasonable explanation of at

least some of the results which we have obtained.

Since Kondo's perturbation treatment is thought to break down below the Kondo temperature T_K, other theoretical attempts have been made to avoid this. Suhl and Wong (1966) produce curves which are smooth through T_K but their results are not given in analytic form and they do not include the field H. Fischer (1968) and Maki (1969) obtain analytical expressions for the thermopower but again they contain no field dependence.

The first discovery of the "giant" thermoelectric power of dilute alloys at low temperatures were made by Borelius et al. (1930, 1932). They studied dilute alloys of iron in Au and Cu and found large negative thermopowers of the order of -10 μV/K. Since then, similar "giant" thermopowers have been observed in a number of other dilute alloys of transition elements in noble metals (as given in review articles by van den Berg (1964) and by Daybell and Steyert (1968). In addition, Coles (1964) has reported a large thermopower for a dilute alloy of Fe in Rh and Gainon et al. (1966), who studied all the rare earths except Pm, report "giant" values for dilute alloys of Ce and Eu in both Au and Ag.

Review of Field Effects

The first observation of the effects of an externally applied magnetic field on one of the "giant" thermoelectric powers was made by MacDonald and Pearson (1957), who found that for alloys of Fe in Cu ranging from 23 to 600 p.p.m. atomic, there was a reduction in the thermoelectric power when a field of up to 11.8 KOe was applied. They showed, however, that this reduction could be wholly accounted for by the effect of magnetoresistance of the alloy so that, at least up to 11.8 KOe, the field appeared to have no effect on the characteristic thermopower of Fe in Cu.

Templeton and MacDonald (1961) who studied the effect of a magnetic field on an alloy consisting of 0.2 at. % Mn in Au found a substantial increase in thermoelectric power with fields of 2.4, 5 and 8 KOe which could not be ascribed to magnetoresistance. On the other hand, Foiles (1968) found no effect due to a magnetic field of up to 11 KOe on Cu-Ni and Cu-Co alloys over the temperature range 4.2 to 20 K.

Berman and Huntley (1963) and Berman, Brock and Huntley (1964) studied alloys of Fe in Au, principally between 200 and 300 p.p.m. atomic Fe, with fields up to 15 KOe and over the temperature range 1.3 to 15 K. They observed an increase in the magnitude of the thermoelectric power with

applied field at all temperatures below about 10K and amounting to as much as 20%. This could not be accounted for by magnetoresistance. They also measured specimens of supposedly pure fine grain gold (99.97% purity) which Huntley (1963) has estimated, from measurements of residual resistance ratio, contained about 50 p.p.m. atomic Fe. This showed about a 10% decrease in the magnitude of the thermoelectric power in a field of 15 KOe and so indicated a strong concentration dependence.

The only theoretical treatment advanced to account for the "giant" thermoelectric power which contained any definite field dependence was that proposed by Kondo (1965) but his formula contained no specific concentration dependence and the very existence of an increase in the magnitude of the thermoelectric power with applied magnetic field in alloys as dilute as 200 p.p.m. atomic seemed to be at variance with his theory because the basic field dependence appeared in the function Q_s $(2\mu_B H/KT)$ which decreases with increasing H.

The Present Experiments

It was thought that the increase in the magnitude of the thermoelectric power found in Au-Fe alloys must in some way arise from an interaction between Fe atoms and so indicate that, at 200 p.p.m. atomic, the alloy was not in the dilution limit for which Kondo's theory had been developed. It accordingly seemed desirable to make field measurements at lower concentrations. We have therefore prepared and studied a range of alloys whose concentrations have been determined and which are significantly more dilute than have previously been available. It also seemed desirable to cover a wider range of applied fields because it was expected that all alloys must ultimately show a decrease in $|S|$ at sufficiently high fields. The apparatus has therefore been designed around a 50 K Gauss superconducting magnet. Finally, it would be of interest to extend the measurements to temperatures well below T_K to see what changes, if any, result from the supposed formation of a bound state. For Au alloys, T_K is believed to be about 1K which is about at the lower limit of temperature attainable by pumping on normal He, so that to reach an appreciably lower temperature would require a further cooling system.

It was decided instead to cover this aspect by including measurements on Cu-Fe alloys, since the Kondo temperature T_K for Cu is above 4K.

CHAPTER 2

APPARATUS AND EXPERIMENTAL METHODS

The apparatus was constructed in the first place with the intention of studying the effects of strong magnetic fields on the thermal conductivities of certain paramagnetic salts in the liquid helium temperature range. This work was intended to follow, and further develop work reported by Berman et al. (1963) and by Brock and Huntley (1968) and both the cryostat and associated apparatus were accordingly constructed along similar lines to those described by Berman and Huntley (1963), by Huntley (1963) and by Brock (1965). Apparatus designed for such measurements is well suited to the study of thermoelectric effects in a magnetic field because the heat flow along the crystal produces a convenient temperature difference in a small space: the whole electrical conductor which is being studied and in which the thermoelectric voltage is produced, can thus be located within a small volume over which a reasonably uniform magnetic field can be maintained.

To adapt the apparatus for work on thermoelectric powers it was necessary only to replace the paramagnetic salt crystal with a rod of high purity quartz ("spectrosil" made by Thermal Syndicate, Northumberland). Berman et al. (1964) have shown

that the thermal conductivity of this material is unaffected by a magnetic field, at least up to 20.6 KOe and over the temperature range 1.2 to 4.3 K. They compared the change in the thermoelectric voltage due to the field for a particular Au Fe specimen mounted first on a "spectrosil" rod and then on a "Teflon" rod. Theoretically, neither rod should show any field effect. The precision of their experiments was such that a difference as small as 0.5% would have been clearly shown. We have extended the range of field strength to 48.1 KOe, using the same technique,with a Rh-Fe specimen and found a small difference, amounting to 2% at 4.6K falling to 1% at 2K, with the temperature difference over the "Teflon" apparently increased relative to that over the "Spectrosil". Our experiment showed a difference of approximately 0.3% at 24.0 KOe.

The design of the equipment, whether for thermal conductivity or for thermoelectric power measurements, includes three main parts:

1) a cryostat, operating between 1 and 5K with associated vacuum pumps and piping;
2) a superconducting magnet;
3) a d.c. voltage measuring system, with 1 nV resolution.

The plan of this chapter is first to describe these parts under equivalent section headings, with a separate section on thermometry, and then to bring the whole together in a final section detailing the measurement procedure. There is no separate section devoted to errors, as the various sources of error are discussed in their appropriate sections. Details of some pieces of the equipment and one ancillary piece are described in appendices A1 to A6.

The Cryostat

The cryostat is shown in fig.2.1 and consisted of a brass vacuum can C within which the whole of the measuring apparatus was suspended by three stainless steel tubes. One of these was .050 inch diameter and connected to a copper gas thermometer bulb G. A second was 1/8 inch diameter and connected to the copper bulb VPb of a vapour pressure thermometer. The third tube, which provided the main support, was 3/8 inch diameter, located centrally and was connected to a copper pot P into which helium could be condensed. This pot could be pumped through the 3/8 inch tube to control the temperature of the whole measuring apparatus at any desired temperature T_o within the range 1.2 to 4.2 K. This pumping tube had a constriction, consisting of a

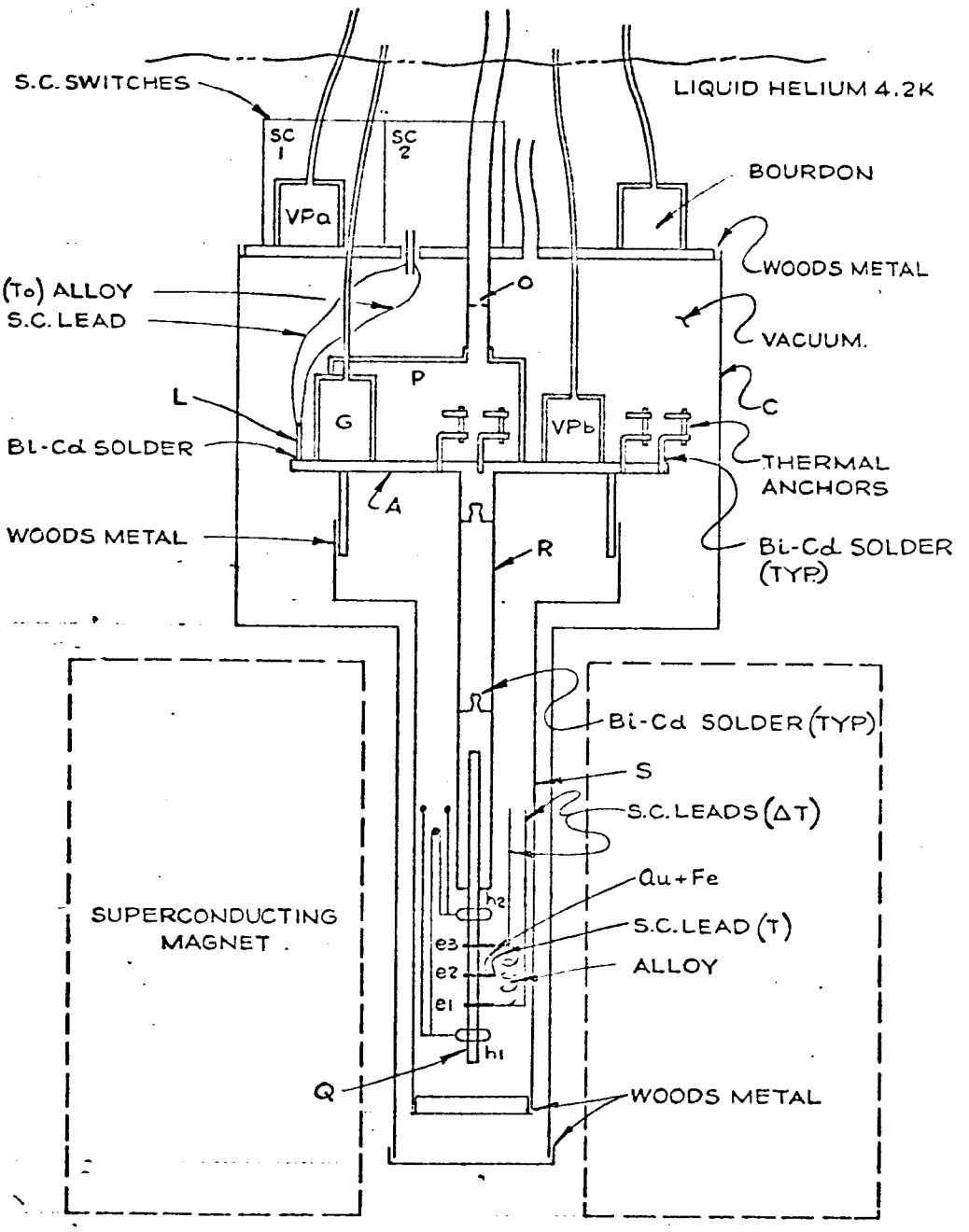

THE CRYOSTAT

FIGURE 2-1

diaphragm with a small hole at 0 to limit flow up the tube of superfluid helium when the temperature was below the λ point.

The three copper pots were mounted on a 1/8 inch thick copper platform A beneath which a 1/2 inch diameter copper rod R extended downwards about 6 inches to support the quartz rod Q at the centre of the superconducting magnet. A copper radiation shield S was also suspended below the platform so that the rod Q and its thermocouple contacts were supported from, and enclosed within copper, all at temperature T_o.

Two heating coils h_1 and h_2 and three thermocouple contacts e_1, e_2, e_3 were mounted on the quartz rod Q in the positions shown in fig.2.1. These are described in detail in Appendices A1 and A2. Current supplied to the lower coil h_1 produced a heat flow along the quartz rod, producing in turn a temperature difference ΔT between contacts e_1 and e_3. The alloy specimen being studied was connected between these contacts. Other connections were also made to these contacts so that the specimen was one arm of a thermocouple sensing the temperature difference Δ T. Since the thermal resistance of this alloy specimen might change in the presence of a magnetic field, it was

desirable that its thermal resistance be large compared to that of the quartz rod between contacts e_1 and e_3 so that any changes due to the field would not significantly affect ΔT. In attempting to achieve this, most of the specimens were in the form of fine diameter wire ($\lesssim$ 0.1 mm. diameter) and were made 50 cm. long. (See Appendix A3 for estimates of the thermal resistances of the Au-Fe specimens compared to that of the quartz rod. The resistances of the Cu, Rh and Au-Ce specimens are considered in the later chapters dealing with these alloys. Calculation of the thermal diffusion times is also included in this Appendix A.3. With such long samples it could be a significant factor in determining the time required for equilibrium to be established. It is shown not to be excessive in the samples studied. Each specimen was enclosed in small diameter Teflon tubing and folded into a compact bundle about 1.1/4 inch long. This was tied to the quartz rod so that most of the specimen was parallel to the rod and in a longitudinal magnetic field which was constant over the specimen, within a few %. The Cu specimens were somewhat different, as described in Chapter 6, but were similarly compact and most of their length was likewise parallel to the field. The third contact, e_2, which was located mid-way between the other two

was used for measuring the mean temperature T with a calibrated thermocouple connected between it and the helium bath.

A further thermocouple contact point was provided on a copper post L attached to the platform A and a second specimen of the alloy being studied was mounted between this and the helium bath for direct measurement of its thermopower over the available temperature range. This could be extended above 4.2K by supplying heat to one of the heater coils h_1 or h_2 with the pot P evacuated.

In all cases the second conductors of the thermocouple were made of superconducting material which cannot produce a thermoelectric voltage so long as it remains superconducting. "Supercon" wire type A25 (Norton International Inc., Natick, Mass.) was used which, according to its specifications, would remain superconducting in the highest fields used in the experiments. In practice no discrepancies or jump discontinuities such as could be attributable to a superconducting transition in these wires were observed in the readings. This wire also had the useful feature that it had a 0.001 inch copper outer layer enabling it to be soldered, but this copper layer also caused excessive heat leaks along the wires. These leaks were shown to exist in a "dry run"

experiment made to test the whole apparatus after it was constructed, in which the thermal conductivity of the quartz rod (Spectrosil) was measured and compared with results given by Brock (1965). The values obtained were about two times too high. The copper cladding was then removed from about 1.5 cm. of each of the three "supercon" wires connected between contacts e_1 and the thermal anchors, after which a repeat measurement of the thermal conductivity of the "Spectrosil" gave results within $\pm$2% of those given by Brock.

The associated vacuum pumps and piping consisted of a more or less standard arrangement with an oil diffusion pump and liquid N_2 trap to provide good vacuum in the cryostat can.

Superconducting Magnet and Magnet Power Supply

Two different superconducting magnets were used in the experiments, the early work being done with one made by Magnion Corporation, which was intended to give 57.2 KOe with a current of 21.4 amps. A power supply was designed for this magnet to work from a 2 volt battery source and using 12 switched resistors with 4 adjustable rheostats for fine control. The circuit is shown in fig.2.2 and included an ammeter with 7 inch mirror scale and 1% accuracy, and a reversible voltmeter to monitor the back e.m.f. from the

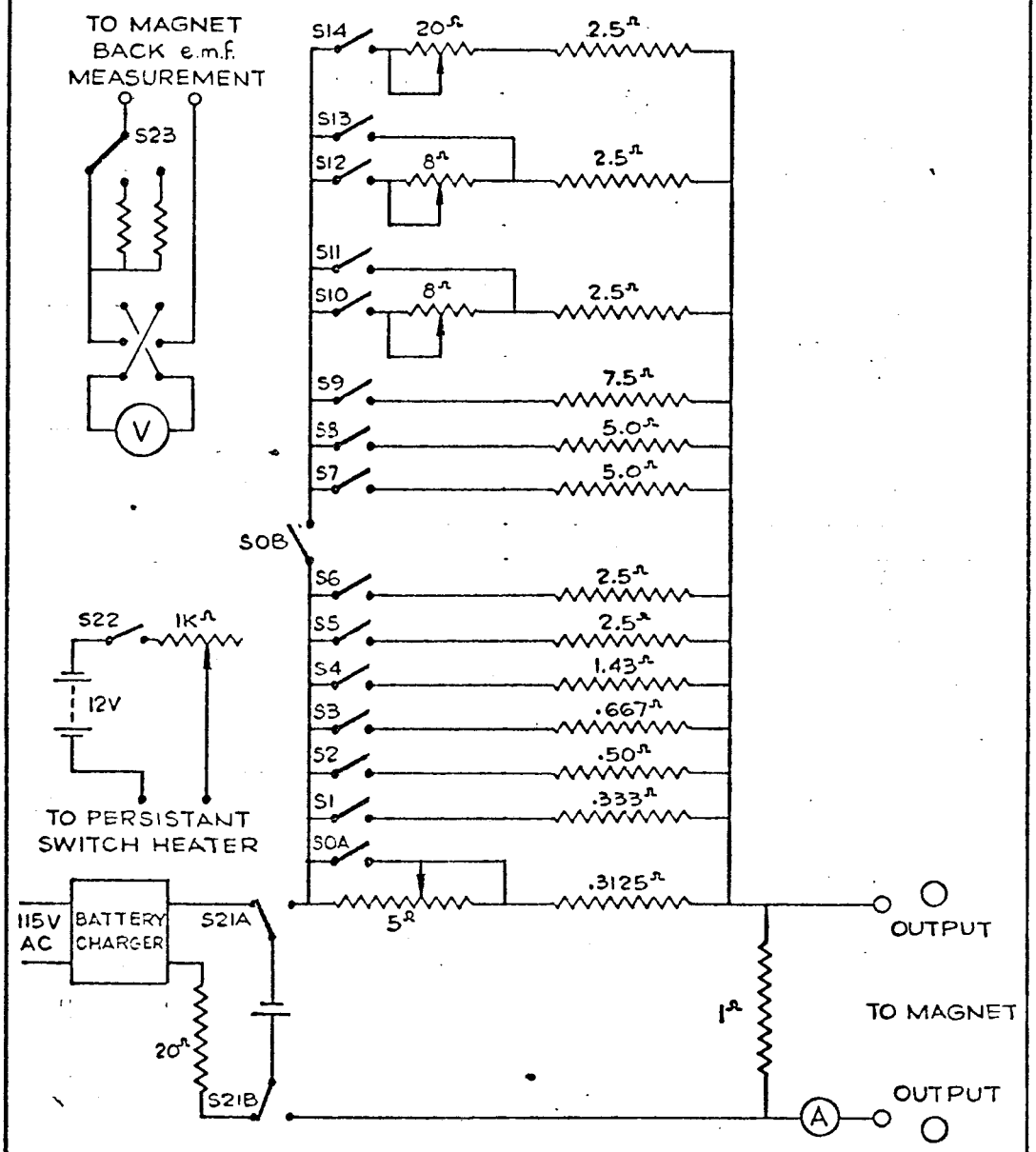

POWER SUPPLY FOR MAGNION
SUPERCONDUCTING MAGNET
FIGURE 2 - 2

magnet with three ranges, 50 mV, 0.5 volt and 5.0 volt. The supply also contained a current source for the persistent switch heater which controlled the magnet shorting switch. A one ohm resistor was connected across the magnet winding as shown, to provide a load into which about half the magnet power would be dumped in the event of it going normal.

Calculation of the magnet coil inductance L, using formulae given by Montgomery (1963) gave L = 19.6 Henry which at 21.4 amps gives a field energy $1/2\ LI^2 = 4500$ joules. Assuming that about half of this is dissipated in the one ohm shorting resistor when the magnet goes normal, the remainder will be dissipated by evaporating about 2.25 litres of liquid helium. To allow for the possibility of this boil-off being rapid, four safety ports were provided at the top of the helium dewar: their design is shown in fig.2.3 and they consisted of a brass disc held in place against a neoprene O-ring by a spring spider. This spider was cut from 10 thou. thick phosphor bronze and the width of the 6 splines was calculated so that the ports would blow if the excess gas pressure inside the dewar exceeded about half an atmosphere, leaving about 20 cm^2 open for helium gas escape. In practice these ports

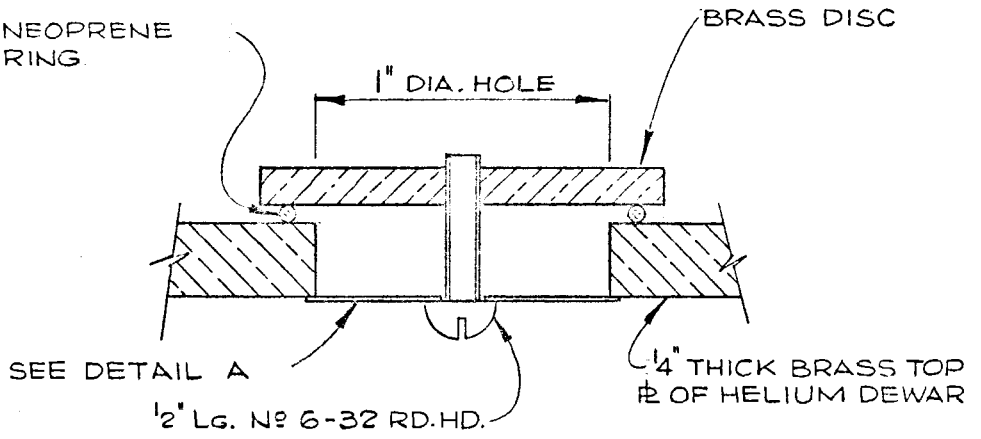

SECTION THROUGH
SAFETY PORT

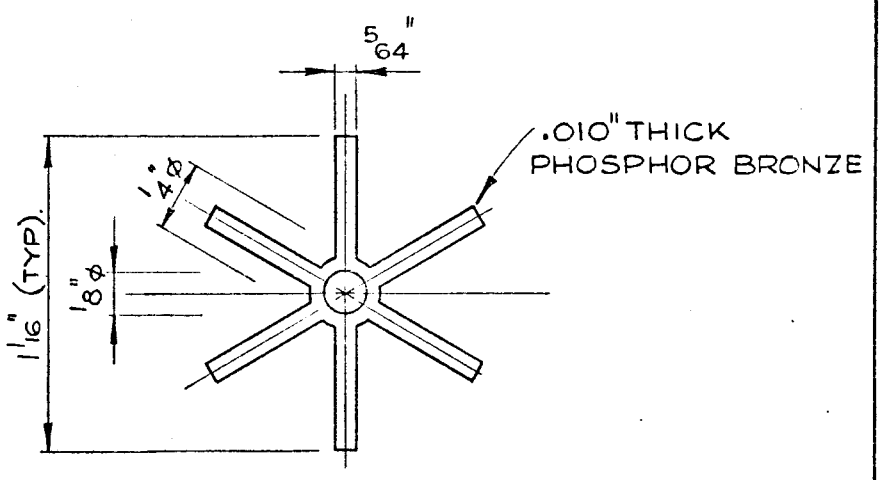

DETAIL A
PRESSURE RELIEF SPIDER

HELIUM BLOW - OFF
SAFETY PORTS
FIGURE 2 - 3

have never blown when the magnet has gone normal and it appears that most of the field energy which is not dumped in the one ohm shorting resistor is dissipated through eddy current heating of the copper in the magnet and in the cryostat and this heat is then passed on comparatively slowly to the liquid helium.

We were never able in practice to operate the Magnion magnet above 38.5 KOe. It went normal just below this point on the first occasion that it was used and in succeeding runs this limiting field became progressively less, eventually reaching 32 KOe. A change was then made to a second magnet which was made by Oxford Instrument Co. and gave a field of 55 KOe with a current of 45.45 amps. Both magnets were calibrated in a separate EPR apparatus using DPPH, with the following result:

Magnion magnet	2.572 KOe/Amp.
Oxford magnet	1.211 KOe/Amp.

Calculation of the inductance of the Oxford magnet using Montgomery's formula gave L = 2.6 Henry and a maximum field energy at 55 KOe of 2690 joules.

The Oxford magnet could not be operated from the supply shown in fig.2.2 which was not capable of delivering 45 amps. A Hewlett-Packard model Harrison 6387A was therefore connected

to the output terminals 0-0 to supply the magnet current. The field was determined from the current readings given by the ammeter in the Hewlett-Packard supply which was the meter used in the calibration. It is therefore the comparative accuracy of this meter rather than its absolute accuracy which is pertinent and the field values are therefore estimated to be correct to $\pm$1% $\pm$100 Gauss or better.

The one ohm shunt resistor remained in circuit during the experiments but not in the calibration. During the experiments, therefore, the current read by the Hewlett-Packard meter included any current passed by this resistor. The resistance of the leads between the terminals 0-0 and the magnet was estimated to be 0.0067 ohm and the current meter readings were therefore reduced by 0.67% when computing the magnet field.

Thermometry

The basic or primary reference thermometers used in the experiments were a helium vapour pressure thermometer VPb, covering the range

$$1.2K \leqslant T \leqslant 4.2K$$

a helium gas thermometer for

$$T \geqslant 4.2K$$

and a second helium vapour pressure thermometer bulb VPa, mounted outside the vacuum can C to read the temperature of the helium bath.

The vapour pressure thermometer bulb VPb which was mounted on the platform A as shown in fig.2.1 was of conventional design with a volume of 5 c.c. Throughout its range of use, this bulb was at a lower temperature than that of the helium bath and the 1/8 inch tube connecting it to its mercury manometer therefore passed up through the helium bath without a surrounding vacuum jacket. The other vapour pressure bulb VPa, however, was provided with a vacuum jacket around its connecting tube, up to the top of the helium dewar, to ensure that the temperature which it read was that of the bulb which was located on the outside of the brass can C, close to the point where the copper wires connected to the Au-Fe reference thermo junctions emerged into,

and made thermal contact with the helium bath. The helium gas thermometer was of the type described by Huntley (1963) and had a 25 c.c. bulb G mounted on platform A as shown in fig.2.1. The dead volume correction was obtained from readings taken at room temperature and with the cryostat immersed in liquid nitrogen. Because of uncertainty as to the exact temperature of the liquid nitrogen (due to the possibility of dissolved oxygen), its temperature was measured by condensing pure oxygen into the vapour pressure thermometer bulb VPb to act as an oxygen vapour pressure thermometer.

The vapour pressure and gas thermometers were used only to calibrate the thermovoltage from a Au-Fe alloy wire which then became a secondary reference. This was used in all later experiments because it was much more convenient to use than the vapour pressure and gas thermometers. Because of the universal use of superconductors for the second elements of all the thermocouples used in these experiments, the thermovoltage developed in a single piece of wire was a practical measureable reality as well as being a valid physical concept and could be directly related to the temperature difference between the ends of the wire. The piece of Au + 230 p.p.m. atomic Fe wire used as the secondary reference was connected

between the central contact e_2 on the quartz rod and the helium bath,and so was also used to measure the temperature at the center of the quartz rod. Its calibration curve is shown in fig.2.4.

At first sight it might be thought that a significant temperature difference could exist during calibration between this thermojunction on e_2 and the platform A on which the vapour pressure and gas thermometers were mounted, due to the quite high thermal resistance of the quartz rod and perhaps also the contact resistances between e_2 and the rod and between the quartz rod Q and the copper rod R. The calibration, however, and all the subsequent measurements of the thermopowers of the other alloys were carried out under equilibrium conditions and a temperature difference could therefore only exist between the thermojunction at e_2 and platform A if there was a heat source or sink at e_2 or on the quartz rod due to heat leaks. Such heat leaks were minimized by

(a) maintaining a good vacuum, $< 10^{-5}$ torr, inside the can C,

(b) surrounding the quartz rod with a copper radiation shield, effectively at the reference temperature T_o, and

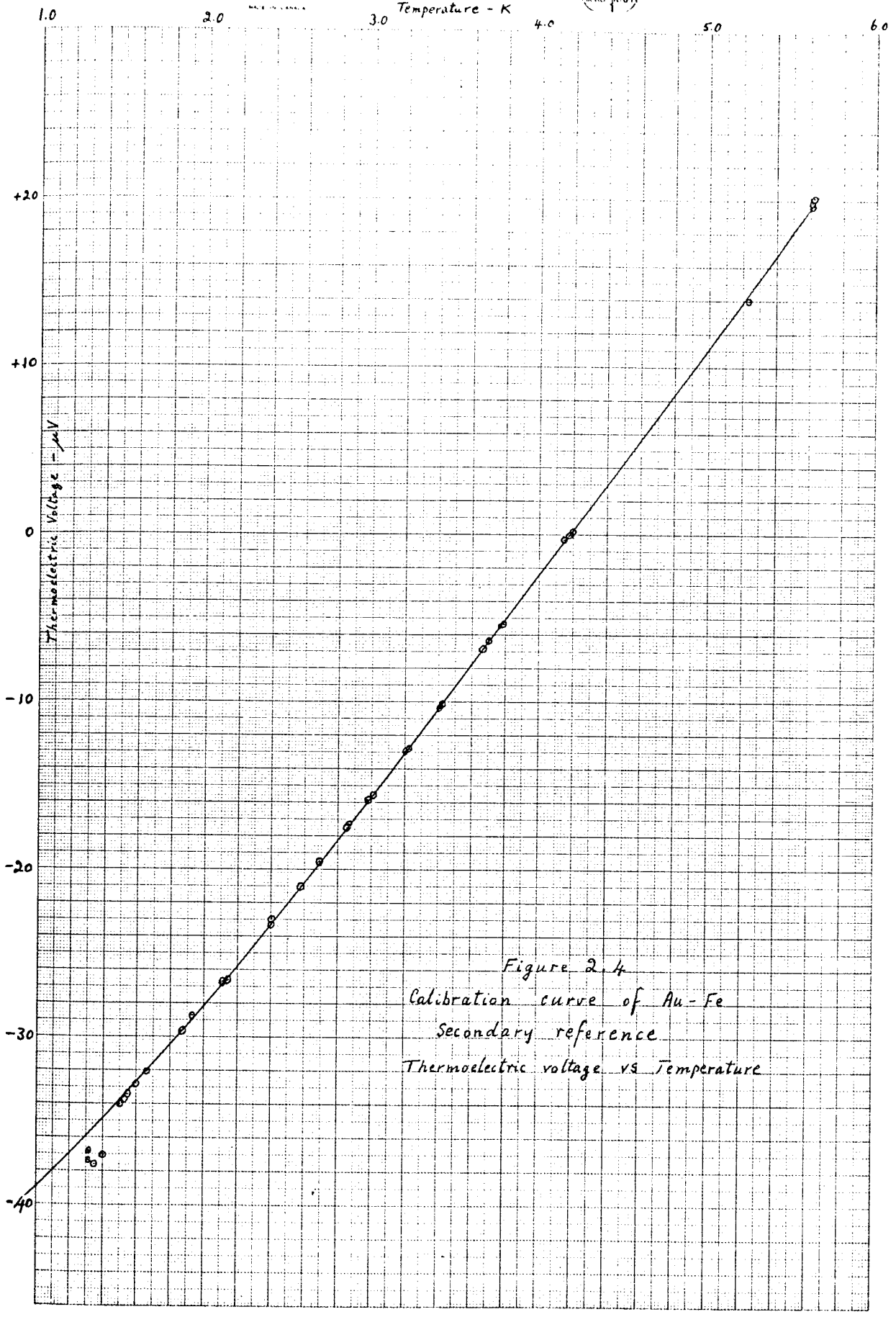

Figure 2.4
Calibration curve of Au-Fe
Secondary reference
Thermoelectric voltage vs Temperature

(c) thermally anchoring all thermocouples and heater wires to the platform A or the gas thermometer bulb G.

The residual heat leaks and resulting temperature difference between e_2 and the platform A are analyzed in Appendix A2, where it is shown that the temperature difference should not exceed 2 mK under the worst conditions with the 0.2 cm. diameter quartz rod and 0.3 mK with the 0.5 cm. diameter rod. This was confirmed experimentally by a repeat calibration in which the reference Au-Fe/superconductor thermojunction was removed from contact e_2 and mounted on the copper post L on platform A. No error due to heat leaks could be detected.

The height of the mercury columns of the vapour pressure and gas thermometers could be read, using a Cathetometer, to 0.05 mm. corresponding to:

above 4.2K	25 mK by gas thermometer
at 4.2K	0.1 mK by vapour pressure thermometer
at 1.6K	2 mK by vapour pressure thermometer

Below 1.6K the vapour pressure thermometer readings became increasingly suspect as the temperature was lowered, as they were incompatible with the thermocouple readings

which previous work with the same Au-Fe alloy, containing between 200 and 300 p.p.m. atomic Fe (Huntley 1963, MacDonald et al, 1962) had shown to be quite regular through this temperature range. The vapour pressure thermometer readings below 1.6K were therefore discarded and a reasonable extrapolation, compatible with earlier work, was used as the calibration graph from 1.6K to 1.2K. In such a relatively short extrapolation and with the reasonable assumption that S goes to zero at 0 K, there is little room for major error to develop, and it is estimated that the error from this cause is less than 10 mK.

The largest source of error over much of the temperature range came from variation in the helium gas pressure over the main helium bath. This was connected to a helium recovery system and the pressure varied in an uncontrolled manner over a range of 0.4 cm Hg. A vapour pressure thermometer was available to read the helium bath temperature but because the change in this temperature occurred in a random and unpredictable manner, and because it was physically impossible for one man to read simultaneously two Hg columns of two vapour pressure thermometers and balance and read a microvolt potentiometer, there was a resultant uncertainty in the helium bath temperature of 6 mK and a corresponding

uncertainty in the calibration due to this cause.

Voltage Measuring Circuit

The circuit for measuring the thermoelectric voltage is shown in fig.2.5 and closely follows that described by Huntley (1963) but with the principal difference that a Keithley nanovoltmeter model No.148 was used in place of a galvanometer, galvanometer amplifier and thermal compensator. Essentially, the Tinsley potentiometer model 5590B, together with a 2 volt battery was used as a d.c. voltage source with 1 μV resolution. The output from this,which could be read from the potentiometer dial settings, was then divided by 1000 by a resistor network consisting of precision resistors R_1 to R_4 to give an output voltage with 1 nV resolution. This voltage was then used to counterbalance the thermoelectric voltage fed through switches S_1 and S_2 and one of the superconducting switches Sc1, Sc2 or Sc3. The Keithley nanovoltmeter was used simply as a null detector but with the useful feature that its zero balance adjustment provided effective means to balance out stray thermal voltages. These were of the order of a microvolt and arose in the leads inside the helium dewar between the superconducting switches and the measuring circuit. These thermal voltages

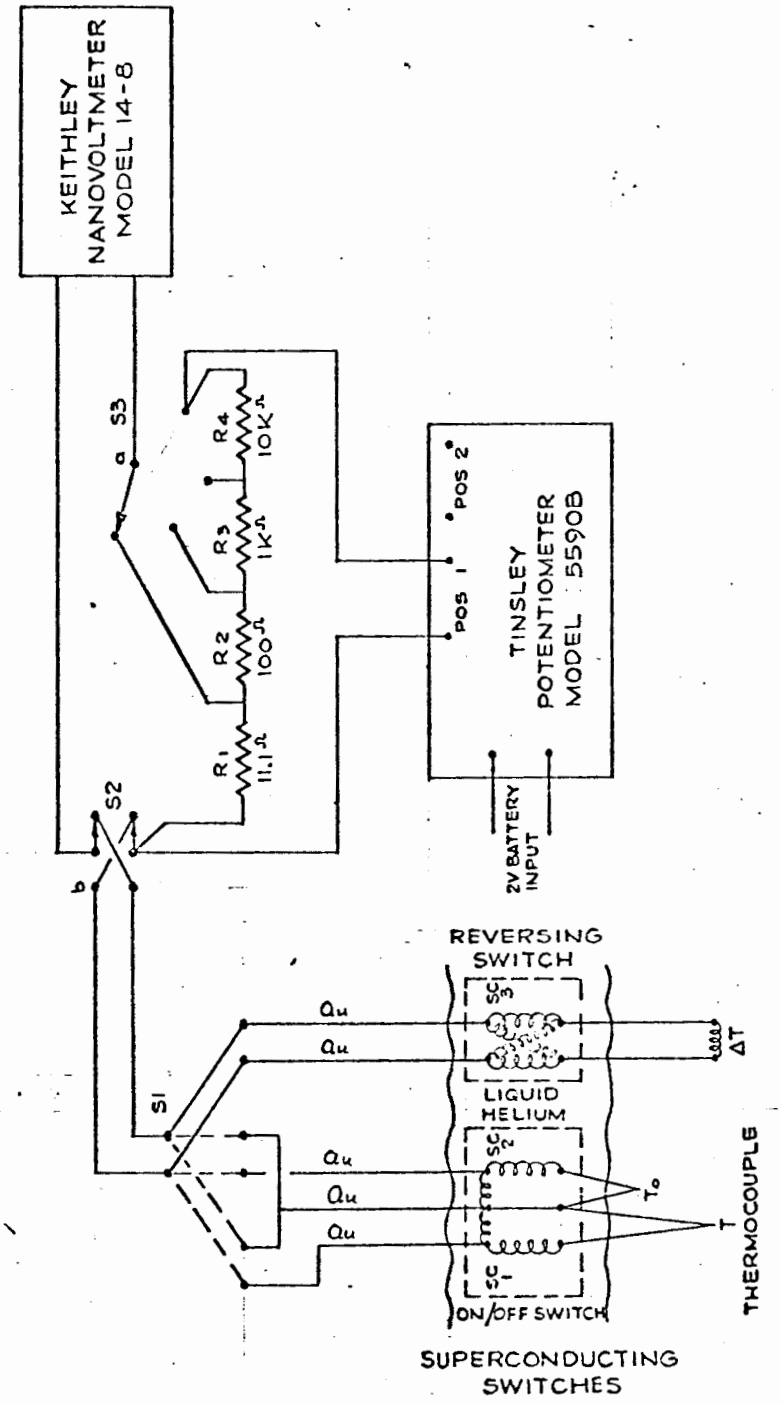

THERMOELECTRIC VOLTAGE
MEASURING CIRCUIT
FIGURE 2-5

were unaffected by operation of the superconducting switches whereas the thermoelectric voltage from the T and T_o thermocouples were switched ON/OFF by switches Sc1 and Sc2 respectively and the voltage from the ΔT thermocouple was reversed by switch Sc3. These superconducting switches were of the type described by Huntley (1963) and were located on the top of the vacuum can C with shielding cans made of superconducting Niobium sheet to shield them from the field of the magnet.

Switch S1 was used to select the thermocouple and switch S2 could be used to reverse the sign of the thermovoltage. Switch S3 could be used to select the division factor provided by the resistor network but was, in fact, kept at the position shown in fig.2.5 throughout the experiments, giving a factor of approximately 1000. When the thermocouple voltage being measured was either switched on-off or reversed by the appropriate superconducting switch it was necessary that the balancing voltage from the Tinsley potentiometer be similarly switched. This was done by switching its battery input and was accomplished in a relay operated control unit, to be described later, which also controlled the superconducting switches.

In operation, the balancing voltage was adjusted with the Tinsley potentiometer controls until no change occurred in the nanovoltmeter reading when both the voltages were switched. In practice, it was not necessary to balance out the stray thermal voltages exactly with the Keithley zero balance control, but necessary only to bring the balance point within the range of the Keithley output meter.

Stray thermal voltages arising outside the helium dewar were kept to a minimum by using an all copper circuit outside the helium bath, except for the dividing resistors R_1 - R_4 which were immersed in an oil bath, and by complete thermal shielding of the entire circuit. The circuit was also well shielded electrically to minimize induced electrical noise. A coaxial cable type NEF-11 made by Northern Electric Company was used and found to be ideal for all interconnections in the voltage measurement circuit between the helium dewar and the oil bath and between the oil bath and the nanovoltmeter. This cable has all copper conductors with a continuous copper foil shield,in addition to a copper braid shield, and has foamed polystyrene insulation between the central and shield conductors, thus providing good thermal as well as electrical insulation of the central conductor. The coaxial construction ensures that the thermal shielding

is uniform along the whole length of all the conductors which is important for minimising thermal voltages.

The thermal shielding proved to be entirely satisfactory and the electrical shielding proved to be effective against all but strong signals fed directly into the laboratory ground line. It was, however, found to be necessary to switch off the magnet power supply and have the magnet operating in persistent mode while any readings of thermoelectric voltages were being taken: large instabilities were otherwise observed. It did not appear that the magnet supply could be affecting the measuring circuit external to the helium dewar to this extent and supply fluctuations could not alter the magnetic field of the superconducting magnet when its circuit was closed through its superconducting shorting switch. It was concluded that, with the magnet supply still operating, and supply current therefore still flowing down the magnet supply leads inside the helium dewar, small fluctuations in this current could directly induce disturbances into the thermocouple circuits in the neighbourhood of the superconducting switches Sc1 - 3, where the leads were unshielded for short distances between the cryostat can and the switches and between the switches and a stainless steel tube which

provided shielding from the neighbourhood of the switches to the top of the dewar. Alternatively, the disturbances could be induced first into the heater leads going to the quartz rod heaters h_1 and h_2 since these leads were unshielded and thence be passed to the thermocouple circuits inside the cryostat can C, where none of the leads were separately shielded from each other. The question was not pursued because it was deemed necessary, in any event, to operate the magnet in persistent mode because small fluctuations in the magnet field would otherwise occur which would directly induce voltages in the thermocouple circuits.

The principal weakness of the voltage measuring circuit was that the nanovoltmeter looked at an input circuit resistance of about 12 ohms (arising principally from R_1 in the voltage dividing network) which caused its response to be slow on the most sensitive ranges. Nevertheless, the thermoelectric voltages to be measured could usually be balanced with assurance against the known voltages from the Tinsley potentiometer to within 1 nanovolt, using the 100 or 300 nV scales in the Keithley nanovoltmeter. These scales were found to provide the best compromise between sensitivity, speed of response and the ease of assessing the mean of a signal containing random noise fluctuations.

The 1 nV precision in the voltage measurement meant that in the calibration of the Au + Fe wire used as the secondary reference, errors in voltage measurement were less than 0.02%, which was an order of magnitude less than the overall error in temperature measurement. In the studies of other alloys the thermoelectric voltages which they produced were generally smaller, so that the 1 nV uncertainty represented a correspondingly larger percentage error but did not exceed 0.3%.

In the study of the variation of the thermoelectric power with applied magnetic field, 1 nV represented from 0.02 to 2.0% uncertainty, depending on magnitude of the thermoelectric voltage which depended on the alloy specimen. It was here that the precision in voltage measurement had its greatest importance. The accuracy in the measurement of the thermoelectric voltage $V(\Delta T,H)$ due to a temperature difference ΔT at field H was at all times limited by a combination of random fluctuations of the signal with a slow drift of the balance point, apparently due to a slow drift of the spurious thermal voltages. Both these effects grew in magnitude with the applied field; thus, at low fields $V(\Delta T,H)$ could always be measured easily and with good assurance to within 1 nV, but at the maximum field the

random fluctuations often had peak values of the order of 30 nV and it became more difficult to assess the true mean balance point, particularly when this balance point was slowly drifting. Rapid switching of the reversing switches could not be used to circumvent this slow drift because operation of the magnetically actuated superconducting switches induced momentary voltage swings as high as 100 nV. In nearly all cases it was nevertheless possible, with patience, to determine the true balance point to within one, or possibly two nV. Sometimes it was necessary first to assess the drift rate and then, with the signal reversed at regular time intervals, to track the position of the mean with a clock, and so to arrive at the correct setting of the Tinsley potentiometer to balance $V(\Delta T,H)$.

In a few of the earlier runs, very much larger fluctuations with occasional peak values of the order of 100 to 300 nV were encountered, mostly at fields above 10 KOe. In these runs the accuracy of some of the points was thereby reduced, but the mean balance point could usually be assessed to within 5 nV. These larger fluctuations were later traced to movement of the whole cryostat relative to the magnet, under the influence of random turbulence in the slowly boiling liquid helium bath, and were subsequently

cured by wedging the cryostat.

On testing the measuring circuit, either with the ΔT thermocouple short circuited or with the whole ΔT circuit at room temperature, stray voltages of the order of 10 to 50 nV were found across the nanovoltmeter input which reversed sign on throwing the reversing switch and could not therefore be attributed to thermals and, furthermore, would show up as errors in the thermocouple readings. These were traced to leakage resistances of the order of 10^9 ohms from the potentiometer and from the nanovoltmeter input to ground, as illustrated in fig.2-6: thus 1 volt was divided across R_1 = 11.1 ohm and the leakage resistances, with the portion appearing across R_1 being read by the nanovoltmeter. The fault could be cured by placing a ground connection anywhere between points A and B and since the T and T_o thermocouples are grounded at the cryostat, an electrical ground was added to one side of the ΔT couple at one of the sapphire thermal anchors.

The voltage dividing network of resistors R_1 to R_4 was first constructed with standard wire wound power resistors but it was found that these did not all have the same temperature coefficients and appreciable changes in their ratios occurred within the prevailing ambient

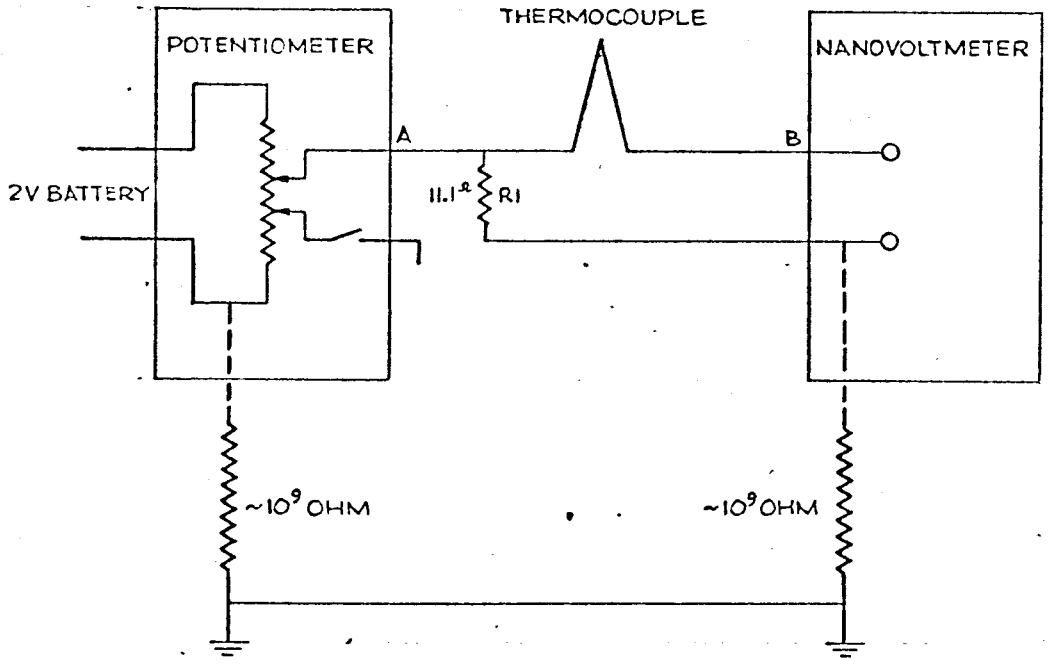

PORTION OF THERMOELECTRIC VOLTAGE MEASURING CIRCUIT SHOWING EFFECT OF LEAKAGE RESISTANCES

FIGURE 2-6

temperature range of $\pm$ 3°C. IRC type AS2 resistors, having temperature coefficients 0.002% per °C were therefore substituted. The division factors which they produced were measured in circuit so as to include the resistance of the wiring exactly as they would be operated. The factors found for the four switch positions were 1.0000, 10.001, 100.205 and 1007.15.

The first control unit which was constructed to fulfil the various measurement switching functions was a simple one using standard unsealed relays to simultaneously operate the superconducting switches and the battery input to the Tinsley potentiometer. It thus avoided the need for simultaneous manual operation of two separate switches but used manual switches in the battery circuits for all other functions. Initially, when the switches and relay contacts were new and clean, this unit was satisfactory but variation of the contact resistances in the battery circuit to the Tinsley potentiometer became noticeable and it was thought that errors could result if they became worse. A number of switches and relays were tested and a type of hermetically sealed relay was found which showed reproducible results with very low contact resistances. The relay unit was then reconstructed as shown in fig.2-7. This new unit was simpler to operate and all

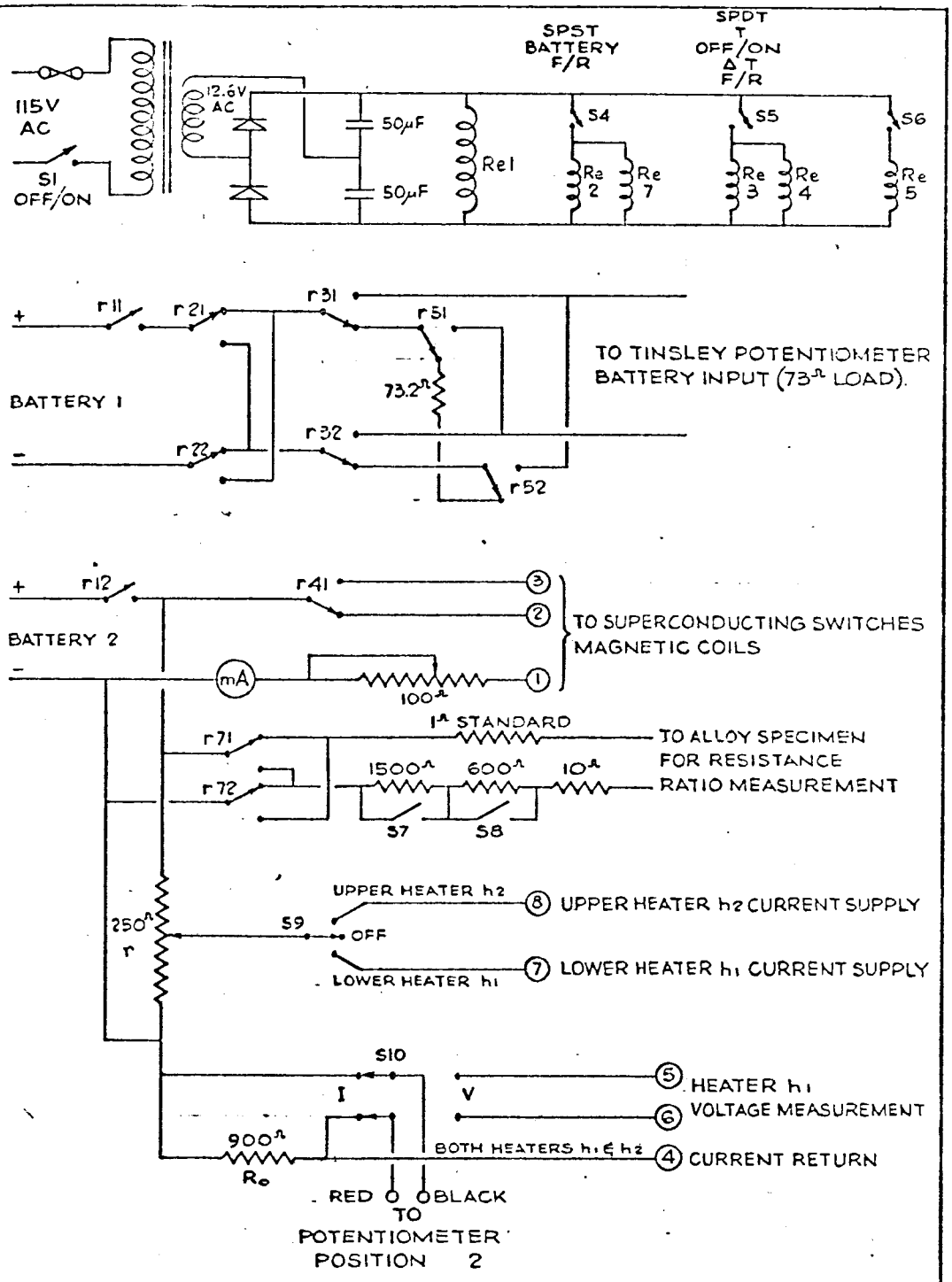

BATTERY SUPPLY AND CONTROL UNIT
FIGURE 2-7

critical circuit changes were performed by the special relays. It also included the circuit supplying the quartz rod heaters h_1 and h_2 which is described in Appendix A1,and the circuit for measurement of residual resistance ratio, which is described in Appendix A6.

Measurement Procedure

The same procedure was used in all the experimental runs and was essentially as follows:

The whole apparatus was first brought to equilibrium at the temperature of the helium bath, about 4.2 K. The lower heater h_1 was then switched on to produce a temperature gradient along the quartz rod and its current adjusted to provide a suitable thermoelectric voltage between contacts e_1 and e_3. The thermoelectric voltage corresponding to ΔT between e_1 and e_3 and to T at e_2 were read at intervals until stable conditions had been reached. The magnetic field was then raised in steps to the maximum value obtainable with the magnet in use. At each step the magnet was put into persistent mode and the magnet power supply switched off before the ΔT thermoelectric voltage was read. After the magnetic field had been returned to zero the ΔT and T thermoelectric voltages were again read. The heater was then switched off.

If any small drift in ΔT had occurred over the field run, this could be allowed for, assuming that the drift rate was constant, by noting the time at which each reading was taken.

Helium was then pumped from pot P to lower the temperature of the apparatus in steps, the temperature being stabilized at each step by means of a manostat (Walker, 1959). This gave a series of temperatures T_o at which the thermoelectric voltages were read from the thermocouple connected between the helium bath and the copper post on platform A and from the reference thermocouple connected between the helium bath and the central contact e_2 on the quartz rod. In the initial and final calibration runs with the Au+230 p.p.m. atomic Fe reference wires in both positions, the helium bath temperature and the temperature T_o were also read by the helium vapour pressure thermometers VPa and VPb respectively, or by the gas thermometer.

Additional magnetic field runs like the one described above at 4.2K, with the lower heater h_1 again switched on, were made at a series of points as the temperature was lowered, usually at about 3.2K, 2.2K and 1.5K.

CHAPTER 3

PREPARATION OF GOLD - IRON SPECIMENS

The need for specimens consisting of more dilute alloys of iron in gold than had hitherto been available has already been discussed in Chapter 1. In order to obtain these with accurately known Fe concentrations it seemed desirable to find a method of specimen preparation other than that of adding iron to pure molten gold because of uncertainties as to the amount of Fe impurity in the supposedly pure Au and the danger of Fe impurity being introduced during handling, and particularly when drawing the alloys into wires. Furthermore, this method could not produce an alloy containing less Fe than was in the most pure gold available. (Later analysis showed that the purest gold available contained about 2.5 p.p.m. atomic Fe). If a method could be found to progressively purify a more concentrated alloy, of say 300 p.p.m., this would seem to be ideal and would be less costly, since Au + .03 at % Fe is commercially available. Furthermore, if this could be done without changing the physical form of the specimens so that subsequent handling of the alloy was minimised, it would seem to be even better. Such a method was therefore sought and successfully found (Walker, 1970).

The method has proved successful, both in producing alloys of controlled composition and as a means of removing trace amounts of Fe to produce high purity gold. This in itself is of value because a principal difficulty in obtaining accurate thermoelectric power, resistivity and other data on dilute alloys of gold with other metals at temperatures below about 20K arises from the very large effects produced by trace amounts of iron. As little as a few p.p.m. of Fe can make it impossible to determine the effects of another alloying element. It is true that the large effects of iron can be eliminated by oxidation of the iron, as has been shown by Worobey et al. (1965) but MacDonald et al. (1962), using gold containing oxidised iron and in which the iron effects were greatly reduced, found that when another metal which they wanted to study was added to the gold, the typical Fe effects reappeared at nearly full strength, presumably because some of the oxygen was taken over by the added metal,leaving enough of the iron unoxidised to again dominate the electron scattering.

Because gold is chemically a highly inert metal, whereas iron is much more strongly reactive, it seemed probable that a chemical means should be available which would convert any iron existing at the surface of a gold specimen

to a volatile iron compound, while leaving the gold unattacked. With suitably elevated temperature the remaining iron inside would then diffuse to the surface and, in turn, be removed.

Chlorine gas is known to react with gold in the temperature range of 140 to 300°C to form either aurous or auric chloride but above 300°C both are unstable and decompose. It was thought, therefore, that if the temperature of the gold was first raised to well above 300°C in a good vacuum before admitting chlorine gas, no reaction should take place between the chlorine and the gold. On the other hand, ferrous and ferric chloride are known to be stable at these temperatures and both are volatile, since ferric chloride boils at 315°C and ferrous chloride sublimes above this temperature.

It was expected that the rate of removal of the iron from the specimens would be limited by the rate of diffusion of the iron to the surface, since the chemical reaction should be relatively quite rapid, and a temperature of 850°C, close to the melting point of gold, was therefore chosen. This choice was, in fact, a compromise determined by the rate of diffusion of the iron, loss of gold through vaporization and the increasing strength of unwanted welds which

formed where two parts of the wire sample came in contact.

Carbon monoxide was considered as an alternative to chlorine gas because it does not react at all with gold, whereas iron carbonyl is stable and boils at 100°C. This was tried first but proved completely unsuccessful, perhaps because ferrous carbonyl is unstable at high temperatures and the formation of ferric carbonyl, $Fe(CO)_5$ would require the simultaneous arrival of five carbon monoxide molecules at an Fe atom site, which is a highly improbable event, except perhaps at much higher pressures than were tried. This was not pursued any further because entirely successful results were then obtained with the chlorine treatment. Since chlorine reacts similarly with Mn, Ni, Co and many other metals, and the resulting chlorides have appreciable vapour pressures at 850°C, we expected that the treatment would be effective also in removing a number of other impurities in the gold.

Measurement of Iron Concentration

The effectiveness of the treatment in removing iron was determined in the first place by measurement of the residual resistance ratio $\frac{R_{4.2}}{R_{293} - R_{4.2}}$ supplemented for the higher purities with measurement of thermoelectric power in the liquid helium temperature range. Confirmation that the iron

was indeed removed and not merely oxidized by the chlorine was obtained by spectrographic analysis.

So long as the iron concentration is large enough to dominate the electron scattering at liquid helium temperatures, its concentration can be determined by assuming that it is proportional to the bulk residual resistance ratio. The bulk ratios can, in turn, be obtained from the measured residual resistance ratios, which include the effect of boundary scattering, using the theory of Sondheimer (1952) and the experimental value obtained by Chambers (1952) for the product of resistivity and electron mean free path in gold.

As the iron concentration is decreased below about 20 p.p.m. atomic, electron scattering by crystal lattice defects becomes increasingly important at liquid helium temperatures and in two of our samples it became the dominant factor; this was demonstrated by measuring the thermoelectric power S at 4.2K, which was found to be about an order of magnitude less in these two samples than in the gold wire with 0.03 at. % Fe before treatment, which had a value S_{Fe} of 13.5 μV/K.

The iron content in these highly purified samples was estimated using the Nordheim-Gorter (1935) relation and

assuming that the thermoelectric power of all electron scattering processes other than by the iron is zero, so that

$$\text{Fe concentration} \propto \rho_{Fe} = \rho \frac{S}{S_{Fe}} \qquad (3\text{-}1)$$

where ρ is the measured value of the residual resistivity and ρ_{Fe} is the part which is due to iron. Beside giving estimates of the iron concentration in the two samples, these thermoelectric power measurements also gave estimates of the residual resistivity due to electron scattering by the crystal lattice defects ρ_{cld}, assuming a simple addition law (Mathiesen's rule)

$$\rho_{measured} = \rho_{Fe} + \rho_{cld} \qquad (3.2)$$

This was then used to determine ρ_{Fe} and hence the iron content in samples of intermediate concentration which had received the same annealing treatment, but in which neither the iron nor the lattice defects completely dominated the electron scattering.

All the experimental data from which the Fe concentrations were determined are collected together in table 3.1, which also shows the various computations.

There is some doubt whether the Nordheim-Gorter rule is strictly applicable to magnetic scatterers like Fe in Au.

This question was examined by Gold et al. (1960), who indicate that Kohler's rule relating the thermoelectric powers to the thermal resistivities, rather than the electrical resistivities, is theoretically more likely to be valid but they reach no definite conclusion. Experimentally, it seems that the Wiedemann-Franz law connecting the two resistivities is correct and applicable to the Au Fe alloys in the liquid He temperature range, at least to within about 10%, as is indicated in Appendix A3. Also, the Nordheim-Gorter rule has been used by several experimenters in interpreting their measurements on dilute magnetic alloys and appears to yield consistent results, as is discussed by Kopp (1969).

Procedure and Results

The gold wire samples ($\sim$ 0.1 mm diameter) were inserted in a long silica tube which was first evacuated and then hydrogen gas admitted to a pressure of about 1 mm Hg. The portion of the tube containing the sample was then inserted in an oven and the temperature raised to 850°C, after which the hydrogen was pumped out. For lower degrees of purification the hydrogen treatment was omitted, but it was then found essential to evacuate the tube to 10^{-5} mm Hg or less to remove all oxygen before the temperature was raised.

TABLE 3.1

SAMPLE	Residual Resistance Ratios $(\rho_r/\rho)_{4.2}$ Measured	Bulk	Crystal Lattice Defects & Other	Fe	Thermo-power at 4.2K $S_{measured}$	Fe Concentration p.p.m. atomic	NOTES
Johnson Matthey .03 at % Au-Fe wire .08 mm.diameter							
XV after 4½ hrs.+3½ hrs. (8 hrs.total) Cl_2 at 850°C & slow cool from 725°C	.001844	.001186	.000955	.000231	S_{Fe}/ 8.0	0.54	Resistance ratio due to Fe calc. from $S_{measured}$ by equation(3.1) hence ratio due to crystal lattice defects (including other scatterers) obtained by equation (3.2) & used for other samples cooled slowly: see also samples II & IX below after long Cl_2 treatment
XV untreated	.1265						Fe concentration obtained by analysis (see Table 3.2).
XIII untreated	.1250	.1253 (mean)	.0015 (est) c.l.d .0178 Sn, Pb	.1060		250	Fe concentration of all other samples calculated from this in the proportion of their Fe resistance ratios. For resistance ratio increment due to Sn, Pb, see Appendix A-7.
I after heat & cool as below plus 62 hrs. CO & quick cool from 850°C	.1244						Samples XIII and XV from spool 3 which appeared to contain no oxidised Fe.
I untreated	.1143						Samples I, II & IV from spool 2. Sample I after 62 hr.treatment by CO which is strong reducer had resistance ratio increased to .1244: concluded that wire from spool 2 contained 228 p.p.m. Fe unoxidised, 250 p.p.m. Fe total.
I after quick cool from 850°C	.1171						
II untreated	.1176	.1160 (mean)	.0015 (est) c.l.d	.0967	13.14	228 unoxidised	
IV untreated	.1152		.0178 Sn, Pb				
VI after 3 hrs.Cl_2 & slow cool from 850°C	.0362	.0362	.00096	.03524	13.7	83.2	T calibration & measurement sample
IVa after 3 hrs.Cl_2 & slow cool from 850°C	.0194	.0194	.00096	.01844		43.5	ΔT measurement sample.This sample treated with sample VI:difference in resultant Fe concentration is thought to be due to presence of oxidised Fe and to inadequate vacuum before Cl_2 treatment.
I after CO treatment as above plus 2½ hrs.Cl_2 & quick cool from 850°C.	.0176	.0176	.0015 (est)	.0161		38.0	
II after 2½ hrs.Cl_2 & quick cool from 850°C	.0127	.0127	.0015 (est)	.0112		26.4	
II after 2½ hrs.plus 15 hrs. (17½ hrs.total) Cl_2 & quick cool from 850°C	.00210	.00145	.00145	-		< .01	Expected Fe conc. from extrapolation of fig.3.1 would be .0004 p.p.m. atomic. This sample provides estimate of resistance ratio due to crystal lattice defects after quick cool from 850°C.
II as above reheated & cooled slowly from 850°C	.00161	.00093	.00093	-		< .01	This sample,with sample IX below & sample XV above,provides estimate of resistance ratio due to crystal lattice defects after slow cool from 850°C.
IX after 25 hrs.Cl_2 & slow cool from 850°C	.00164	.00096	.00096	<.00007	S_{Fe}/ 24.3	< .16 unoxidised	Limiting Fe concentration & residual resistance ratio calculated on the assumption that $S_{measured}$ is wholly due to Fe, which is probably an overestimate(see chap.4).
XV after 4½ hrs.Cl_2 at 850°C & slow cool from 725°C	.00497	.00440	.00096	.00344		8.12	
Cominco 99.9999% Au.wire .1 mm. dia.							
III untreated	.0098	.0098	.0088	.0010		2.25	Fe concentration obtained by analysis(see Table 3.2).Resistance ratio due to Fe calculated from this.
III after ½ hr.H_2 & 15 hrs. Cl_2 & quick cool from 850°C	.00143	.00092	.00092	-			
III as above reheated & cooled slowly from 850°C	.00114	.00060	.00060	-			
XVI after ½ hr.H_2 & 69½ hrs. Cl_2 & very long cool;	.000561	.000010	.000010	-		< .15	Spectrographic analysis detected some Fe.
after standing 2 days at 23°C	.00139	.00087	.00087	-			
XVII after ½ hr.H_2 & 72 hrs. Cl_2 & very slow cool	.00135	.000825	.000825	-		.07	Fe concentration obtained by analysis (see Table 3.2); probably oxidised.

S_{Fe} is characteristic thermoelectric power of Fe in Au at 4.2K.

Iron oxide, like most other metal oxides, is not volatile below the melting point of gold and its presence appears to inhibit the diffusion of the iron to the surface.

After pumping out the hydrogen and with the gold specimens at 850°C, chlorine gas was admitted slowly to a pressure between 0.1 and 0.3 mm Hg.

After the required treatment time, the chlorine gas was pumped out to 10^{-4} mm Hg or less and the temperature then maintained for at least an hour to allow the remaining iron to diffuse uniformly throughout the sample. The temperature was then reduced to 725°C for half an hour before switching off the oven and allowing the sample to cool slowly to room temperature. This procedure allowed some of the crystal lattice defects to anneal out and gave reproducible results.

The variation of iron concentration with chlorine treatment time is shown in fig.3.1 for gold wire 0.08 mm diameter initially containing 250 p.p.m. atomic Fe. It is seen that a 10 hour treatment reduces the iron concentration by three orders of magnitude. The two points obtained with wires treated in Cl_2 for three hours are thought to be high because of an inhibiting effect of iron oxide. These specimens were not first treated with either H_2 or CO to reduce any oxide present and, as shown below and in the notes in

Figure 3-1

Change of iron concentration with chlorine treatment time at 850°C for gold wires 0.08 mm diameter originally containing 250 p.p.m. atomic Fe.

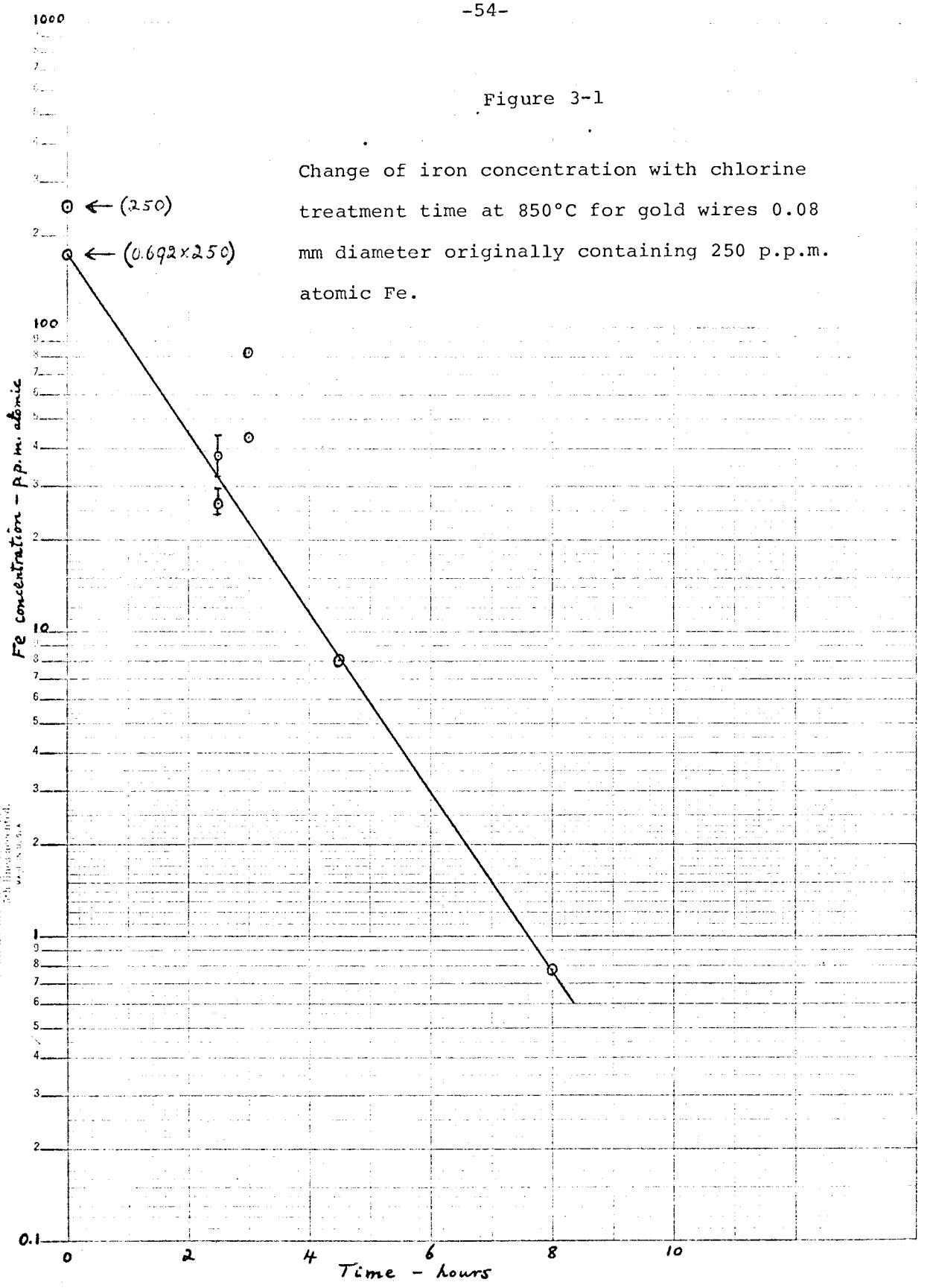

table 3.1, it seems almost certain that the spool of wire from which they were cut contained about 20 p.p.m. oxidised Fe. It should be noted that the sample treated for 8 hours, which reduced its Fe concentration to 0.54 p.p.m. atomic Fe, received its treatment in two stages: the first stage was a 4½ hour Cl_2 treatment which reduced its Fe content to 8 p.p.m. atomic and was followed by a heat treatment in vacuum, long enough to distribute the remaining Fe uniformly throughout the sample. The second stage, which included the remaining 3½ hour Cl_2 treatment, thus started fresh with a uniformly distributed sample and so the initial removal of Fe at the start of this second stage was faster than if the whole 8 hours had been run continuously. This faster initial period is allowed for in the diffusion equation (3.3) below by the factor 0.692, and in fig.3.1 the initial point for zero Cl_2 treatment time is at a concentration of 0.692 x 250 p.p.m. atomic Fe. We have correspondingly allowed for the two step treatment of the 8 hour point in fig.3.1 by raising it to correspond to an Fe concentration of 0.54/0.692 = 0.78 p.p.m.

A further sample of this alloy was treated with chlorine for 25 hours but without first using hydrogen to reduce any metal oxide which may have been present. The resulting

wire specimen had a small thermoelectric power which could be explained using the Nordheim-Gorter relation as due to 0.16 p.p.m. atomic Fe, but this had both temperature and magnetic field dependence which did not wholly conform to our data on other gold-iron samples and it is thought that the small thermoelectric power may have been due to some other cause, or to some other impurity. Extrapolation of fig.1 to 25 hours would leave less than 10^{-6} p.p.m. at. Fe. The sample was analysed spectrographically using carrier distillation, as described by Tymchuk et al. (1965,67), with the results given in table 3.2 and it is concluded that most, if not all of the 0.67 p.p.m. atomic Fe found in it was in the oxidised state. Further evidence pointing to the existence of appreciable amounts of iron oxide in this wire in its untreated state is that its residual resistance ratio was increased by treatment at 850°C with carbon monoxide gas from about .114 to .124, as shown in table 3.1. Since the electron scattering is here dominated by the unoxidised iron present, this indicates that about 20 p.p.m. atomic Fe was originally present as oxide.

Table 3.2 also includes the result of a half hour hydrogen and 72 hour chlorine treatment of a sample of Cominco 99.9999% pure gold wire 0.10 mm. diameter.

TABLE 3.2

Spectrographic Analysis

By Carrier Distillation Of Samples Of Gold Wire

Before and After Treatment with Chlorine Gas

Impurity	Gold wire 0.08 mm diameter spec. pure plus 0.03 at.% Fe.[a]		Gold wire 0.10 mm diameter 99.9999% pure.[b]	
	Untreated	Treated Cl_2 25 hrs. at 850°C	Untreated	Treated H_2 half hr. Cl_2 72 hours at 850°C
	p.p.m. atomic	p.p.m. atomic	p.p.m. atomic	p.p.m. atomic
Iron	250	0.67	2.25	0.07
Tin	100 to 130	~2.5		
Lead	10 to 20			
Silicon	<7	<7	1.7	1.7
Aluminum	not visible	<7	0.7	0.7

[a] Johnson, Matthey Metals Ltd., London, England, Spool 3

[b] Cominco American, Spokane, Washington, U.S.A.

The spectrographic analysis of both samples confirms that iron was indeed removed by the treatment and shows that it was also effective in removing tin. Another Cominco sample, sample XVI, after treatment with H_2 for ½ hour and Cl_2 for 69¼ hours at 850°C was given a long, slow anneal procedure (725°C ½ hour, 450°C 4½ hours, 275°C 12 hours, 100°C 12 hours, 40°C 18 hours) and was then found to have a bulk residual resistance ratio in excess of 10,000, as indicated in table 3.1. After the slow cool, this sample was slid out of the annealing tube and into place on the holder for measuring its residual resistance ratio, virtually without handling. Two days later, after handling twice but without removal from the holder, the measured resistance ratio had changed to a value of .00139, comparable to that found for samples III and XVII, and indicating a bulk value of .00087. It is possible that this change was all due to additional lattice defects produced by handling, but it must be remembered that the Cl_2 treatment would leave the wire surface exceptionally clean: the boundary scattering may therefore have been appreciably less than normal when the resistance ratio was first measured. Even so, the measured ratio of .00056 is a low value. It would be of interest to measure a sample after Cl_2 treatment and slow cooling, without

removing it from the annealing tube and with vacuum or a He atmosphere maintained around it.

Diffusion Rate of Iron in Gold

As a by-product, the work here yielded a value for the diffusion rate of iron in gold. This is obtained from the slope of the graph in fig.3.1. According to Jost (1960) the change in the average iron concentration after time t due to outward radial diffusion in long cylindrical specimens for which the surface concentration is maintained equal to zero, is given by

$$\frac{\bar{c}}{c_i} = 0.692\ e^{-t/\tau} \qquad (3.3)$$

where c_i is the initial concentration, except for a short initial period, less than about one time constant τ. The diffusion coefficient D is obtained from the measured time constant as a function of the cylinder radius r.

$$D = \frac{r^2}{5.78\ \tau} \qquad (3.4)$$

The value of D which we obtain for the diffusion of iron in gold at 850°C is $5.19 \pm 0.08 \times 10^{-10}$ cm^2 sec^{-1}. Kubaschewski and Ebert (1944) have reported values for a gold-iron alloy containing 15.6 at. % Fe over the temperature range from 753°C to 1003°C. Interpolating from their graph of log D versus the reciprocal of the temperature

gives about 20×10^{-10} cm^2 sec^{-1} at 850°C. Since it appears (see Jost, 1960) that D generally increases with concentration, their data is not inconsistent with ours. At 15.6 at.% Fe in Au the iron is diffusing through a mixture of the two metals, rather than through gold. Our value, obtained at extreme dilution, would seem to represent the true value for the diffusion of iron in gold.

CHAPTER 4

EXPERIMENTAL RESULTS ON ALLOYS OF Fe IN Au

The thermoelectric powers of five dilute Au-Fe alloys were studied, varying in concentration from 230 p.p.m. to $<.16$ p.p.m. atomic Fe and prepared as described in the previous chapter.

The effect on these thermoelectric powers of an externally applied magnetic field was studied for four of them containing 230, 43, 0.54 and $<.16$ p.p.m. atomic Fe at a series of fixed temperatures between 1.2K and 6.75K, and the variation of the thermoelectric powers with temperature at zero applied field was obtained for three of the same alloys containing 230, 0.54 and $<.16$ p.p.m. and for one containing 83 p.p.m. atomic Fe.

Thermoelectric Power vs. Temperature

The experiments yielded a series of measurements of the thermoelectric voltage developed across an alloy sample connected between one point at a fixed temperature (helium bath) and a second point at a variable temperature. They thus provided directly a plot of thermovoltage vs. temperature (of the second point) for each of the alloy samples studied. The thermoelectric powers of the samples are then given by the

slopes of these curves (see equation (1.1) in chapter 1). The slopes vary with temperature and we thus obtain plots of $S_{measured}$ vs T.

The results of our measurements have been plotted in fig.4.1 for the characteristic thermoelectric powers S_{Fe} due to the Fe, using equation (3.1) in chapter 3 and the resistivity data for the alloys computed in table 3.1. In this table the part of the residual resistance ratio which is due to Fe is calculated by subtracting the portions due to crystal lattice defects and other impurities from the measured total ratio or from its computed bulk value, as given by Appendix A.6. The portion due to crystal lattice defects and impurities not removed by the Cl_2 treatment was measured in samples which had been given long enough treatment to remove virtually all the Fe and other removable impurities and which had then been given the same annealing procedure as the sample being computed. The portion of the residual resistance ratio due to removable impurities, shown by the analysis to be Sn and Pb, was computed as shown in Appendix A.7. The resulting computed values of the resistance ratio due to Fe, in addition to being used to calculate S_{Fe} from $S_{measured}$, was used to obtain the alloy concentrations by direct proportion to the original untreated alloy which was chemically analysed.

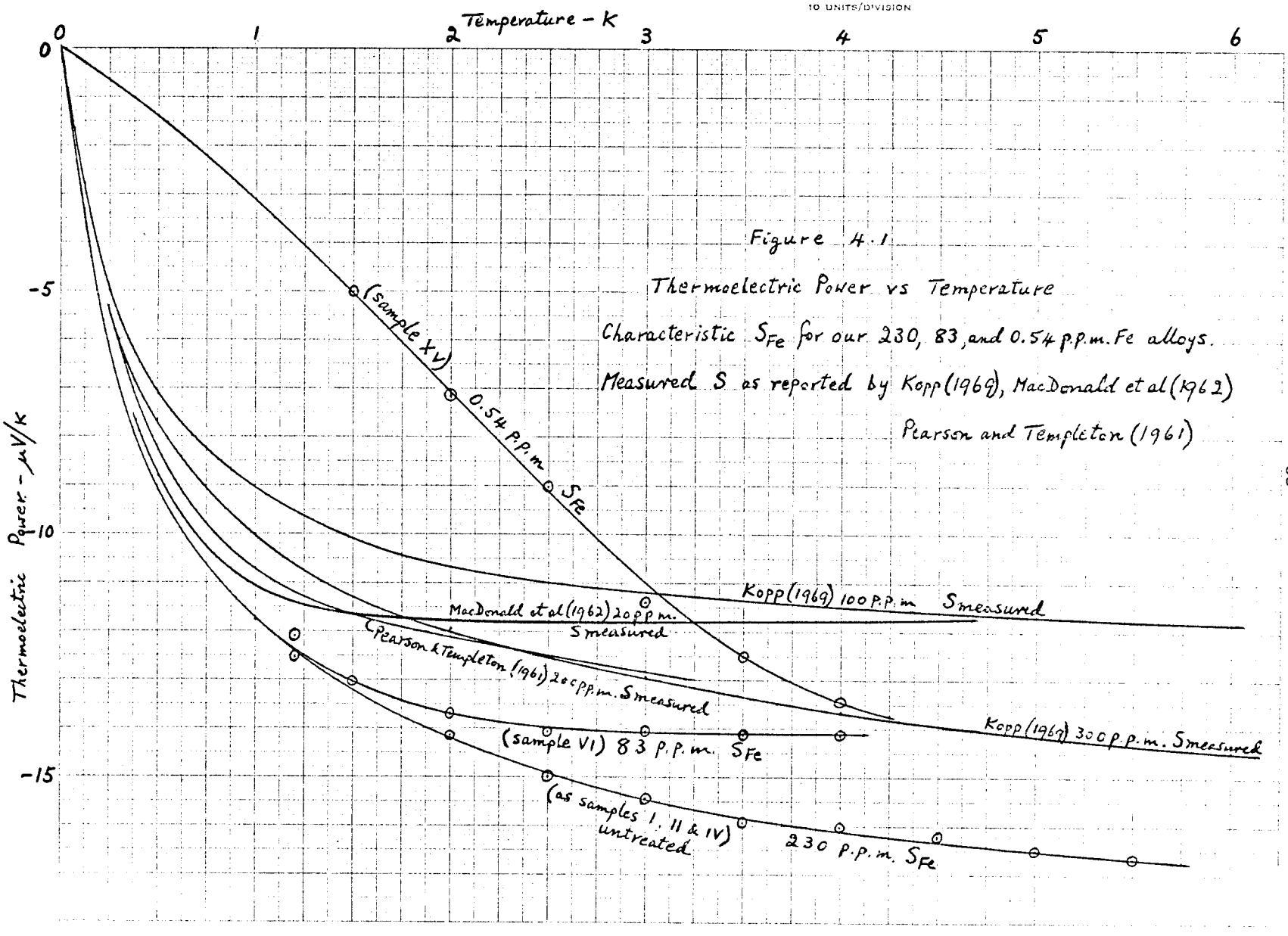

Figure 4.1

Thermoelectric Power vs Temperature

Characteristic S_{Fe} for our 230, 83, and 0.54 p.p.m. Fe alloys.

Measured S as reported by Kopp (1969), MacDonald et al (1962)

Pearson and Templeton (1961)

It can be seen in fig.4.1 that S_{Fe} is greatest over the whole temperature range for the alloy containing 230 p.p.m. Fe and reaches a value exceeding 16.5 μV. At somewhat lower concentration of Fe the magnitude of the characteristic thermopower S_{Fe} appears to be maintained at the lowest temperatures but does not rise as high as S_{Fe} for the 230 p.p.m. alloy. The curve for the 0.54 p.p.m. alloy shows that at much lower concentrations S_{Fe} falls steeply below 4K and becomes almost proportional to T. The exact position of this curve for S_{Fe} for the 0.54 p.p.m. alloy is uncertain because the ratio of the characteristic thermopower S_{Fe} to the measured thermopower $S_{measured}$ is not known with certainty, but this ratio cannot differ greatly from 8.0 without giving a value for the residual resistance ratio due to crystal lattice defects and other scatterers, which is in disagreement with values found for other samples with the same annealing treatment.

The thermoelectric power of the most highly purified specimen containing $<$0.16 p.p.m. atomic Fe is not separately shown in fig.4.1 because the observed thermoelectric voltage was everywhere proportional to that observed for the 230 p.p.m. alloy, being always smaller by a constant factor of 24.3 over the whole temperature range and so its thermoelectric power curve would have the same shape as the more concentrated alloy.

It does not therefore exhibit the more rapid fall off below 4K which is characteristic of the 0.54 p.p.m. alloy. As suggested in Chapter 3, the observed small thermoelectric voltage may have been due to some other cause, not Fe; the reduction factor of 24.3 for the observed thermoelectric power, combined with the observed residual resistance ratio for this alloy of 0.00164, sets an upper limit of 0.16 p.p.m. atomic for the unoxidised iron content.

Included for comparison in fig.4.1 are results reported by Pearson and Templeton (1961), by MacDonald et al (1962) and by Kopp (1969). These are reproduced as reported by the authors and are not adjusted to the characteristic thermopowers S_{Fe}, with the result that trends are not easily discerned. Insufficient accurate data are given by the authors to make the adjustments with certainty; nevertheless, with some reasonable assumptions it is possible to deduce probable S_{Fe} curves and these are given with our curves in fig.4.2, with encouraging results. The calculations are as follows:

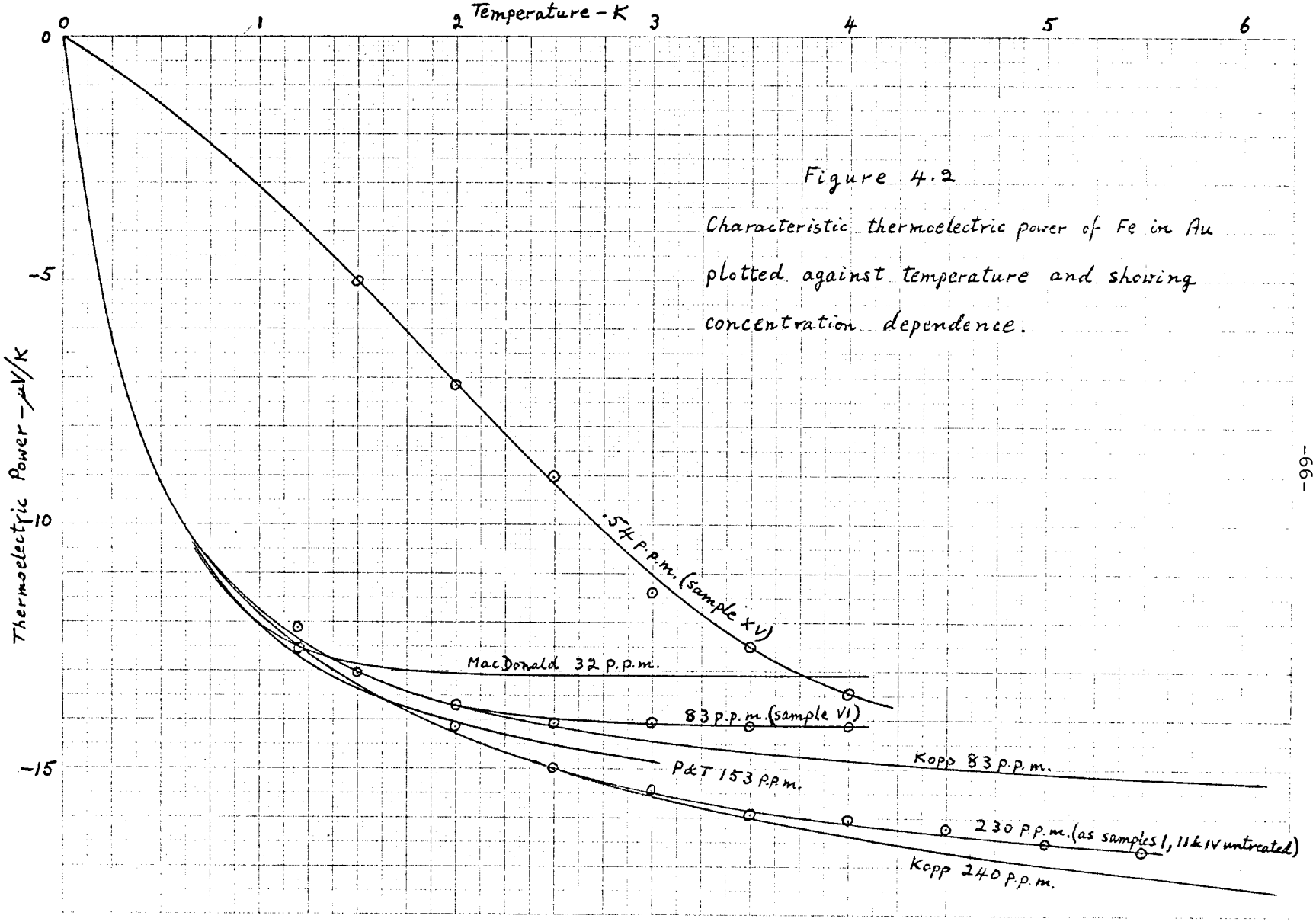

Figure 4.2

Characteristic thermoelectric power of Fe in Au plotted against temperature and showing concentration dependence.

Kopp's alloy nominally .03 at % Fe gave measured thermoelectric powers close to those found for our 230 p.p.m. alloy, which also was nominally .03 at % Fe with the same purity specification and was obtained from the same supplier at about the same time. Our measured residual resistance ratio was .1160 for spool 2 and .1253 for spool 3, in general agreement with Kopp's measurements which gave the resistivity at 4.2K as 264 nΩcm, corresponding to a residual resistance ratio of .120. It is reasonable, therefore, to assume that both wires contained the same impurities and, as received, had the same number of lattice defects. The same factor 1.20 should therefore be used in translating his measured data to characteristic thermopower S_{Fe}. This, of course, brings his curve into substantial agreement with our 230 p.p.m. curve, as shown in fig.4.2. It also yields a value for the magnitude of S_{Fe} at its maximum, at a temperature of about 10K of 18.4 μV/K.

One important point of disagreement between our data and Kopp's concerns the concentrations of the alloys. The analysis of such dilute alloys is very difficult, and in each case has to be based on some reference sample. Kopp had his samples analysed for him in London, whereas our concentrations are all based on an analysis performed for us in Ottawa. For the

nominally .03 at.% Fe in Au wire obtained by both of us from Johnson Matthey, Kopp's analysis showed 300 p.p.m. in agreement with the nominal specification, whereas ours showed 250 p.p.m. Fe. Our analysis gives the incremental residual resistance ratio due to Fe in Au as $4.24 \pm .10 \times 10^{-4}$/p.p.m. atomic Fe, in excellent agreement with a plot of residual resistance ratio against Fe concentration given by Macdonald et al (1962) which has a slope of 4.25×10^{-4}/p.p.m. atomic Fe. Kopp, on the other hand, quotes .82 nΩcm/p.p.m. atomic Fe, corresponding to residual resistance ratio increment of 3.73×10^{-4}/p.p.m. atomic Fe. A method for accurately determining the concentrations of these dilute alloys has recently been developed by Loram et al (1970) and we can therefore expect that this matter of concentration will eventually be resolved. In the meantime, and to maintain a common basis for comparison, we have used the Ottawa analysis and in comparing Kopp's results have adjusted his concentrations accordingly. Thus, for the .03 at.% alloy the residual resistance ratio of .120 obtained above from Kopp's data gives .101 for the portion due to Fe (after allowing for other impurities and lattice defects) and gives 240 p.p.m. atomic Fe for the concentration of his alloy. The curve in fig.4.2 is labelled accordingly.

It should be noted that if the Ottawa analysis is shown eventually to be wrong, it is only the concentrations as labelled on the curves which have to be changed. The residual resistance ratios are not affected, nor are the factors used to convert $S_{measured}$ to S_{Fe}.

Kopp's alloy nominally .01 at.% Fe was shown by his London analysis to contain 100 p.p.m. atomic Fe and so, by the Ottawa analysis, the concentration would be expected to be 83 p.p.m. atomic Fe. This means a residual resistance ratio due to the Fe content of .0353. Kopp gives the total resistivity of this sample as 100 nΩ cm, corresponding to a total residual resistance ratio of .0455. These values give a factor of 1.29 for $S_{Fe}/S_{measured}$. Using this brings his curve into close agreement with our curve for the same concentration up to 2.5K; above this temperature his curve shows a continued increase in the magnitude of the thermoelectric power, whereas our curve becomes essentially flat.

The resistance ratios calculated above for Kopp's sample give a resistance ratio increment of .0102 due to lattice defects and other impurities, corresponding to a residual resistivity of 22.5 nΩ cm, rather than the value of 18 nΩ cm assumed by Kopp. These values are an order of magnitude greater than those of our annealed and purified alloys and it is perhaps

worth noting that because our 83 p.p.m. sample was both well annealed and purified of other scatterers it had a measured thermoelectric power as high as any reported so far for a Au-Fe alloy below 4K, despite the flattening of its response curve above 2.5K.

MacDonald's alloy nominally .002 at.% Fe has a thermoelectric power curve which is similarly flat above about 1.5K. To adjust the measured curve to the characteristic thermoelectric power S_{Fe} it is necessary to know the residual resistance ratio of the alloy, which is given by MacDonald et al as .0151, and the portion which is due to Fe which must be estimated. Since we do not know the Fe concentration accurately, this residual resistance ratio due to Fe must be estimated by other means.

The alloy was made by adding approximately 20 p.p.m. at.Fe to proof plate gold and MacDonald et al give a graph of residual resistance ratio vs. Fe concentration for a range of alloys prepared in this way: extrapolating this graph to zero added Fe indicates that the residual ratio of the proof plate gold was .004. The thermoelectric power of the proof plate gold was also measured and showed that it already contained some magnetic scattering impurity. A factor of 1.6 would bring $S_{measured}$ for this proof plate gold to equality with S_{Fe} of other Au-Fe alloys below 1K. Assuming, therefore, that the magnetic scattering

impurity in the proof plate gold was Fe, the portion of the residual resistance ratio due to Fe was .004/1.6 = .0025 ; this gives its Fe concentration to be 6 p.p.m. atomic and the portion of the residual resistance ratio due to crystal lattice defects and other impurities to be .0015; (this is the same as the value derived in table 3.1 for crystal lattice defects and scatterers other than Sn and Pb in our original Au-Fe alloy). The ratio due to Fe in the .002 at.% alloy is therefore estimated to have been .0151-.0015 = .0136 giving $S_{Fe}/S_{measured}$ = 1.11 and the alloy concentration to have been 32 p.p.m. atomic Fe. The curve for MacDonald et al in fig.4.2 is drawn and labelled accordingly. Pearson and Templeton's alloy, nominally .02 at.% Fe can be brought into general agreement with the other alloys using a factor for $S_{Fe}/S_{measured}$ = 1.16. They give the residual resistance ratio for the alloy as .075 and, with the above factor, this gives the residual resistance ratio due to Fe as .065 and hence the alloy concentration of unoxidised Fe as 153 p.p.m. atomic. This bears the same ratio to the nominal concentration as does our 230 p.p.m. alloy.

The resulting curves in fig.4.2 all follow the same general trend, except for the one for our very dilute alloy containing 0.54 p.p.m. atomic Fe, whose concentration is about 2 orders of magnitude smaller than the others. From 240 p.p.m. to 32 p.p.m.

the characteristic thermoelectric power S_{Fe} decreases with concentration above some minimum temperature, the decrease extending progressively further toward zero K as the concentration decreases. The S_{Fe} curve for 0.54 p.p.m. atomic Fe indicates that this trend does not continue indefinitely and it would be of interest to obtain additional curves between 30 p.p.m. and 0.5 p.p.m. atomic Fe. The following information is available in this region but contains some uncertainties. The data of MacDonald et al (1962) for proof plate gold which has been estimated above to have contained 6 p.p.m. atomic Fe, follows the trend of the higher concentrations. We have also estimated the thermoelectric power of the ΔT sample supposedly containing 0.54 p.p.m. atomic Fe which was connected between contacts e_1 and e_3 on the quartz rod Q to study the effects of applied magnetic fields. This sample was cut from the same spool of wire and was treated in Cl_2 at the same time as the 0.54 p.p.m. sample used to obtain the plot in figs.4.1 and 4.2, and so was presumed to be the same alloy. The thermoelectric power in this case is determined by measuring the heat input to the crystal heater and so calculating the temperature difference between contacts e_1 and e_3 using the measured thermal conductivity of the quartz rod. The measured thermoelectric voltage between e_1 and e_3 thence

directly yields the thermoelectric power of the alloy. For the more concentrated alloys, the results obtained in this way agree closely with the values obtained as described above from the thermoelectric voltage vs temperature plots from which the curves in figs.4.1 and 4.2 are obtained, but for the supposedly 0.54 p.p.m. sample these ΔT measurements give results differing markedly from the results of the thermoelectric voltage vs temperature plot. The accuracy with which the thermoelectric power can be determined from the ΔT measurements on this sample is not good, because the heat inputs to the quartz rod in this case were only noted approximately, but they indicate an almost constant thermoelectric power over the whole temperature range measured from 4.4K down to 1.4K, in agreement with the trends noted above for the more concentrated alloys. The explanation may be that the ΔT sample contained a slightly higher Fe concentration, and there is some evidence that its concentration was in fact slightly greater than 1 p.p.m. atomic Fe, and it may be that the very different behaviour shown in figs.4.1 and 4.2 for the 0.54 p.p.m. alloy only appears below 1 p.p.m., or it may be that the curve for the 0.54 p.p.m. alloy in figs.4.1 and 4.2 is incorrect and is the result of some apparatus effect.

It is worth noting that the general trend,seen in fig.4.2,

of increasing characteristic thermoelectric power with increasing concentration, is the opposite of the trend seen at higher concentrations, above .03 at.% Fe in Au, in the results reported by MacDonald et al (1962). This perhaps indicates a maximum in the characteristic thermoelectric power in the region of .03 at.%. It is possible, however, that the apparent increase with concentration seen in fig. 4.2 is the result of a breakdown in the Nordheim-Gorter rule as applied to these alloys.

Effects of Magnetic Field on Thermoelectric Power

The change in the thermoelectric power resulting from the application of an external magnetic field was studied in the Au-Fe alloys containing 230 p.p.m., 43 p.p.m., 0.54 p.p.m. and <0.16 p.p.m. atomic Fe. The results are plotted for each alloy separately in figs.4.3 to 4.6 as the fractional change $\Delta S(H)/S(o)$ vs field H for a range of fixed temperatures T. As can be seen, the effect of the field in general is to decrease the thermoelectric power, except for the most concentrated alloy containing 230 p.p.m. atomic Fe in which it produces an increase at moderate field strengths, followed by a decrease at higher fields. The increase in moderate fields was found by Berman et al (1964) and the later decrease has been confirmed by Berman et al (1968). Our measured results

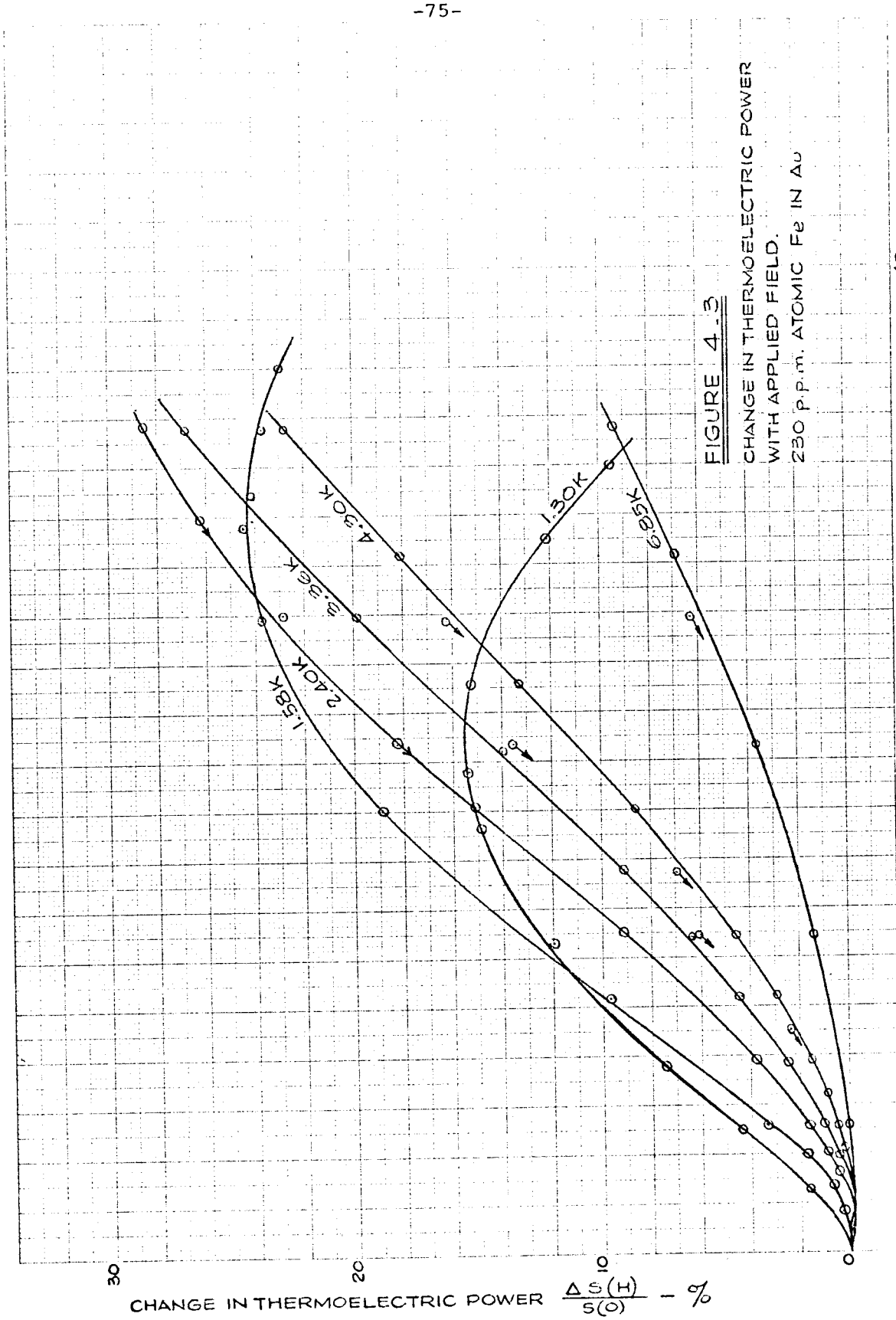

FIGURE 4_3
CHANGE IN THERMOELECTRIC POWER WITH APPLIED FIELD.
230 p.p.m. ATOMIC Fe IN Au

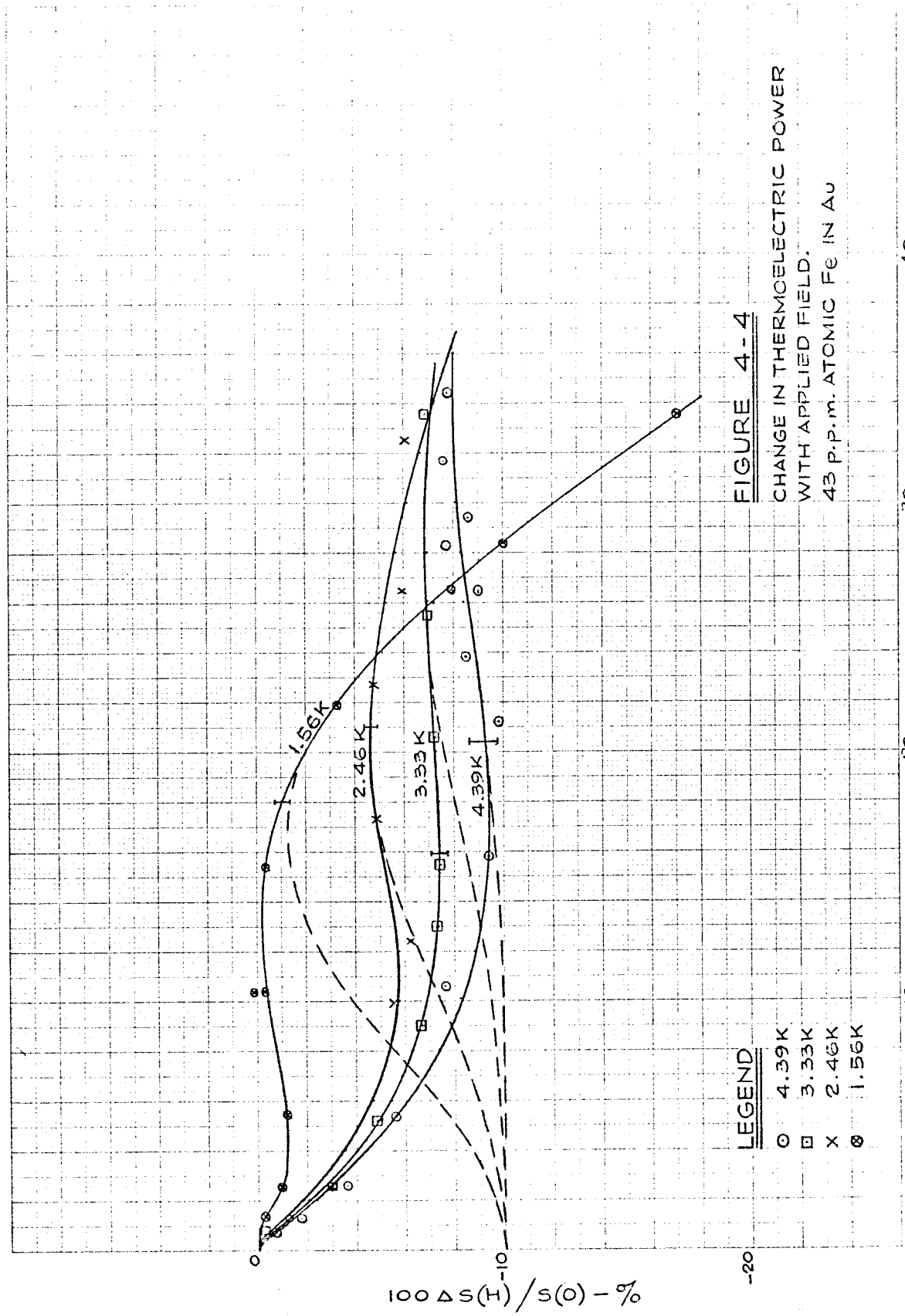

FIGURE 4-4

CHANGE IN THERMOELECTRIC POWER WITH APPLIED FIELD.
43 P.P.M. ATOMIC Fe IN Au

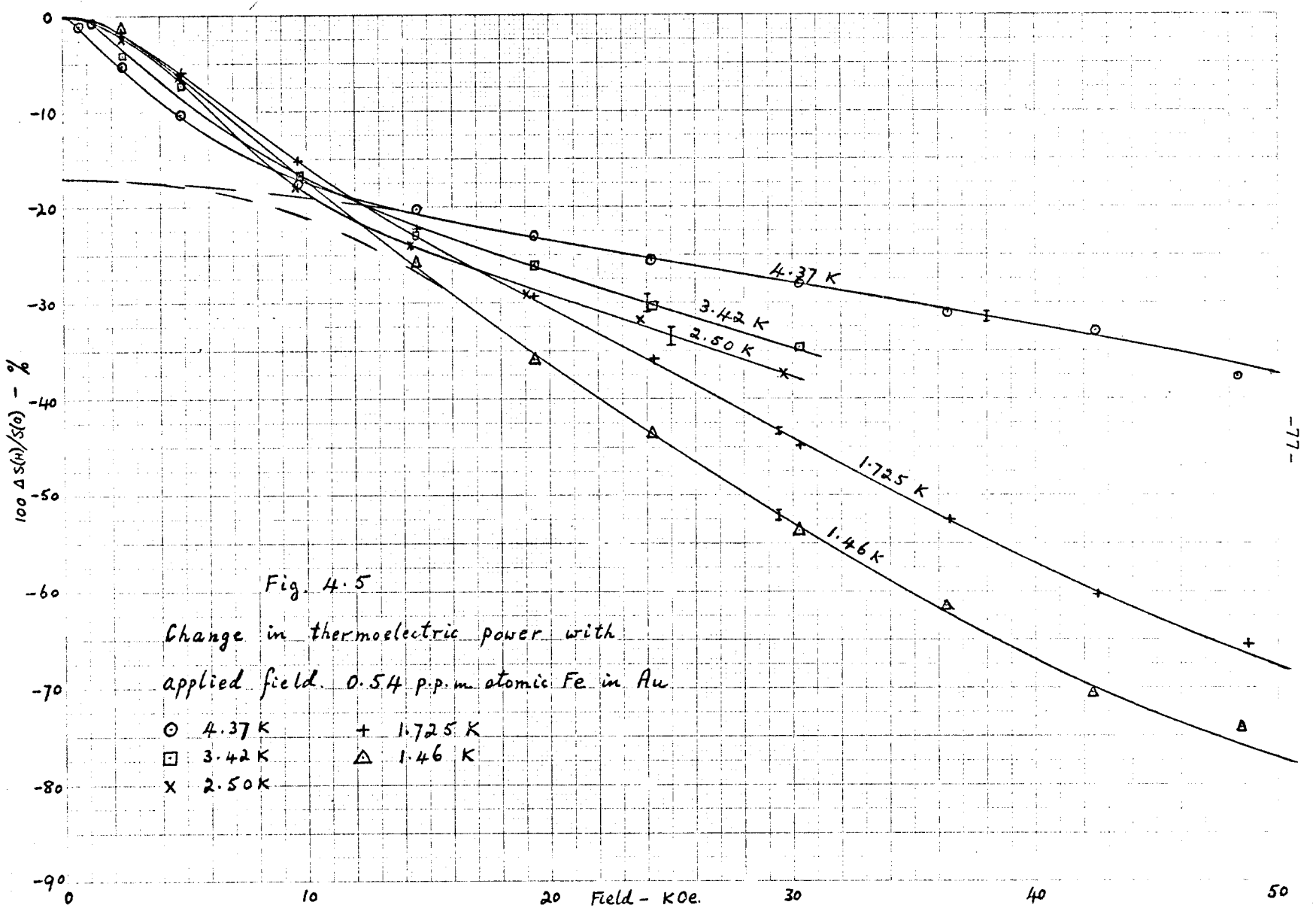

Fig. 4.5

Change in thermoelectric power with applied field. 0.54 p.p.m atomic Fe in Au

⊙ 4.37 K + 1.725 K

⊡ 3.42 K △ 1.46 K

× 2.50 K

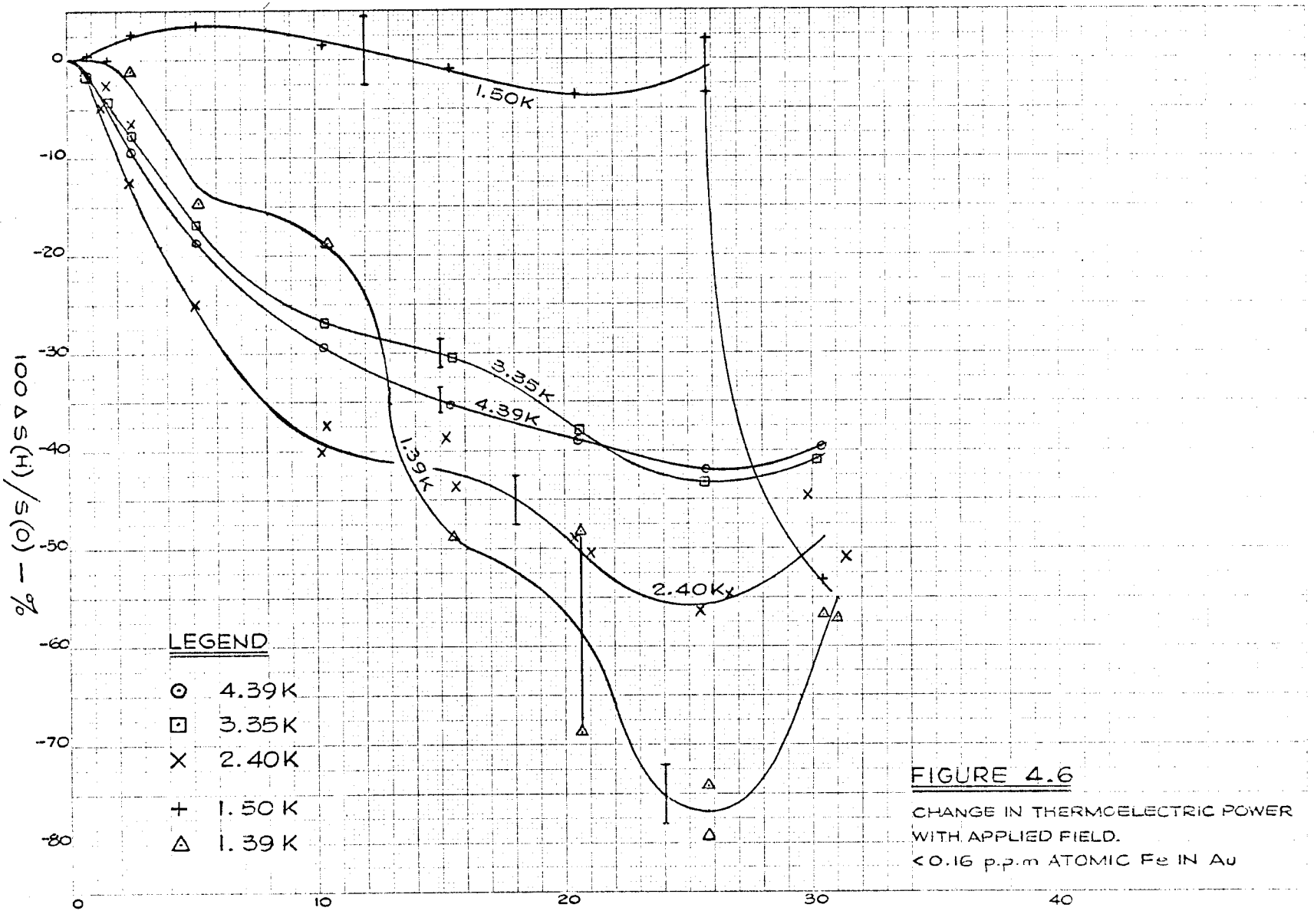

FIGURE 4.6

CHANGE IN THERMOELECTRIC POWER WITH APPLIED FIELD.
<0.16 p.p.m ATOMIC Fe IN Au

differ from theirsin some significant details which are discussed below; perhaps the most peculiar behaviour is in the 43 p.p.m. alloy for which a decrease is followed by an increase, followed by a decrease.

Berman et al (1964) give their results plotted against $H/_T$; there is some theoretical justification for this, but the theory is unsatisfactory and the $H/_T$ plot does not bring the experimental results at different temperatures into exact agreement and, in fact, succeeds only in producing a somewhat confused picture. We have felt it desirable first to present the measured results as clearly as possible. Error bars have been added to figs.4.4, 4.5 and 4.6, showing the estimated error at high fields for each curve. No bars are shown in fig. 4.3 for the 230 p.p.m. atomic Fe alloy because the estimated errors are about the same as the line widths.

In figs. 4.7 to 4.10 the curves have been redrawn so as to directly compare the four alloys at a series of fixed temperatures 4.35K, 3.37K, 2.45K and 1.56K. When making the measurements we attempted to repeat the same set of temperatures for each alloy but did not succeed in doing so exactly, with the result that small temperature differences exist. Except for the 0.54 p.p.m. alloy below 2K, the differences from one of the chosen temperatures does not exceed 3% at most

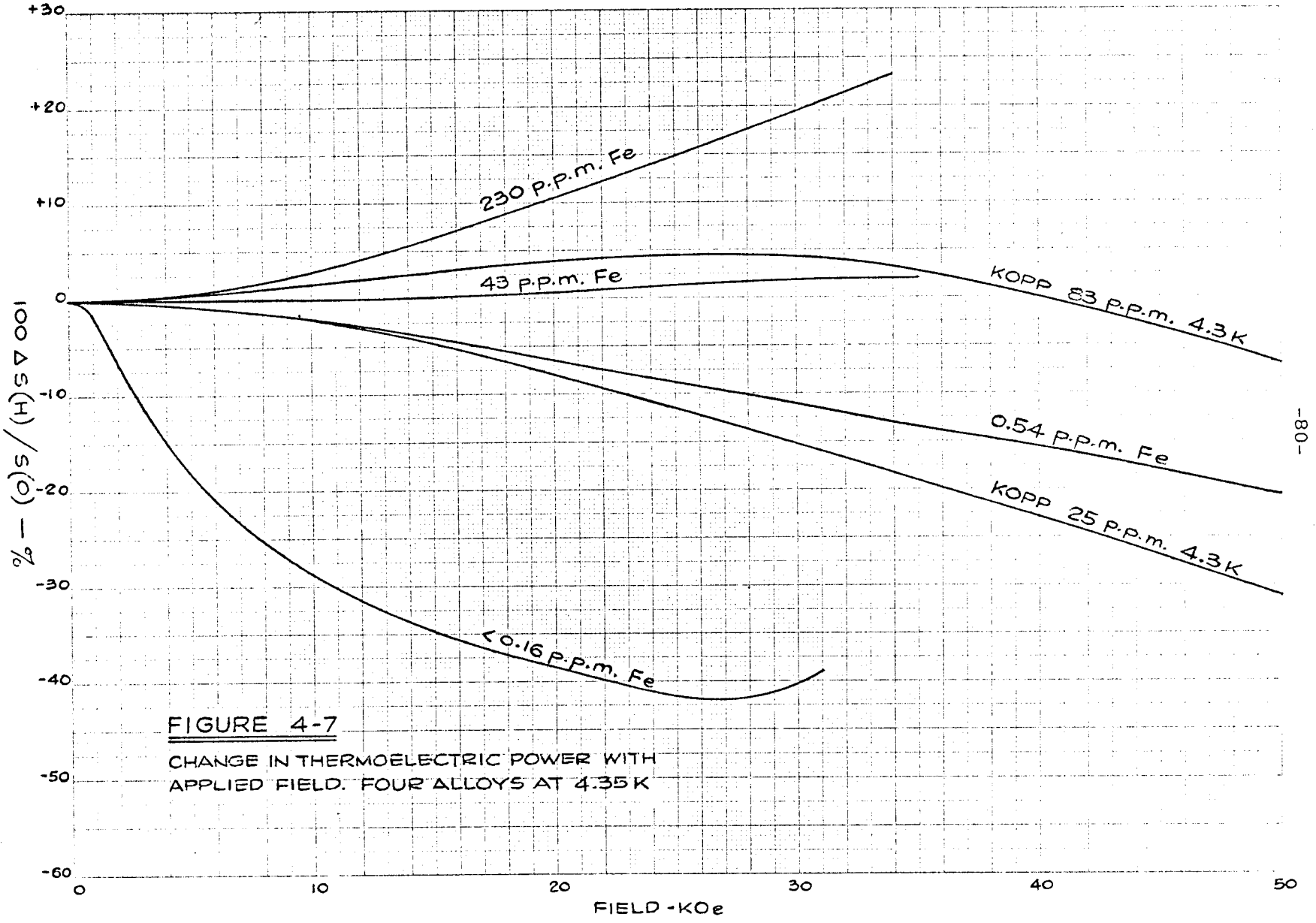

FIGURE 4-7

CHANGE IN THERMOELECTRIC POWER WITH APPLIED FIELD. FOUR ALLOYS AT 4.35K

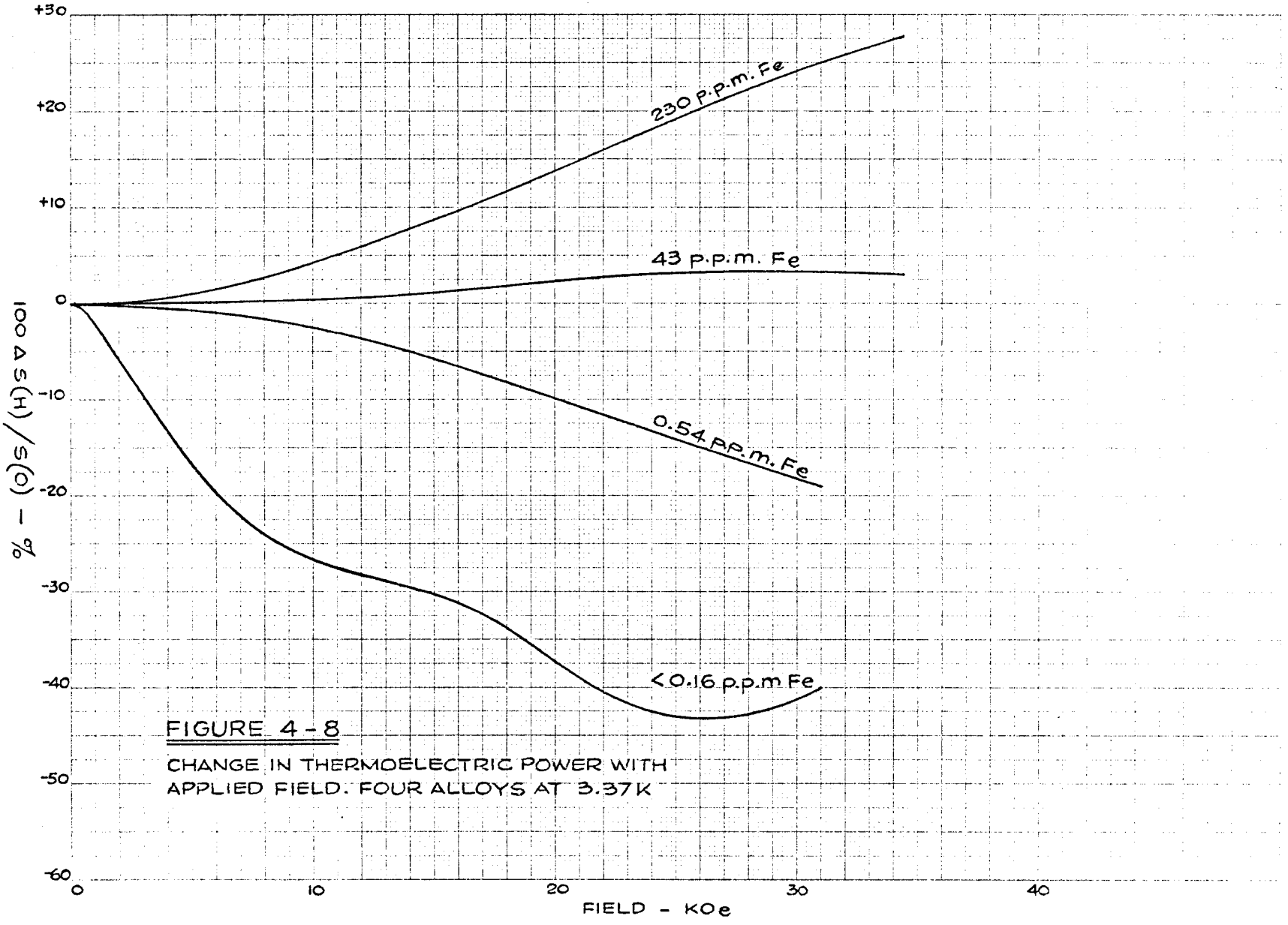

FIGURE 4-8

CHANGE IN THERMOELECTRIC POWER WITH APPLIED FIELD. FOUR ALLOYS AT 3.37K

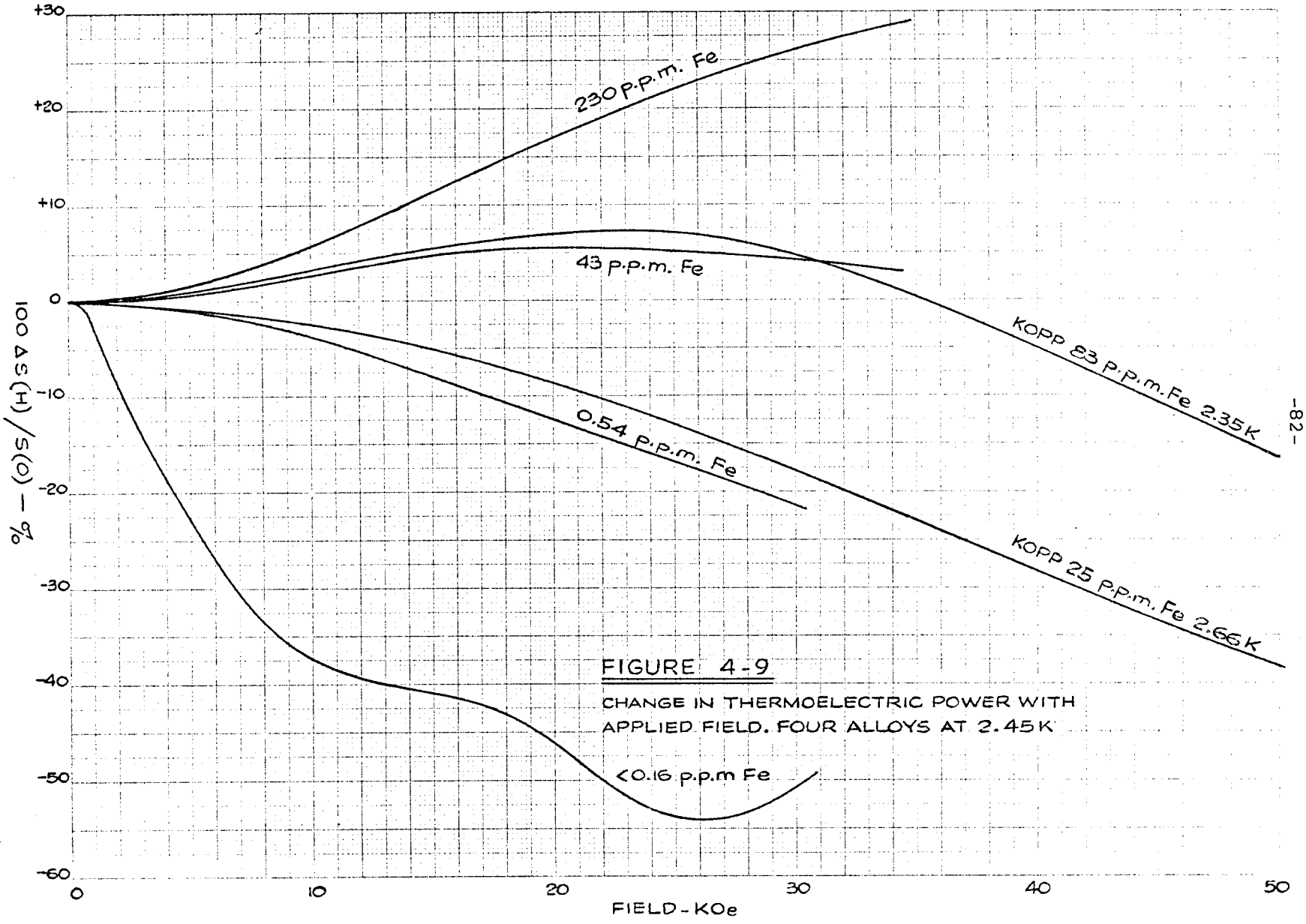

FIGURE 4-9

CHANGE IN THERMOELECTRIC POWER WITH APPLIED FIELD. FOUR ALLOYS AT 2.45K

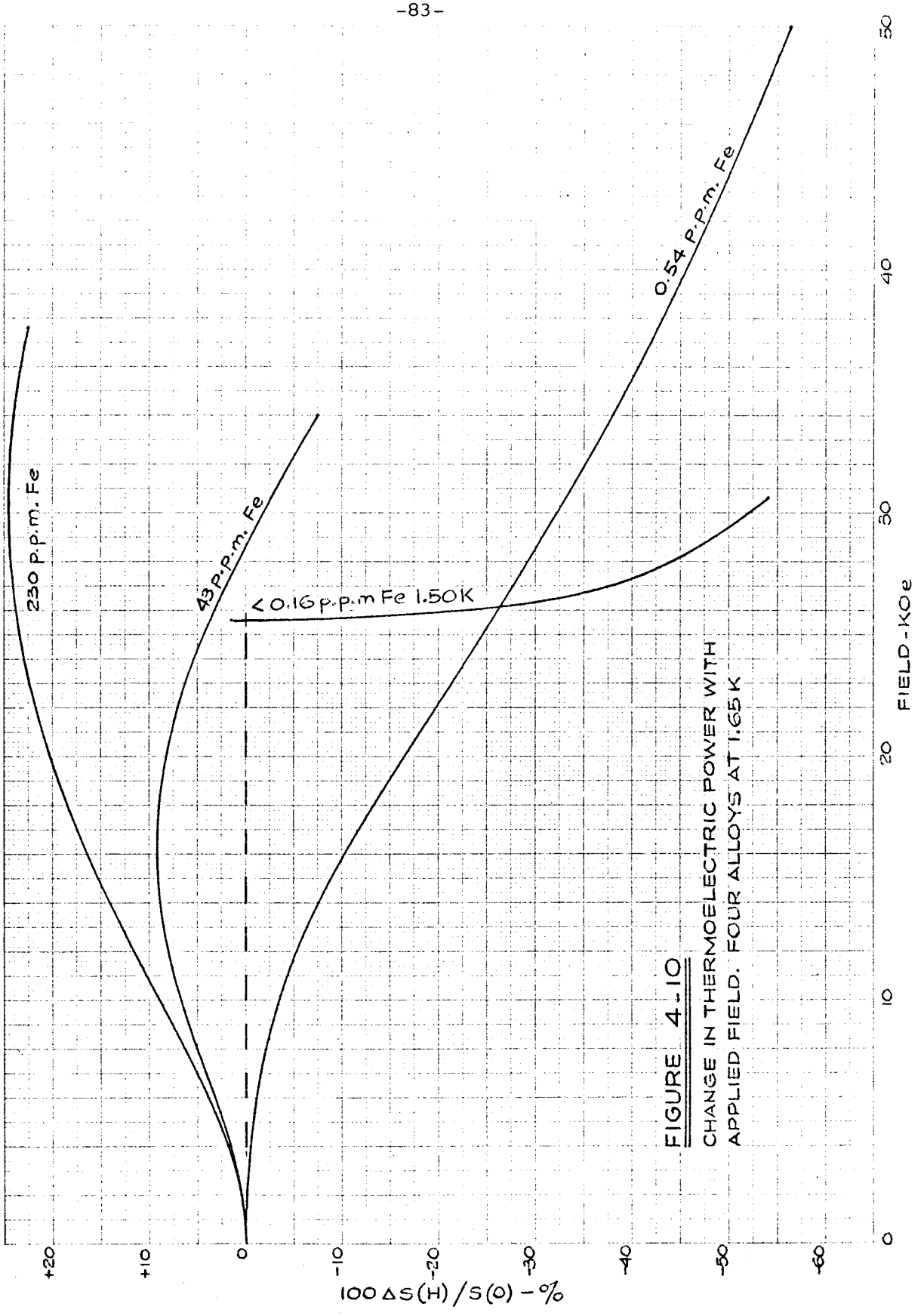

FIGURE 4-10

CHANGE IN THERMOELECTRIC POWER WITH APPLIED FIELD. FOUR ALLOYS AT 1.65 K

and the approximate $H/_T$ dependence has accordingly been used to adjust the measured curves to the chosen temperatures by adjusting the field value H by an amount $\delta H = H\, \delta T/T$ where δT is the difference between the temperature T of the measurement and one of the chosen temperatures. It can be shown by comparing two experimental curves at different temperatures that the δH adjustment computed in this way is correct to within 15%, so that with δT less than 3%, the overall error resulting from the adjustment is less than 0.5%. For the 0.54 p.p.m. atomic Fe alloy below 2K, measurements were not made at, or close to one of the chosen temperatures but at 1.725K and 1.46K, about equally spaced above and below the chosen temperature of 1.56K. Adjustments to 1.56K have accordingly been computed separately from each of the two measured temperatures using the δH approximation and a mean curve has been drawn between them. This mean curve differs from each of the two computed curves by only $\pm$ 1.2%.

In drawing the curves of figs.4.7 to 4.10, other adjustments have also been made to eliminate what is believed to be an anomalous effect due to the presence of Pb in our alloys; the chemical analysis reported in table 3.2 showed between 10 and 20 p.p.m. atomic Pb in the original alloy. Reference has already been made to the peculiar form of our curves for the 43 p.p.m. atomic Fe

alloy as shown in fig.4.4, but the effect is seen most strikingly in our curves for the 230 p.p.m. alloy, although its magnitude here is much smaller. At 6.85K, 4.30K and 3.36K in the 230 p.p.m. alloy it appears as a small initial negative excursion of $\Delta S(H)/S(o)$ at very low fields; this is shown more clearly in the expanded plots of fig.4.11. The effect is still discernible at lower temperatures as seen at (d) and (e) in fig.4.11, but appears as an inflection in the curves rather than a negative minimum. It is possible that this anomaly is merely an apparatus effect, but if so, it should appear unchanged in all our curves, both for the other Au-Fe alloys and for the Cu-Fe, the Rh-Fe and the Au-Ce alloys; it was looked for in these but could not be seen. If, on the other hand, it was a genuine effect due to the Fe in the Au it should have been noticed by other workers in the field, notably at Oxford where it was looked for but not seen (Kopp - private communication). We are led, therefore, to suspect an impurity present only in our alloys, although we must recognise that the effect, as seen in the 230 p.p.m. atomic Fe alloy has a maximum magnitude of only 0.26%, whereas most of the Oxford measurements only had a precision of 1% and their limit of detection was reported to be ¼%. The effect is clearly seen in our data for this alloy because we had a

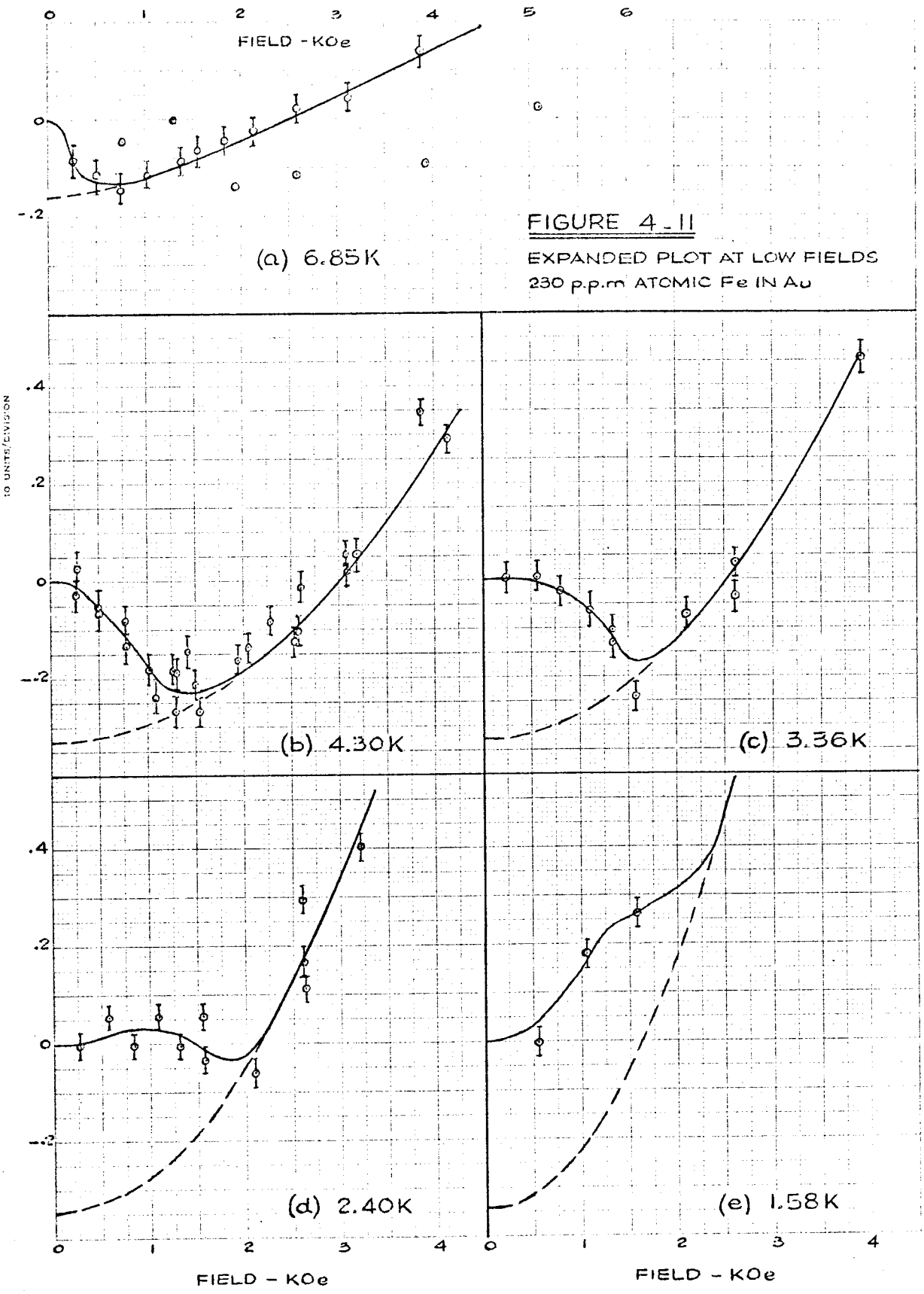

FIGURE 4-11

EXPANDED PLOT AT LOW FIELDS
230 p.p.m ATOMIC Fe IN Au

precision of 0.1% and a limit of detectability of 0.02%. In the more dilute alloy, however, containing 43 p.p.m. atomic Fe, the anomaly has a magnitude of about 10% and this could not have been missed at Oxford. Furthermore, we would not expect an effect due to Fe to increase in size by nearly two orders of magnitude when the Fe concentration was decreased.

In order to analyze the anomaly, we note that the field dependence of the thermoelectric power can be represented by a general formula of the form

$$\Delta S(H)/S(o) = \alpha + \beta H^2 + \gamma H^4 + \delta H^6 + \text{----} \quad (4.1)$$

where α, β, γ, δ etc. are constants at any one temperature. Odd powers of H are excluded because the thermoelectric power is independent of field direction. At sufficiently low fields the first two terms must dominate and, in fact, we find for all the curves in fig.4.3., except the one at 6.85K, that their early parts, up to fields of about 5 KOe, closely fit a simple quadratic if we exclude the region at very low fields where the anomalous negative dip occurs. The extrapolations of these simple quadratic forms to H = o have been added as dashed curves to fig.4.11. The curve at 6.85K was obtained with a rather large heat input to heater h_1, which produced a 3.1K temperature drop along the length of the specimen and this distorted the simple

quadratic form. From fig.4.11 it can be seen that the small anomalous dip has the character of a small step change with a magnitude of 0.33%, except again for the curve at 6.85K, where it appears to be about half as big. The steps occur near a critical field H_c which is a function of temperature. The steps are not sharp but extend over a range of field strength about H_c, which has been chosen at the point where the step is half complete. A sharp change with field would not be expected because the field of the superconducting magnet used in these experiments was only constant within 0.1% over a 1 cm. cube and so varied somewhat over the length of the alloy specimen which was nearly 4 cm. long. Also, there was a temperature drop of about 0.2K along the length of the specimen in all except the run at 6.85K, as noted above. These effects, however, could not wholly account for the spread. In fig.4.12 we have plotted H_c directly against T and from this it appears that H_c will tend to zero a little above 7K. The effect will therefore disappear above this temperature. The effect thus has the unmistakable character of a superconducting transition in Pb which, according to Franck and Martin (1961) occurs in zero field at 7.193K. The only questions are whether Pb present in an alloy to the extent of only a few parts per million can exhibit superconducting behaviour and, if so, what do our results mean in terms of its

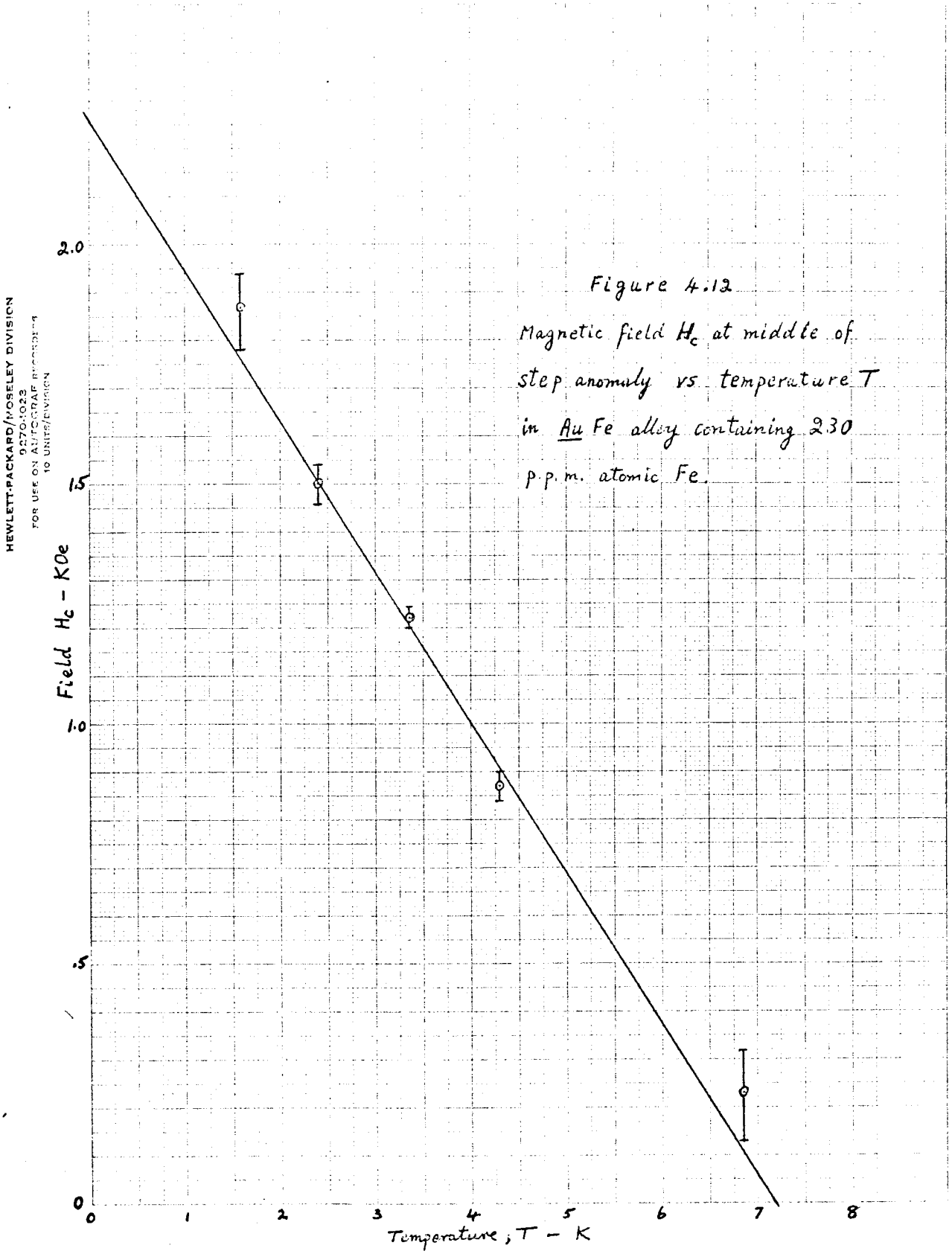

Figure 4.12

Magnetic field H_c at middle of step anomaly vs temperature T in Au Fe alloy containing 230 p.p.m. atomic Fe.

effect on the electron scattering. Part of the answer is provided by Hansen (1958), who states that Pb is completely insoluble in Au below 500°C, so that even if the alloy was quenched from above this temperature some of the Pb would likely be present as separated occlusions in the Au, and in our 43 p.p.m. atomic Fe alloy which was cooled slowly from 850°C, virtually all the Pb would undoubtedly separate. Thus, we can be reasonably certain that our samples contained separated Pb metal. Below 7.19K in zero field, this separated Pb would be superconducting and when the field H_c was applied, or the temperature was raised above 7.19K, the Pb would go normal.

If the quantity of separated Pb present had been sufficient to produce macroscopic superconductivity its effect would have been to short out all, or part of the thermoelectric voltage, so that on going normal the observed thermoelectric voltage would increase. Clearly this was not the case, and would scarecly be expected with as little as 10 to 20 p.p.m. atomic Pb distributed throughout the Au. It is conceivable that the presence of superconducting Pb could affect the electron scattering in such a way as to change directly the thermoelectric power of the Au Fe alloy, but it seems more likely that the effect on the measured thermoelectric power was due to a resistivity change. The direction of the observed

change means that in the superconducting state the Pb contributes less to the resistivity of the alloy than when it goes normal.

To understand this we need to know how the separated Pb will contribute to the electron scattering in the Au. When normal, its effect must be essentially that of boundary scattering at each interface between Au and Pb and so may well depend on how the Pb is distributed. Thus, a small number of large occlusions should have less effect than a large number of small ones for the same total concentration of Pb. When the Pb is superconducting, the same boundaries exist separating normal and superconducting material and they will still scatter the conduction electrons: the difference, according to theory communicated to us by Bardeen, is that those electrons which are scattered at the boundaries are totally reflected as holes and so make no resultant contribution to the electrical resistivity.

We can verify that the 10 to 20 p.p.m. atomic Pb known to be present in the alloys was sufficient to produce changes of the observed magnitude if we assume that in the superconducting state the separated Pb makes no contribution to the resistivity of the alloy and that in the normal state it contributes to the electron scattering to the same extent as

when dissolved in Au. In the 230 p.p.m. alloy the total residual resistance ratio was .1160, so that a reduction of 0.33% in $S_{measured}$ would be produced by an added resistance ratio increment of .00038: this would be produced by only 2.8 p.p.m. atomic separated Pb if it contributed to the electron scattering to the same extent as when dissolved in Au. Since the alloy contained over 10 p.p.m. atomic Pb it is probable either that it was present in a small number of large occlusions, which would contribute less to the electron scattering than if it was dissolved, or that much of it was quenched in solution and so did not contribute to the anomaly.

For a superconducting transition in bulk material we might expect H_c to be proportional to T^2 since the formula

$$H_c = H_o \left(1 - \left(\frac{T}{T_c}\right)^2\right) \qquad (4.2)$$

is approximately true in some cases, where H_o is the critical field at T = 0K and T_c is the transition temperature at zero field. In our alloys, however, it seems certain that the Pb occlusions will be small enough that their dimensions are less than the London penetration depth λ . The critical field will therefore be a function of these dimensions and so will vary from one particle to another. Also, since λ is a function of

temperature, the resultant relation to be expected between T and H_c is uncertain. The experimental points in fig.4.12 indicate that the relationship is linear. Extrapolation to T = 0K indicates a critical field H_o at zero K of about 2.3 KOe, which is considerably larger than the value for bulk Pb of about 0.75 KOe. The London theory indicates that the enhancement of the field should be on the order of λ/R, where R is the radius of the superconducting filaments or particles, but Tinkham (1958) has shown that this should probably be $\lambda \xi^{1/2}/R^{3/2}$ where ξ is Pipard's coherence length. Bean et al (1962) studied this question experimentally by forcing Hg into pores of about 30 Å radius in Vycor glass. They found enhancements greatly exceeding those predicted by the London theory and more likely to agree with Tinkham's formula.

Turning now to the 43 p.p.m. Fe alloy, examination of fig.4.4 clearly shows the existence of the same anomalous features as the 230 p.p.m. alloy with initial negative dips followed by a rise to a maximum, but the initial drops are much larger and extend to higher fields; the curves also have the same basic character that the steepest drops occur at progressively higher field strengths as the temperature is lowered. Analysis along the lines used above for the 230 p.p.m. alloy

is not possible and exact interpretation of the curves must await the development of an exact theory for the true form of the S_{Fe} vs H dependence. In the meantime, it is evident from the 4.39K curve in fig.4.4 that the extrapolation to zero field in the absence of the anomaly must be to $< -9.5\%$ on the vertical axis because the measured curve has a minimum at this value. At the same time, the subsequent maximum in the measured curve is quite shallow, so that the zero field intercept cannot be much less than -9.5%. We have added dashed line extrapolations which seem intuitively reasonable to fig. 4.4 and these intercept the vertical axis at -10.2%. These curves,with the anomalous dips removed, are plotted in figs. 4.7 to 4.10. Since the residual resistance ratio of this alloy was .0194, an anomalous decrease in $S_{measured}$ of 10.2% would require an added resistance ratio increment of .00220, which would be produced by 16.2 p.p.m. atomic separated Pb if its contribution to the electron scattering was the same as for dissolved Pb. This is larger than was found for the original alloy, but after the Cl_2 treatment at 850°C when the Pb would dissolve, the alloy was cooled quite slowly to room temperature and during this time all the Pb not removed by the treatment would separate out. Since its diffusion rate would be greatly reduced as the temperature dropped, the Pb would remain

finely divided in a large number of small occlusions. Analysis of the critical fields H_c along the same lines as used for the 230 p.p.m. alloy gives $H_o \simeq 9$ KOe with a spread of the transition to at least 15 KOe, in agreement with the above conclusion that the Pb was present in smaller occlusions.

The curves of fig.4.5 for the 0.54 p.p.m. Fe alloy have the same initial steep negative slope which decreases at higher fields and again the point at which the slope is steepest moves to higher fields as the temperature is lowered. The anomaly, therefore, still appears to be present but it is less sure and the curves are even less readily analysed as there are no longer any maxima. Again, the curve at 4.37K is useful in setting an upper bound because between 15 KOe and 40 KOe the experimental points lie on a straight line and it is plausible that the anomaly produces the steeper slope below 15 KOe. Continuation of the straight line portion to zero field gives an intercept with the vertical axis at -14% and the true intercept must be below this, unless our interpretation is incorrect. Dashed extrapolations have been made to have a horizontal tangent at zero field and to be smooth extensions from the straight line portions of the experimental curves.

They are also in agreement with the theory of Weiner and Beal-Monod (1970), as discussed in the next chapter. The resulting intercept with the vertical axis is at -17% and the anomalous change in $S_{measured}$ due to the Pb is therefore assumed to be 17% in this alloy. The residual resistance ratio in this alloy was .001844, so that the assumed 17% decrease in $S_{measured}$ would be produced by an added resistance ratio increment of .00038, giving a separated Pb content of 2.8 p.p.m. atomic, on the same basis as assumed for the other alloys. Since this alloy was treated with Cl_2 for 8 hours at 850°C, it is to be expected that its Pb content would be reduced since $PbCl_2$ boils at 950°C and so would be expected to have an appreciable vapour pressure at 850°C. Again, in plotting figs. 4.7 to 4.10, the dashed extrapolations have been used to remove the anomalous dips. The decrease in the Pb concentration from that of the 43 p.p.m. atomic Fe alloy with the extra 5 hours Cl_2 treatment yields a value of 2×10^{-10} $cm^2/sec.$ for the diffusion coefficient of Pb in Au, which is not unreasonable. If the initial steep drops found for the 0.54 p.p.m. alloy are not due to Pb anomaly, this diffusion coefficient would have to be much larger and would indicate too high a Pb concentration in the original 230 p.p.m. atomic Fe alloy. Nevertheless,

the existence of the low field anomaly in this very dilute alloy is in doubt, since the adjusted curves for this alloy in figs. 4.7 to 4.10 are not entirely compatible with the others, but the evidence is inconclusive. Additional information which is pertinent to this question comes from our attempts to make Au Ce alloys, as reported in Chapter 7, but this is also inconclusive. These alloys were made by adding Ce to gold wire obtained from a different source - 99.9999% pure gold from Cominco - which did not contain Pb; nevertheless, the magnetic field curves obtained for them are essentially identical to the measured curves for the 0.54 p.p.m. Fe alloy before adjustment, as shown in fig.4.5. The Cominco Au wire was also free of Fe and it has therefore to be assumed that up to about 2 p.p.m. atomic Fe was introduced via the Ce; it is entirely possible that some Pb was also introduced by the same mechanism.

It seems reasonably certain that the anomalous dips observed at low fields in the 230 p.p.m. and 43 p.p.m. atomic Fe alloys, and seen in figs. 4.3, 4.4 and 4.11, were due to superconducting transitions occurring in a few parts per million of Pb present as separated occlusions in the Au alloy. It is remarkable that superconducting behaviour can be exhibited in such finely divided Pb, present in concentrations

of only a few parts per million. This behaviour was not, of course, observed macroscopically as superconductivity and was observable only through secondary effects of the electron scattering. It might be termed microscopic superconductivity.

While some doubt may be felt to exist as to the correct interpretation of the anomaly, there is little doubt that an anomaly does exist and we can have reasonable confidence in the correctness and accuracy of the adjusted curves as given in figs. 4.7 to 4.10. Thus, in the 230 p.p.m. alloy, the anomaly has a peak magnitude of only 0.26% and since it has been analysed as shown in fig. 4.11 to within better than 10%, any residual error in our curves for $\Delta S(H)/S(o)$ is entirely negligible. In the 43 p.p.m. alloy the magnitude of the anomaly is believed to be 10.2% with outside limits on this of $\pm$0.7%; it thus contributes a possible error of less than 1% to the curves for this alloy in figs. 4.7 to 4.10. Only for the curves of the 0.54 p.p.m. alloy is there any appreciable doubt and these curves should be repeated with an alloy of higher purity and preferably with apparatus designed to give higher sensitivity. Allowance must also be made in these very dilute alloys for the effect of the negative magnetoresistance component due to Fe in Au; this negative component

was measured by Berman et al (1964) and becomes an appreciable factor (of the order of 10%) at this dilution, at which the Fe no longer dominates the scattering. The accurate determination of the negative magnetoresistance component as it exists in very dilute alloys is not entirely straightforward, as Rohrer (1969) has pointed out, because of the effect of internal fields which change with the concentration.

The general character of the curves in figs. 4.7 to 4.10 conforms well to the theoretical predictions of the impurity pair model of Huntley and Walker (1969) and to some of the predictions of the theory of Weiner and Béal-Monod (1970); this will be examined more closely in the next chapter. The curves also appear to agree reasonably well with results reported by Kopp (1969), although there are differences. Two of Kopp's curves for each of two of his alloys containing nominally .01 at.% Fe and .003 at.% Fe are included in figs. 4.7 and 4.9. For comparison with our curves based on our Ottawa analysis, these are labelled 83 p.p.m. and 25 p.p.m. atomic Fe respectively. As the field is increased, Kopp's curves drop off faster than would be expected according to our data, but in comparing his curves with our 230 p.p.m. and 43 p.p.m. curves, this trend can be accounted for by the probable errors of measurement, together with the larger com-

petitive scattering in Kopp's alloys which would increase the effect of magnetoresistance and cause them to drop faster at higher fields.

The relative positions in figs. 4.7 and 4.9 of Kopp's curves for 25 p.p.m. atomic Fe and ours for 0.54 p.p.m. atomic Fe are certainly not as would be expected and the discrepancies can not be accounted for by magnetoresistance and experimental error. If the data for our 0.54 p.p.m. alloy is plotted in figs. 4.7 to 4.10 as measured, instead of according to the interpretation given above, their positions relative to Kopp's curves are more satisfactory but their shapes are not. A possible explanation is that in these very dilute alloys the magnitude and number of Fe-Fe interactions are dependent on the annealing treatment which the alloy has undergone, so that their field response is a function of their thermal history. Thus, the long slow cool from 850^{o}C to room temperature which our 0.54 p.p.m. alloy received may have favoured the formation of impurity pairs. An alternative explanation is that most of the Fe in Kopp's 25 p.p.m. alloy was oxidized; the analyses which were performed for him would not differentiate between oxidized and

unoxidized Fe and, unfortunately, he does not report any other measurements which could add further information.

The curves obtained on the alloy containing <0.16 p.p.m. atomic Fe follow the main trend in falling off rapidly with applied field, but show no definite signs of a low field anomaly. The apparent oscillations in these curves are peculiar, but fall within the range of probable error for these curves so that their existence is not certain, except for the rise which appears at the maximum field in all but the curve obtained at 1.50K. The curve at 1.50K is distinctly different from all the others, with no known cause: it was obtained first with steadily increasing field and repeated, starting at maximum field. The detailed behaviour of this alloy is not understood and may be due to very small quantities of several impurities. Further investigation could only be fruitful if accompanied by careful analysis.

CHAPTER 5

THEORY

Kondo (1965) was the first to provide a theory for the giant thermoelectric power in dilute magnetic alloys using second Born approximation for the scattering amplitude. He did not explicitly allow for an externally applied magnetic field, but his result is given as a function of the field H at the impurity atom sites. Huntley and Walker (1969) showed that this could account, at least qualitatively, for the experimental results by assuming that the field H was the resultant of the externally applied field and an internal field arising from simple Fe-Fe pair interactions, and there appeared reason to expect that quantitative agreement might be achieved if the proper form for the interaction could be discovered. In this direction, the theoretical work of Marshall (1960) and of Klein (1964) appeared to offer some hope of success. This is described in more detail below.

More recently, Weiner and Béal-Monod (1970) have given a theoretical derivation explicitly for an applied magnetic field and again using the second Born approximation, but assuming no internal fields due to interaction between the magnetic impurity atoms. Their theory is therefore only

applicable to alloys in the limit of extreme dilution, or when the applied magnetic field is strong enough to swamp the effect of any internal field.

Weiner and Béal-Monod Theory and Comparison with Experiment

Only our Au alloy containing 0.54 p.p.m. atomic Fe is sufficiently dilute for the theory of Weiner and Béal-Monod to be applicable to our results. The formula which they obtain for the field dependent thermoelectric power is:

$$\frac{S(H)}{S(0)} = \left\{ \frac{1}{2S(S+1)\sinh^2\frac{\alpha}{2}} \left[\alpha\langle S_z\rangle + \frac{\alpha^2}{2}\langle S_z^2\rangle - 3\alpha^2\langle S_z\rangle^2 \right] - \frac{1}{(2\pi n(E_F)V)^2} \cdot \frac{\alpha^2\langle S_z\rangle^2}{S(S+1)\sinh^2\frac{\alpha}{2}} - \frac{\langle S_z\rangle}{\pi^2 n(E_F) J S(S+1)} I(\alpha) \right\} \frac{\rho(H)}{\rho(0)} \tag{5.1}$$

where $$I(\alpha) = \int_0^\infty du \, \ln\left|\frac{u-\alpha}{u+\alpha}\right| \frac{u}{4\sinh^2\frac{u}{2}} \left\{ 1 - \frac{u}{2}\coth\frac{u}{2} \right\}$$

and where $\alpha = g\mu_B H/KT$, $n(E_F)$ is the conduction electron density of states at E_F and $\rho(H)$ is the field dependent resistivity: they have assumed that the exchange integral J for the scattering of conduction electrons is small compared to the potential scattering integral V which, according to Kopp (1969), appears to be valid for the dilute Au-Fe alloys; he experimentally obtains the values: J= -1.0eV and V=2.4eV.

In the low field limit, $\alpha \ll 1$ this formula predicts

$$\frac{\Delta S(H)}{S(o)} \propto -M^2 \qquad (5.2)$$

where M is the magnetisation, which at sufficiently low fields must be proportional to H and in the high field limit, $\alpha \gg 1$

gives $$\frac{S(H)}{S(o)} \propto \frac{T}{H} \qquad (5.3)$$

Weiner and Béal-Monod indicate that they expect the low field proportionately to $-M^2$ to be valid up to $g\mu_B H/KT < 1$ and the high field condition to be good for $g\mu_B H/KT > 2$.

All our curves for the alloy containing 0.54 p.p.m. atomic Fe as given in fig. 4.5 are swamped in the low field region by the low field anomaly and we are not able to remove it precisely by independent means, so that comparison with theory in this region is not possible. Instead, we have assumed the Weiner and Béal-Monod theory to be correct and have drawn the dashed extensions in fig. 4.5 to be in conformity with an H^2 law. This sets the zero field intercept at $100\ \Delta S(H)/S(o) = -17.0 \pm 1.0\%$.

In the high field region our curve for the 0.54 p.p.m. alloy obtained at 1.46K provides the best comparison with the theory and here the effect of the low field anomaly is

less important. This curve has been replotted in fig. 5.1 against $1/H$ with the low field anomaly removed by adding 17.0% to the experimental values of $100\ \Delta S(H)/S(o)$. Our experimental points have been included in this figure, which clearly shows the linear $1/H$ dependence as predicted by Weiner and Béal-Monod above a field of about 35KOe (which corresponds to $\alpha \simeq 3$). Note that the extrapolation of the straight line portion of our curve passes through the origin indicating zero S at infinite applied field.

Our data on the 230 and 43 p.p.m. atomic Fe alloys all show effects which are thought to be due to Fe-Fe interactions and to fairly strong fields of internal origin. Since our applied fields were not high enough to swamp these, we can not compare our results on these alloys with the theory of Weiner and Béal-Monod.

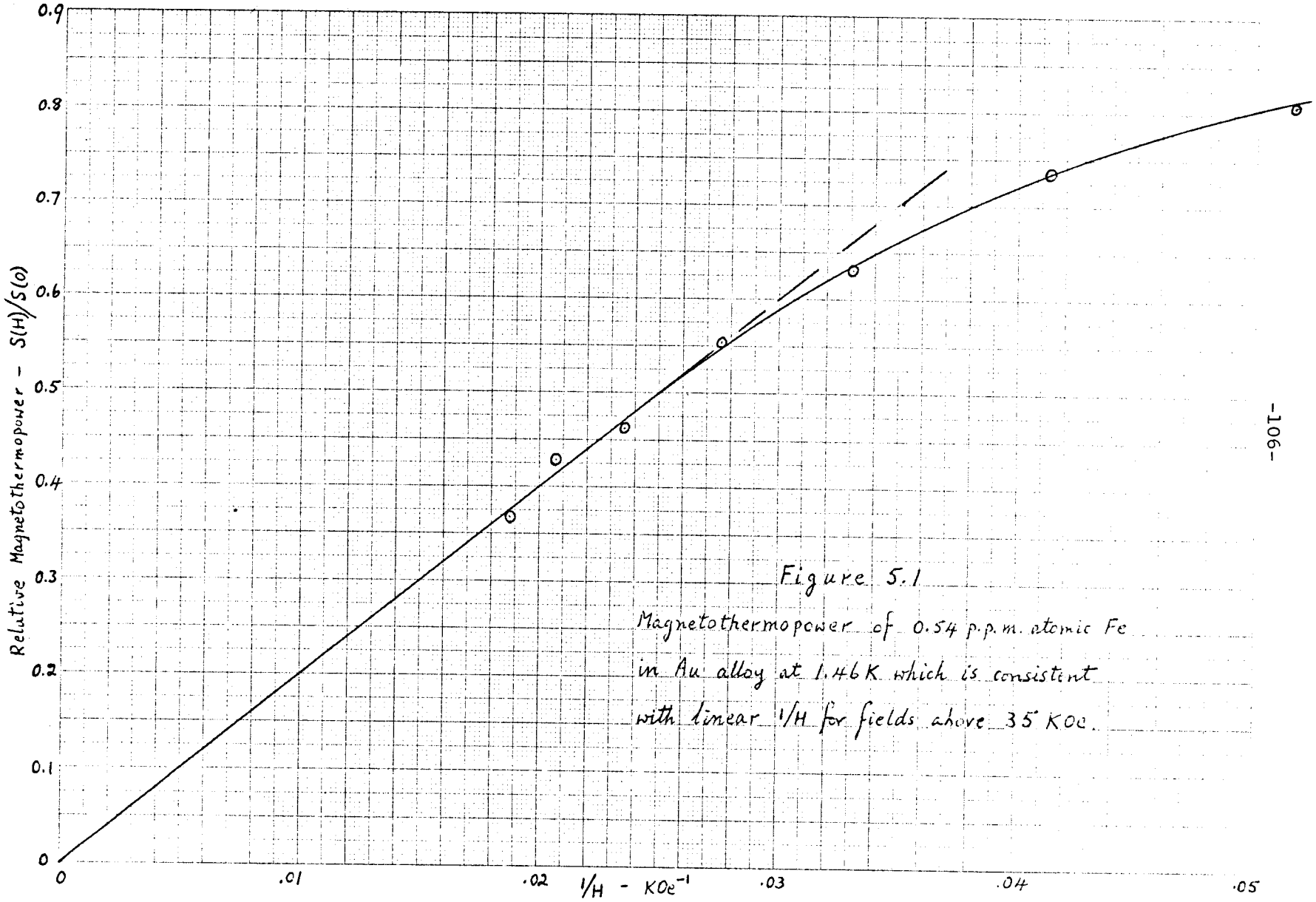

Figure 5.1

Magnetothermopower of 0.54 p.p.m. atomic Fe in Au alloy at 1.46 K which is consistent with linear 1/H for fields above 35 KOe.

Kondo Theory with Pair Interaction Model and Theories of Marshall and Klein

Kondo's (1965) perturbation calculation yielded a formula for the thermoelectric power of dilute alloys containing localised magnetic impurities which is a function of the magnetic field H at the impurity atom sites:

$$S = A \frac{\kappa}{e} \int_0^\infty \rho(2\mu_B H)\, Q_S\left(\frac{2\mu_B H}{\kappa T}\right) d(2\mu_B H) \tag{1.4}$$

He gave an explicit form for the function Q_S

$$Q_S(x) = -2\,\mathrm{cosech}^2(x/2)\left\{1-(x/4)\coth(x/2)-(x^2/8)\coth^2(x/2)\right\}$$
$$+\left\{4S(S+1)\right\}^{-1}\left\{\coth(x/2)-(2S+1)\coth\left((2S+1)x/2\right)\right\}$$
$$\times\left[-6\coth(x/2)\,\mathrm{cosech}^2(x/2)\left\{1-(x/12)\coth(x/2)-(x^2/12)\coth^2(x/2)\right\}\right.$$
$$\left.+3\,\mathrm{cosech}^4(x/2)\left\{1+(x/4)\coth(x/2)\right\}\right] \tag{5.4}$$

and the constant A he gave as

$$A = 4\pi^2\left[n(E_F)\right]^2 V J \left(R_{mag}/R\right) \tag{5.5}$$

where R_{mag} is the resistivity component due to scattering by the exchange interaction alone and R is the total resistivity, so that in the absence of other scattering centres

$$R_{mag}/R = J^2 S(S+1)/\left\{V^2 + J^2 S(S+1)\right\} \tag{5.6}$$

Kondo says nothing about the field distribution function $p(2\mu_B H)$ and a suitable form for this has been the source of some speculation. Berman et al (1968) assumed a three dimensional random distribution of the impurity spins with a reflected Gaussian distribution for $p(H)$, centred at an average field H_o and with a width mH_o so that:

$$p(H) = \frac{1}{\sqrt{2\pi}\, m H_o}\left[\exp\frac{-(H-H_o)^2}{2(mH_o)^2} + \exp\frac{-(H+H_o)^2}{2(mH_o)^2}\right] \qquad (5.7)$$

but no values of m and H_o could be found which would yield a fit to the observed data of S vs T with zero applied field and no value of applied field would produce an increase in S, as observed at all temperatures for the alloys containing more than 100 p.p.m. atomic Fe.

Huntley and Walker (1969) considered the effect of impurity Fe atoms interacting in pairs, producing an internal field H_i at each atom which was either parallel or anti-parallel to an applied field H (an Ising model). There are four possible states for such a system with energies as shown in fig. 5.2. The resultant field at one of the Fe atom sites is $H + H_i$ with probability P_+ and is $H-H_i$ with probability P_-. Using the canonical distribution for the states, these probabilities are given by:

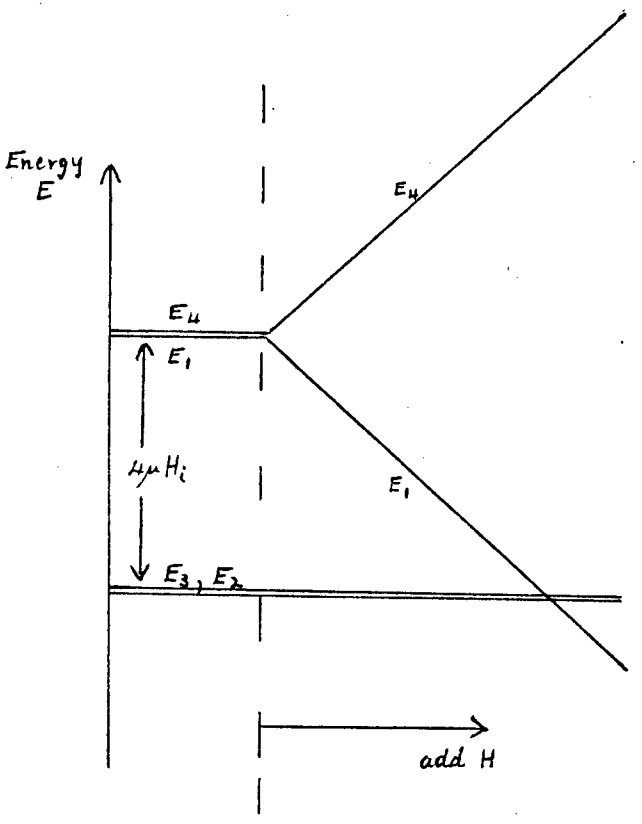

Fe_1	Fe_2
Both spins parallel to external field H	
$E_1 = +\mu H_i - \mu H$	$+\mu H_i - \mu H$
$E_2 = -\mu H_i - \mu H$	$-\mu H_i + \mu H$
$E_3 = -\mu H_i + \mu H$	$-\mu H_i - \mu H$
Both spins antiparallel to external field H	
$E_4 = +\mu H_i + \mu H$	$+\mu H_i + \mu H$

Figure 5.2

Spin energy states in an internal field H_i with added external field H. — Ising model.

$$p_+ = \left(e^{x_i} + e^{-x-x_i}\right) \Big/ \left(2e^{x_i} + e^{-x-x_i} + e^{x-x_i}\right)$$

$$p_- = \left(e^{x_i} + e^{x-x_i}\right) \Big/ \left(2e^{x_i} + e^{-x-x_i} + e^{x-x_i}\right) \qquad (5.8)$$

where $x = 2\mu_B H/KT$, $x_i = 2\mu_B H/KT$ and positive values of x_i apply to antiferromagnetic coupling.

Kondo's theory for the thermoelectric power then gives

$$S(H,T) = S_0 \left\{ p_- Q_S(x-x_i) + p_+ Q_S(x+x_i) \right\} \qquad (5.9)$$

in which we choose the value of Q_S for $S = \frac{1}{2}$, as indicated by Du Chatenier and Miedema (1966) to be appropriate for Fe in Au. For $S = \frac{1}{2}$ equation (5.4) simplifies to

$$Q_{1/2} = (x^2/12)\,\mathrm{cosech}^2(x/2)\left\{1 + (4/x)\tanh(x/2)\right\} \qquad (5.10)$$

This simple model gave the set of curves shown in fig. 5.3 for different values of H_i which qualitatively have the essential features of our experimental curves, as shown in figs. 4.7 to 4.10. They conform with the expectation that the internal field at an impurity atom should increase with concentration.

It is clear that the assumption of a single value for H_i in a given specimen is an over-simplification and that we must in fact assume some field distribution. Marshall (1960), who discusses this problem in relation to specific

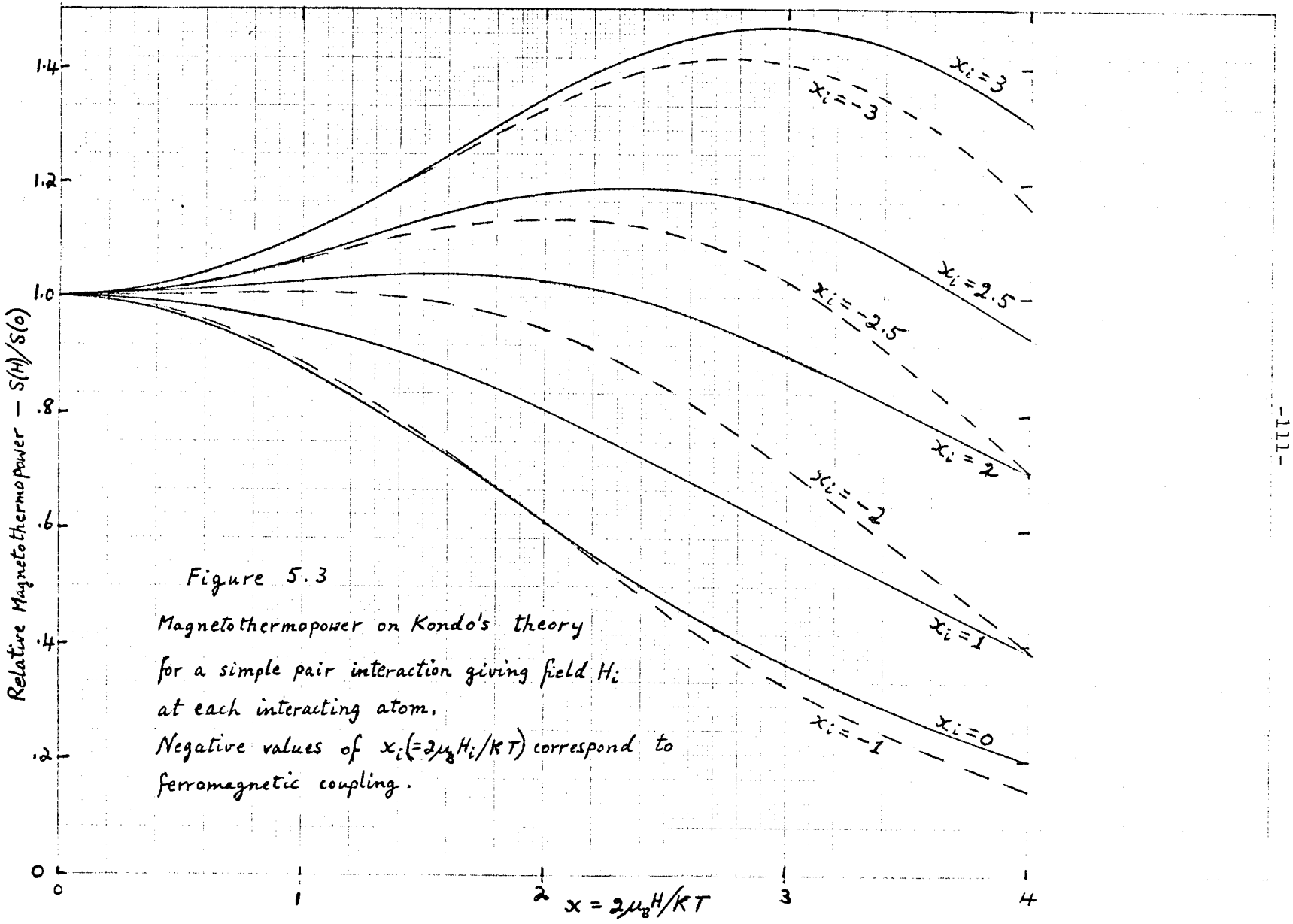

Figure 5.3

Magnetothermopower on Kondo's theory for a simple pair interaction giving field H_i at each interacting atom. Negative values of $x_i (= 2\mu_B H_i / KT)$ correspond to ferromagnetic coupling.

heat in dilute alloys, starts with a single field value as obtained in a regular lattice by the Weiss molecular field method, and shows a corresponding δ-function distribution, "a" in fig. 5.4, which is reproduced from his paper. He then modifies this to allow for fluctuations in H by using the Bethe-Peierls method which considers a central spin surrounded by r nearest neighbours whose spins may be parallel or antiparallel to the central spin (Ising model) and so contribute a total of $2r + 1$ possible values for H at the central spin; their probabilities are given by standard Bethe-Peierls theory. This distribution for H is shown as "b" in fig. 5.4, but he notes that this is only really applicable to a regular lattice and that in a dilute randomly distributed alloy there will in general be only one nearest neighbour. Marshall accordingly considers finally a modification of the Bethe-Peierls method needed to account for the non-uniform distance of near neighbours which,he says, reduces the tendency for their spin orientations to be all alike because of their non-uniform interactions with one another and with the central spin. The result is a broadening of the two peaks and a shift of their maxima toward lower $|H|$, which is shown schematically by his curve "c" in fig. 5.4. The shape of this curve is not intended

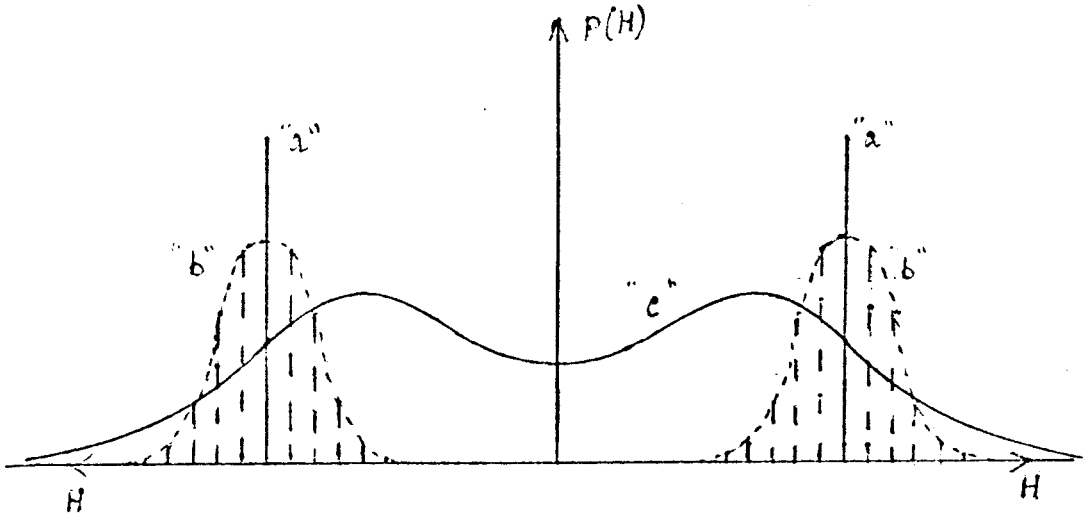

Figure 5.4

Schematic field probabilities at low T
(Taken from Marshall 1960)

for "a" Regular lattice, Weiss molecular field

"b" Regular lattice, Bethe-Peierls model.

"c" Dilute alloy.

to be a precise prediction but he does envisage a substantial value for p(H) at H = 0.

Klein (1964) makes a more precise calculation of a distribution curve like "c" of fig. 5.4 in which he assumes a Ruderman-Kittel (1954) - Yosida (1957) fluctuating potential as the interaction mechanism between the magnetic impurity atoms in an Ising model. Following a statistical theory developed by Klein and Brout (1963) for dilute ferromagnets which assumes that no long-range order exists in the solid, he divides the space around the central spin into an inner and an outer part which contribute components H_1 and H_2 respectively to the field at the central spin. Any impurity atom in the alloy can, of course, be this "central" one and none are peculiar. The inner part encompasses the magnetic impurity atoms whose spins are correlated with the central spin and has a radius R_c given for T = 0 by:

$$R_c \approx 0.51\ c^{-1/3}\ d \qquad (5.11)$$

This is obtained from a self consistent calculation of the spin correlation function for spins at large distances from the origin and R_c is the radius at which the correlation falls to zero; d is the lattice constant and c is the magnetic impurity concentration. Most of the field at the

central spin comes from the magnetic impurity atoms which are located within the inner part and whose spins are closely correlated with the central spin. Klein concludes that there are, on the average, about 2.3 of these other impurity atoms in the inner volume. It can be seen from equation (5.11) that this volume increases as the alloy concentration decreases so as to keep this average number of closely correlated spins constant. Klein assumes that the impurity atoms are all located on regular lattice sites of the host metal and hence that the field component H_1 at the central spin has a limited number of discrete values, giving a discrete probability distribution $p(H_1)$ for H_1.

The spins in the outer region make only a small contribution to the field at the central spin because their effect is largely screened out by the fluctuating potential. Furthermore, they are uncorrelated with the central spin and are randomly oriented with respect to it. A statistical model due to Margenau and Watson (1936) is therefore used to obtain a continuous distribution $p(H_2)$ for H_2.

The two field components H_1 and H_2 are taken to be approximately independent random variables and the probability distribution $p(H)$ of the total field is therefore obtained by the convolution of the two probability distributions $p(H_1)$

and $p(H_2)$. Since the spins located in the inner volume contribute a large spread in effective fields, whereas the outer volume contributes comparatively little, the character of the total probability distribution p(H) is primarily determined by the inner region and the outer region serves only to make the distribution continuous by filling in the gaps between the discrete values of H_1. Like Marshall, Klein obtains a substantial value for p(H) at H = 0, with even smaller humps on either side than shown in fig. 5.4.

At this point it is important to consider the experimental evidence.

Experimental Evidence and Critique of Theories

In principle, the internal magnetic field in an alloy can be determined in a Mössbauer experiment, as pointed out by Marshall et al (1964), although the interpretation is not entirely straightforward. Mössbauer experiments on dilute alloys of transition elements in noble metals have been reported by a number of workers, including Marshall et al (1964), Borg et al (1963), Henry (1963), Gonser et al (1965), Window (1967,b, 1969), Window and Johnson (1969), but all of these have been at concentrations of the transition element between 0.5 and 5 at.%, which is several orders of magnitude

higher than in the experiments reported here. Furthermore, it has become apparent that in the present state of theoretical development, the results obtained on one system, for example Cu Mn, can not be used to predict expectations for another system such as Cu Fe. Nevertheless, some important facts emerge.

Window (1967a,b) performed Mössbauer experiments on a number of alloys, including Au Mn, Au Cr, Au Fe, Au Co, Au V, Ag Mn and Cu Mn, in the concentration range 3.5 to 6 at.% and found internal fields of the order of 100 KOe in all except the Au Co and Au V: in these two,the experiments indicated no internal fields but the precision was such that fields <8 KOe could have been present. He gives more complete details of his results on Au Mn containing 5 at.% Mn (see Window, 1967a). For this he used ^{119}Sn at less than 1 at.% to determine the field distribution,and the best fit to his experimental points showed a zero probability for field strengths below 17 KOe, in marked contrast to the distributions proposed by Marshall and by Klein. Window comments that his experimental results appear to certainly indicate either ferromagnetic order extending over greater distances than is expected on Ruderman-Kittel-Yosida theory, or a long wavelength spiral alignment of spins. It is unfortunate that the measurement of the internal fields has

not been carried to lower concentrations,but the difficulties are considerable. The observed trends which have been reported indicate that the magnitude of the fields at the impurity site falls with concentration, as we would intuitively expect, or perhaps it is more accurate to say that the probability of an impurity atom being located in a high field decreases as the concentration decreases. Nevertheless, the experiments on the magnetothermopower of dilute Au Fe alloys reported in chapter 4, as well as those of Berman et al (1964), Berman et al (1968) and Kopp (1969) all show effects which, if they are to be explained along the lines proposed by Huntley and Walker (1969) require internal fields at the magnetic impurity sites with maxima in their probability distributions in the region of 10 to 100 KOe. It is noteworthy that at a concentration as low as 43 p.p.m. atomic Fe for which the average Fe-Fe spacing is about 20 lattice constants, the curves in figs. 4.7 to 4.10 show maxima in the thermoelectric power at fields between 15 and 30 KOe (depending on temperature), requiring maxima in the internal field distributions at about these same field values. This means either that fields of the order of 15 to 30 KOe extend out to 20 lattice constants, or that a substantial fraction of the Fe atoms are spaced much closer than the average of 20 lattice constants.

Marshall (1960) avoids any quantitative predictions for his field distribution, but the form of his curve "c" as drawn, is not adequate to explain the observed results and, in fact, the distribution which he gives at "b" (see fig. 5.4) appears more in conformity with the experimental results on the thermoelectric power of Au Fe alloys and with the field distributions reported by Window. Such a δ-function distribution which is obtained from Bethe-Peierls-Weiss theory applied to a ferromagnet has to be modified if it is to be applied to a random dilute alloy, but it seems that this modification has to be less drastic than that proposed by Klein. Klein's theory predicts double peaked distributions but the heights of the peaks above the probability at H = 0 are at least an order of magnitude too low. It is significant that any one of the experimental curves for the thermo-electric power of dilute Au Fe alloys can be fitted to within about 10% by a curve of the simple pair interaction model of Huntley and Walker (1969). For these, the δ-function peaks occur at fields of the order of 10 to 100 KOe, with zero probability of an internal field less than this. It is, of course, equally true that they can be fitted by a combination of several such curves and by a continuous distribution of such

curves, as pointed out by Huntley and Walker (1969), but it is equally evident that the resultant probability distribution for the field must be strongly peaked in the appropriate region between 10 and 100 KOe, with the probability of an Fe atom being located in a zero field being at least an order of magnitude less than the probability at the maxima of the distribution.

Both Marshall and Klein have claimed success for their theories in explaining the results of specific heat and magnetisation studies (specifically on Cu Mn), but it seems that these properties are less sensitive to the height and location of the maxima of the field distribution than are the magnetothermopowers.

An alternative explanation advanced by Overhauser (1959, 1960, 1963) for the internal fields, is that they arise from long-range antiferromagnetic coupling by linear spin density waves. This theory is equally successful in providing an explanation for the specific heat results on Cu Mn and it appears that it may be able to account for the long-range fields needed to explain our magnetothermopower measurements in Au Fe, but Marshall et al (1964) were unable to obtain good fits to their Mössbauer results in Cu Fe alloys using the Overhauser theory, and Marshall (1960) has

pointed out that the fundamental objection raised by Yosida (1957) to Zener's theory of ferromagnetism applies also to the Overauser theory, namely, that the interaction between the localised spins and the conduction electrons is treated only in first order perturbation theory, whereas the total energy change appears finally as a second order quantity in the interaction. Yosida emphasises that it is necessary to work consistently to second order.

It does not seem that a complete understanding of the origin of the internal fields is possible at this time, but measurements of the magnetothermopower of dilute alloys clearly provide a sensitive indicator and, in conjunction with the results of Mössbauer experiments, point to the need for a theory giving strongly peaked field distributions. It is possible that this may require only a modification of existing theory within the framework of the Ruderman-Kittel-Yosida interaction mechanism. It is worth noting, however, that the Ising model which was used by Huntley and Walker, as well as by Klein and by Marshall, is thought to be incorrect. A Heisenberg model, which allows for more general spin orientations, see Ziman (1964, chapter 10) is considered to be appropriate for dealing with spin interactions of the Ruderman-Kittel-Yosida type. When applied to our simple pair interaction

model for spin 1/2 particles, the Heisenberg model would give a total of four energy levels instead of three, one for antiferromagnetic and three for ferromagnetic spin alignment.

The experimental results, both on internal fields and on magnetothermopower, show a definite correlation with the Kondo temperature T_K. Thus, Au Mn alloys which have the lowest T_K show the largest internal fields in Window's Mössbauer experiments performed at 4.2K, which for Au Mn alloys is well above T_K. The internal fields were also found to be large at 4.2K in Au Fe and Au Cr alloys whose T_K is also below 4.2K, but were $<$8 KOe in Au Co and Au V, for which $T_K \sim$100K. Au Mn alloys also show the largest increase in the magnitude of their thermoelectric power with applied field as seen by Templeton and MacDonald (1961), who measured an alloy containing 0.2 at.% Mn in Au and over the temperature range 1.5 to 4K found more than 100% increase in the magnitude of the thermoelectric power in an applied field of only 8 KOe. This is larger by an order of magnitude than the effects we have observed in Au Fe alloys. In the other direction, Kopp's measurements on Au Fe alloys, which were carried to temperatures below T_K show a marked reduction both in the height of the maximum in the thermoelectric power and the strength of the applied field at which it occurs. Thus,

at 0.4K, which is below T_K in Au Fe alloys, his .03 at.% Fe alloy shows only about a 12% increase occurring at 11 KOe, whereas at 1.19K which is at, or just above T_K, the increase is 20% occurring at 22 KOe. In Cu Fe alloys whose T_K is well above 4K, our experiments between 1.5 and 4.5K as reported in the next chapter show only a decrease in thermoelectric power with applied field. This correlation with T_K is in line with the theory of Rivier and Zuckerman (1968) and others, which predicts the progressive formation of a bound state and the screening out of the magnetic impurity interaction below T_K. On the basis of this correlation we can expect an increase in the thermoelectric power with applied field in the liquid helium temperature range in Ag Mn and Cu Mn alloys, as well as in Au Cr alloys, but only a decrease in Au Co and Au V alloys.

CHAPTER 6

EXPERIMENTS ON Cu Fe ALLOYS

Previous thermoelectric power measurements on Cu Fe alloys in a magnetic field had been made by MacDonald and Pearson (1957) at concentrations of 23, 52 and 610 p.p.m. atomic Fe and up to fields of 11.8 KOe. They claimed that the changes which they observed in S due to H over this range could be accounted for entirely by the effect of magnetoresistance. It seemed desirable to extend the measurements to higher fields with better precision, to check this and see if we could detect an additional direct effect of the field on the thermoelectric power such as was observed in Au Fe alloys. If such a direct effect exists, and there seemed good reason to suppose that it should, we wished to see if it is the same as that observed in Au Fe alloys, or if the field behaviour of these dilute magnetic alloys changes on going to temperatures well below the Kondo temperature T_K, which in Cu Fe alloys was known to be well above 4K. (Daybell et al (1969) have estimated that T_K is $\approx$18K for Fe in Cu).

Magnetoresistance affects the measured thermoelectric power S_m indirectly through the Nordheim-Gorter rule,

equation (3.1) so that

$$S_m(H) = S_{Fe}(H)\frac{\rho_{Fe}(H)}{\rho_{total}(H)} \qquad (6.1)$$

In this equation, only the field effects due to changes of intrinsic scattering cross section are included. As we have pointed out, (Huntley and Walker, 1969), it is only the negative magnetoresistance component due to the effect of the field on the electron scattering arising from the s-d exchange interaction which is involved.

Preparation of Samples

As in the case of Au, we wished to prepare samples of dilute alloys of accurately known composition and containing the smallest possible amount of other impurities.

The chlorine treatment method, developed for Au alloys and described in Chapter 3, could not be used for Cu because copper chlorides are stable to high temperatures and the Cu would therefore be attacked. Nevertheless, it seemed desirable to follow the same principle as used for Au alloys, of minimizing the handling of the alloy and so, if possible, to produce it in the form of a wire by a diffusion process. It was accordingly decided to start with high purity Cu sheet, which was available in a purity of 99.999%. Fe could be deposited on the surface of this sheet by vacuum evaporation

and then uniformly distributed throughout the sheet by diffusion at a suitable temperature in vacuum. Finally, the sheet could be photo-etched into the desired form of a long conductor.

Specimens of the copper sheet 1 inch by 1/2 inch were first cleaned, to remove surface contamination, by electro-polishing. This served also to reduce the sheet thickness from its original value of .0127 cm to about .01 cm. Three such specimens were then placed in the electron beam vacuum evaporator and approximately 75 Å Fe deposited on one, 25 Å Fe on another, and none on the third, to act as a control. The three specimens were then placed in a silica tube which was first evacuated: H_2 gas was then admitted to about 1 mm. pressure and the temperature raised to 850°C. After 15 minutes the H_2 gas was pumped out and the vacuum maintained at 2×10^{-5} torr with the oven at 850°C for about 36 hours. The specimens were then annealed by gradually lowering the temperature over a period of five and a half days to room temperature.

It was noted at this stage that the control specimen had only about four or five crystal boundary lines crossing it, whereas the other two specimens had many more, the specimen to which 25 Å Fe had been added showing macroscopic

crystals of the order of 0.5 cm across and the specimen with 75 Å Fe showing crystallites of the order of 0.1 to 0.2 cm across. In both the specimens containing Fe a number of black lines were apparent, coinciding with crystal boundaries.

The final stage in the sample preparation was to mount the prepared copper foils on an insulating backing and photo-etch them, so as to produce a flat non-inductively wound coil approximately 26 cm long and approximately 2×10^{-4} cm cross section, as shown in fig. 6.1, which shows a photograph of one of them. This procedure was pure art and many attempts were made before a successful procedure was evolved. This procedure was as follows: The specimen was first cleaned by dipping in 8% HCl for 30 seconds, then dipped in full strength KOR etch-resistant solution (supplied by Eastman Kodak Company) and whirled for 30 minutes in the dark until dry. A photographic negative had been prepared with the pattern as shown in fig.6.1 by photographic reduction from an original made with 1/8 inch black tape and this negative was placed in contact with one face of the copper foil and exposed for 20 minutes at 25 inches from a tungsten lamp (Electro Optics Associates type L101). The whole of the

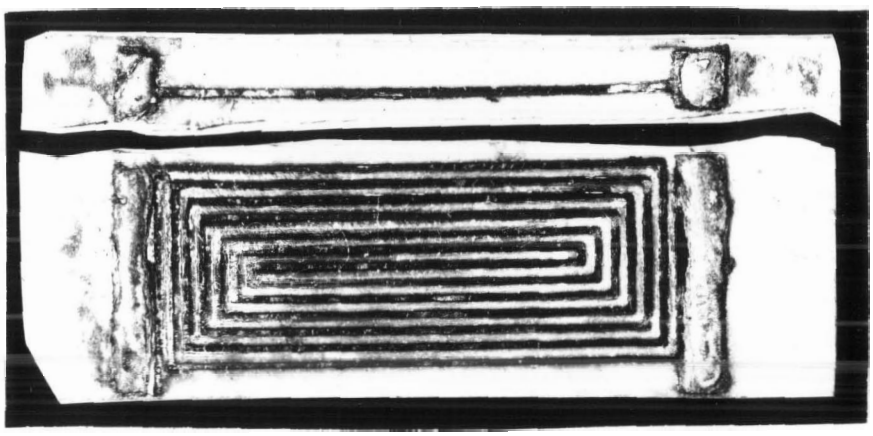

Figure 6.1

Photograph of typical Copper sample enlarged 2.6 times, showing flat ΔT coil and straight T_o specimen

other face, or back of the specimen was then exposed in the same way with no negative. The specimen was then gently shaken in Xylene for 2 minutes and spray washed with distilled water, using a power spray, to remove all unexposed KOR. The specimen was then mounted on a thin stycast lo-K plate,using just enough Eastman 910 cement to hold it, ensuring that no cement contacted the front face of the specimen. Stycast lo-K is a composite dielectric material (obtained from Emerson & Cuming Inc., Canton, Mass.) with a coefficient of thermal expansion which is not too different from that of copper. Finally, the specimen was mounted in a stirred etch solution consisting of M/5 Ammonium Persulphate with M/5 Sodium Chloride heated to about 70°C. This etch solution dissolved the Cu from areas which were not protected with exposed KOR. The etch proceeded faster near the edges of the specimen, so that it had to be removed and progressively protected inwards from the edges with additional exposed KOR to maintain a uniform cross-section for the coil conductor. The etch was complete in about 1½ hours.

It was noted that the black lines seen along the crystal boundaries, and mentioned above, were in fact more numerous than seen on the surface and were slow to etch:

some which bridged adjacent turns of the copper coils had eventually to be cut away. It was strongly suspected that they were composed of separated Fe which had come out of solution during the 5½ day slow cool from 850°C, and the results reported below on their thermoelectric power and residual resistance ratios confirm this. Hansen (1958) indicates that Fe solubility in Cu at room temperature is very low; at 200°C he gives 1.3×10^{-5}% by weight as the probable solubility.

A further three specimens were accordingly prepared, following the same procedure as above, but with ½ hour in H_2 at 850°C after the 36 hours vacuum diffusion and finally, with ½ hour in vacuum at 725°C, after which the specimens were cooled quickly to room temperature by removing the silica tube in which they were contained from the oven. These specimens did not have the black lines seen in the earlier specimens and all three had essentially the same appearance, with only a few crystal boundary marks.

Experimental Results and Discussion

a) Resistivities and Fe Concentrations

Residual resistance ratio measurements for the six specimens are reported in Table 6.1 and clearly show that essentially all the Fe deposited on the first set of specimens had come out of solution: this is seen from the fact that the residual resistance ratio of the pure Cu control to which no Fe was added is higher than the other two, showing that it in fact contained more impurities in solution. This, at first sight, appeared surprising but because some, at least, of the other impurities present in the copper would be soluble in Fe they would be partially leached from the Cu by the Fe as it separated out. It is seen that the specimen on which more Fe was deposited shows a larger decrease in the residual resistance ratio, roughly in proportion to the amount of added Fe.

The resistance measurements on the second set of specimens shows that with a reasonably quick cool, all the Fe does not come out of solution in the Cu, but indicates also that it did not all stay in solution in our specimens. This is made more definite with the aid of our thermoelectric power measurements and we are able to estimate the resulting concentration of dissolved Fe, using data given by Kjekshus

TABLE 6.1

RESIDUAL RESISTANCE RATIOS, THERMOELECTRIC POWERS AND Fe CONCENTRATIONS OF Cu Fe ALLOYS

	Residual Resistance Ratios $(\rho r/\rho)_{20}$			Thermopower at 4.2K	Fe Concentrations p.p.m. atomic
	Measured	Other	Fe	$S_{measured}$ $\mu V/K$	
Cu control slow cool	.00145		.0000505	0.376	0.06
+25 Å Fe " "	.00138				
+75 Å Fe " "	.00112		.000073	0.703	0.09
Cu control quick cool	.0199	.0199			
+25 Å Fe " "	.0249	.0202	.00466	2.025=S_{Fe}/5.34	5.6
+75 Å Fe " "	.0762	.0373	.0389	5.51 =S_{Fe}/1.96	47.0

and Pearson (1962) and by Daybell and Steyert (1968b). Kjekshus and Pearson measured the thermoelectric powers of several Cu alloys, including two containing nominally 25 p.p.m. and 75 p.p.m. atomic Fe, for which they found $S_{measured}$ at 4.186K to be 9.25 μV/K and 10.0 μV/K respectively. They give the residual resistivities of these alloys as .03193 $\mu\Omega$cm and .08555 $\mu\Omega$cm respectively and, making reasonable assumptions, we can compute the value of the characteristic thermoelectric power of Fe in Cu at 4.186K to be 10.8 μV/K. Using this value in equation (3.1) given in Chapter 3, in conjunction with our measured thermoelectric powers and measured residual resistance ratios, gives the resistance ratio component $(\rho_{Fe}/\rho)_{20}$ due to the Fe in our Cu alloys as

alloy with 75 Å Fe added, $(\rho_{Fe}/\rho)_{20} = .0389$

" " 25 Å Fe added, $(\rho_{Fe}/\rho)_{20} = .00466$

To obtain the dissolved Fe concentrations from these, we must know the incremental resistivity due to Fe in Cu. An accurate value for this cannot be obtained from the data of Kjekshus and Pearson because they only give nominal concentrations for their alloys, but Daybell and Steyert (1968b) measured the residual resistance of Cu alloys

containing 63 and 22 p.p.m. atomic Fe prepared from high purity Cu and at 4.2K give 90 nΩcm and 32.6 n Ω cm respectively for their resistivities. From these, with the assumption that the resistivity due to other scatterers is the same in both alloys, we obtain a value of 1.40 n Ω cm/p.p.m. atomic Fe for the incremental resistivity of Fe in Cu. Taking the resistivity of pure copper at 20°C to be 1.693 $\mu\Omega$cm we find the dissolved Fe content of our alloys to be:

alloy with 75 Å added Fe contained 47 p.p.m. atomic Fe in solid solution

alloy with 25 Å added Fe contained 5.6 p.p.m. atomic Fe in solid solution

(we note that 25 Å Fe added to a Cu specimen .01 cm thick would give a concentration of 25 p.p.m. atomic Fe). It also appears that the true dissolved Fe content of Kjekshus and Pearson's nominally 25 and 75 p.p.m. alloys were 19.2 and 57.5 p.p.m. respectively.

We can use a slight modification of this same calculation procedure to estimate the small residual amount of Fe which remained in solution in the first set of specimens after the slow cooling from 850°C. This first set of specimens, including the copper control, had magnetothermopower

characteristics, as described below, which were markedly different from those observed in the second set, due to Fe, and the obvious inference is that the thermoelectric power observed in the first set, including the Cu control, was at least in part due to some impurity other than Fe. At the same time, the specimen on which 75 Å Fe had been deposited had a thermoelectric power which was slightly higher than was measured in the pure Cu control, so it evidently contained some Fe. If we call the other impurity responsible for part of the thermoelectric power "impurity x" (recognizing, of course, that it may be Fe), we can write the following equation relating the measured thermoelectric power and residual resistance ratios to the characteristic values for Fe and impurity x:

$$\left(\frac{\rho_r}{\rho}\right)S_{measured} = \left(\frac{\rho_{Fe}}{\rho}\right)S_{Fe} + \left(\frac{\rho_x}{\rho}\right)S_x \qquad (6.2)$$

where (ρ_r/ρ) is the measured residual resistance ratio of the alloy and ρ_{Fe} and ρ_x are the residual resistivity components due to Fe and impurity x respectively. Applying this to the Cu control in which we assume there was only impurity x, gives $(\rho_x/\rho)S_x = .000545$. (If impurity x is Fe, this indicates that the Cu control contained .061 p.p.m. atomic Fe). This result can then be

applied to the specimen on which 75 Å Fe had been deposited and in which the quantity of impurity x is assumed to be unchanged to give ρ_{Fe}/ρ = .0000225 and shows the residual (or additional) Fe concentration still in solution after slow cooling to be .027 p.p.m. atomic Fe.

The results of all these calculations are included in Table 6.1 with the Fe concentrations and resistance ratios for the slowly cooled specimens shown on the assumption that impurity x is Fe, as is indicated in the discussion of the magnetothermopower in the penultimate section of this chapter.

In these calculations we have assumed that the characteristic thermoelectric power due to Fe in Cu at 4.2K is not a function of concentration, at least below 65 p.p.m. atomic Fe. In Au-Fe alloys the results discussed in Chapter 4 indicated a fairly small but definite concentration dependence at 4.2K over this same concentration range, but not below about 1K. In making comparisons to Cu Fe alloys, it is probably better to use the same value of T/T_K, rather than the same T and we can therefore conclude that for Cu Fe at 4.2K, for which $T/T_K < 1$, the characteristic thermoelectric power S_{Fe} will be concentration independent in the range of interest in the above calculations.

b) Thermoelectric Power vs Temperature

Our data for S_{Fe} vs T is shown in fig.6.2 for the two specimens containing 47 p.p.m. and 5.6 p.p.m. atomic Fe, and this is compared with the curve published by Kjekshus and Pearson (1962) for their nominally 75 p.p.m. alloy, adjusted to S_{Fe} using their published resistivity data for this alloy. The results show exact agreement over the range of temperature studied.

c) Effect of Magnetic Field on S_{Fe}

The change in the thermoelectric power due to the application of external magnetic fields of up to 50 KOe to our Cu specimens containing 47 p.p.m. and 5.6 p.p.m. atomic Fe are shown in fig.6.3. In this figure, the percent change $100\,\Delta S_m(H)/S_m(o)$ is plotted against field H for a series of fixed temperatures. The most surprising feature of the curves for both alloys is the small difference between curves for different temperatures over the range from 4.5K to 2.6K compared to the differences from 2.6K to 1.6K. Apart from this, the thermoelectric power is seen to fall off with applied field, as was expected.

The curves do not seem to have reached the high field region where, according to the theory of Weiner and Béal-Monod (1970), $S(H) \propto T/H$, but the form of the curves does

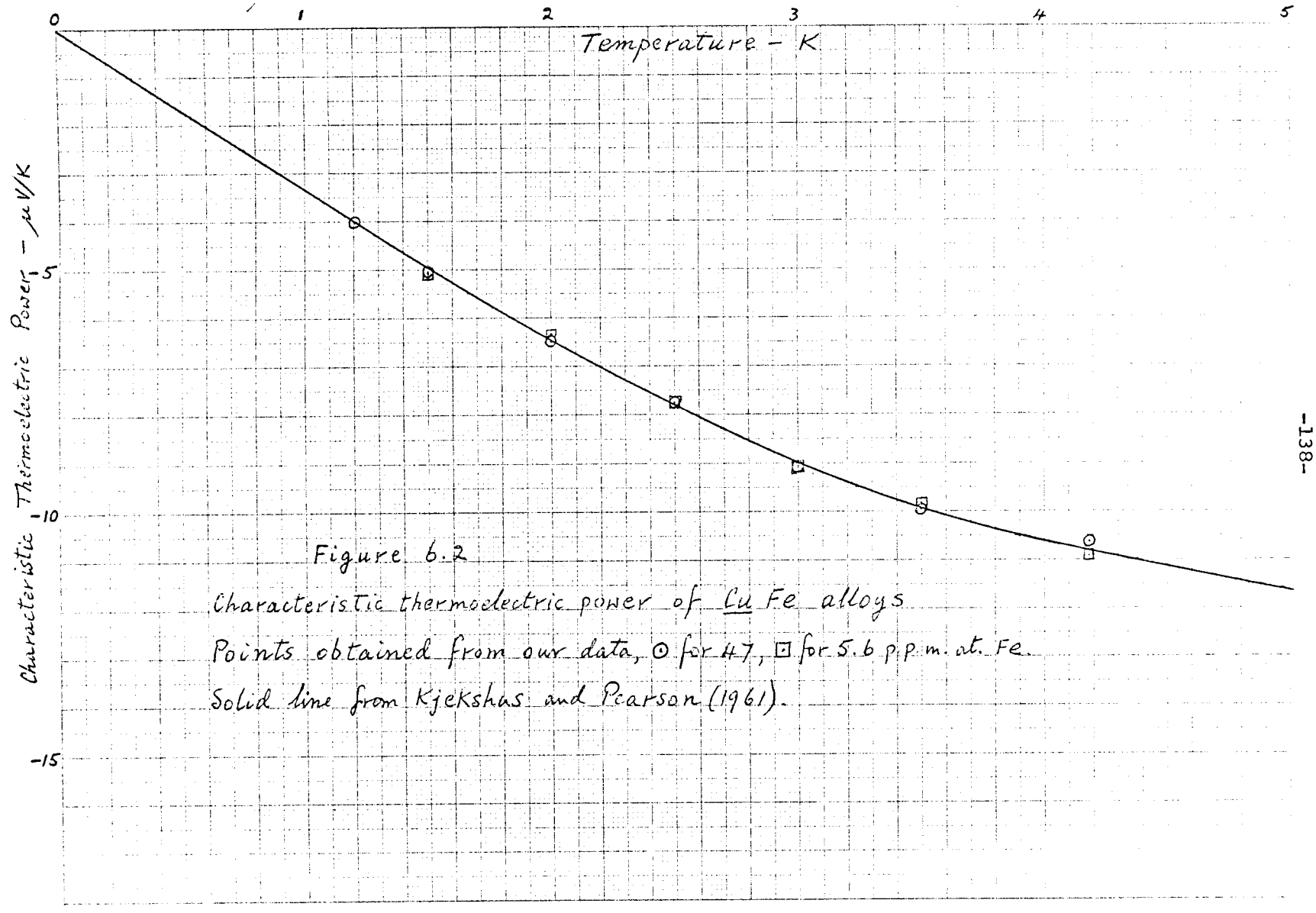

Figure 6.2

Characteristic thermoelectric power of Cu Fe alloys

Points obtained from our data, ⊙ for 4.7, ⊡ for 5.6 p.p.m. at. Fe.

Solid line from Kjekshus and Pearson (1961).

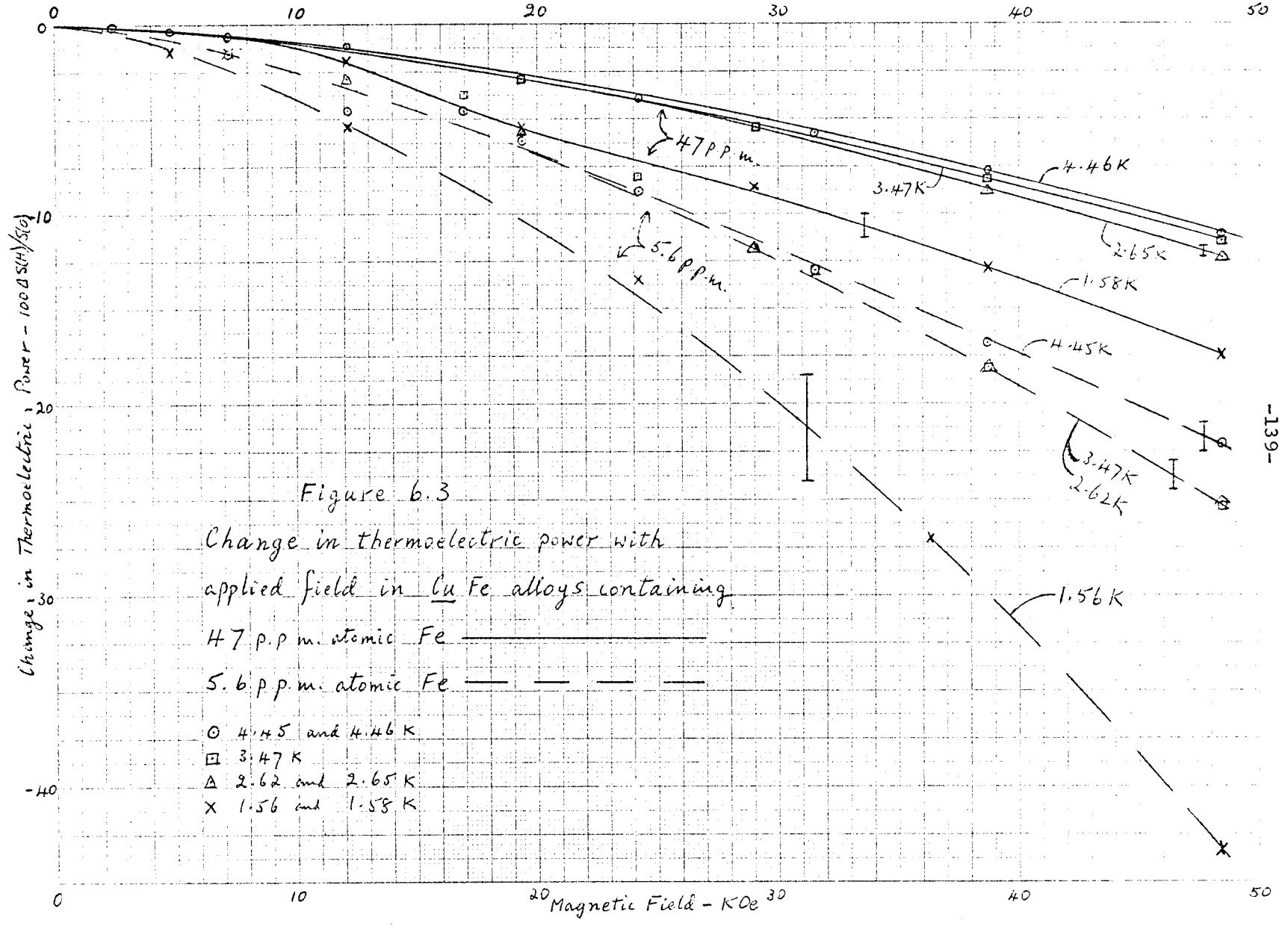

Figure 6.3

Change in thermoelectric power with applied field in Cu Fe alloys containing

47 p.p.m. atomic Fe ————————

5.6 p.p.m. atomic Fe — — — —

⊙ 4.45 and 4.46 K
⊡ 3.47 K
△ 2.62 and 2.65 K
× 1.56 and 1.58 K

not indicate the presence of magnetic impurity interactions and the theory of Weiner and Beal-Monod should therefore be applicable over the whole range of field strengths measured. Detailed comparison is beyond the scope of this chapter, but the peculiar temperature dependence noted above would seem to be at variance with their predictions.

The specimens, whose physical form is shown in fig.6.1, were mounted in our apparatus so that the magnetic field was applied parallel to their length so that 82.4% experienced a longitudinal field and 17.6% a transverse field.

d) Magnetoresistance Correction

We must now try to determine how much of the change in $S_m(H)$ was due to the effect of magnetoresistance, $\rho_{Fe}(H)$ in equation (6.1), in order to determine the true effect of the applied field on the characteristic thermoelectric power $S_{Fe}(H)$.

The magnetoresistance of dilute Cu Fe alloys has been measured recently by several workers, Muto et al (1964), Monod (1967) and Rohrer (1969). Of these, Muto et al were unable to separate the negative s-d component from the normal positive component and their results are, therefore,

of no use to us. Monod measured an alloy said to contain 110 p.p.m. Fe and he shows a graph of the resistivity as a function of temperature in zero field and in a field of 20 KOe, from which he has subtracted the normal positive magnetoresistance. He showed also that the negative s-d component is independent of field direction. Rohrer measured a more concentrated alloy, said to contain 0.08 at.% Fe, and he shows graphs of the negative magnetoresistance component $\Delta \rho_{Fe}(H) / \rho(o)$ for a series of temperatures from 2.17 K to 35K with applied fields up to 200 KOe. Rohrer states that his results show a negative magnetoresistance component 4 times larger than reported by Monod and there is therefore uncertainty as to the magnitude of the corrections to be applied to our data. In order to establish that there is a real change in S_{Fe} due to the field, we have used Rohrer's results to calculate the maximum magnetoresistance correction and we have done this at the maximum field of 48.4 KOe for each of our alloys at 4.45 K and at 1.57 K.

Rohrer shows $100 \Delta \rho_{Fe}(H) / \rho_{total}(o) = -4.8\%$ in a field of 48.4 KOe at 4.16 K, and -6.3% at 2.17 K. We can use Monod's results, which cover a wider temperature range, to estimate the amounts by which these values should be

adjusted for 4.45K and 1.57K and obtain -4.7% and -7.0% respectively. Since Rohrer's Fe concentration was large enough for the Fe to dominate the scattering, we can assume $\rho_{total}(o) = \rho_{Fe}(o)$ and write

$$\Delta\rho_{Fe}(H)/\rho_{Fe}(o) = -0.047 \text{ at 48.4 KOe and 4.45K}$$
$$= -0.070 \text{ " " " " 1.57K}$$

In order to see the effect that this has on our measured thermoelectric powers and to derive the net effect of the applied field on the characteristic thermoelectric powers $\Delta S_{Fe}(H)/S_{Fe}(0)$, we transform equation (6.1) to

$$\frac{\Delta S_{Fe}(H)}{S_{Fe}(0)} = \frac{\frac{\Delta S_m(H)}{S_m(0)}\left(1+\frac{\Delta\rho_{Fe}(H)}{\rho_{Fe}(0)}\cdot\frac{\rho_{Fe}(0)}{\rho_{tot.}(0)}\right) - \frac{\Delta\rho_{Fe}(H)}{\rho_{Fe}(0)}\left(1-\frac{\rho_{Fe}(0)}{\rho_{tot.}(0)}\right)}{1+\frac{\Delta\rho_{Fe}(H)}{\rho_{Fe}(0)}} \qquad (6.3)$$

which contains measured quantities. Based on Rohrer's data for the magnetoresistance of Cu Fe alloys we therefore find, at 48.4 KOe for our 47 p.p.m. alloy

at 4.46K, $\frac{\Delta S_m(H)}{S_m(0)} = -11.1\%$, $\frac{\Delta S_{Fe}(H)}{S_{Fe}(0)} = -8.9\%$

at 1.58K, " $= -17.7\%$, " $= -15.4\%$

for our 5.6 p.p.m. alloy

at 4.45K, $\frac{\Delta S_m(H)}{S_m(0)} = -22.4\%$, $\frac{\Delta S_{Fe}(H)}{S_{Fe}(0)} = -19.3\%$

at 1.56K, " $= -43.7\%$, " $= -40.3\%$

The effect of magnetoresistance is therefore seen to be quite small, even on the basis of Rohrer's data, and would account for less than 1% of the change in the measured thermoelectric power on the basis of Monod's data.

e) Effect of Magnetic Field on Specimen from which Fe Separated and on Cu Control

The curves showing the change of thermoelectric voltage with applied field for the first set of Cu Fe specimens, cooled slowly from 850°C, are shown in figs. 6.4 and 6.5, the first (fig.6.4) being for the specimen on which 75 Å Fe had been deposited and the second (fig.6.5) being for the pure copper control. The measurement precision in both these figures was poor, as indicated by the error bars, because the thermoelectric voltage S(0) developed in the specimens was only about 50 nV in all except the one curve in fig. 6.4 taken at a mean temperature of 6.9 K for which S(0) was 200 nV. Despite the resulting uncertainty, both sets of curves clearly have two main features in common which are entirely absent from the Cu Fe curves of fig.6.3. Both show initial sharp drops in thermoelectric power at low fields of the order of a few KOe and in both, this is followed by an increase to a maximum. The curves thus bear

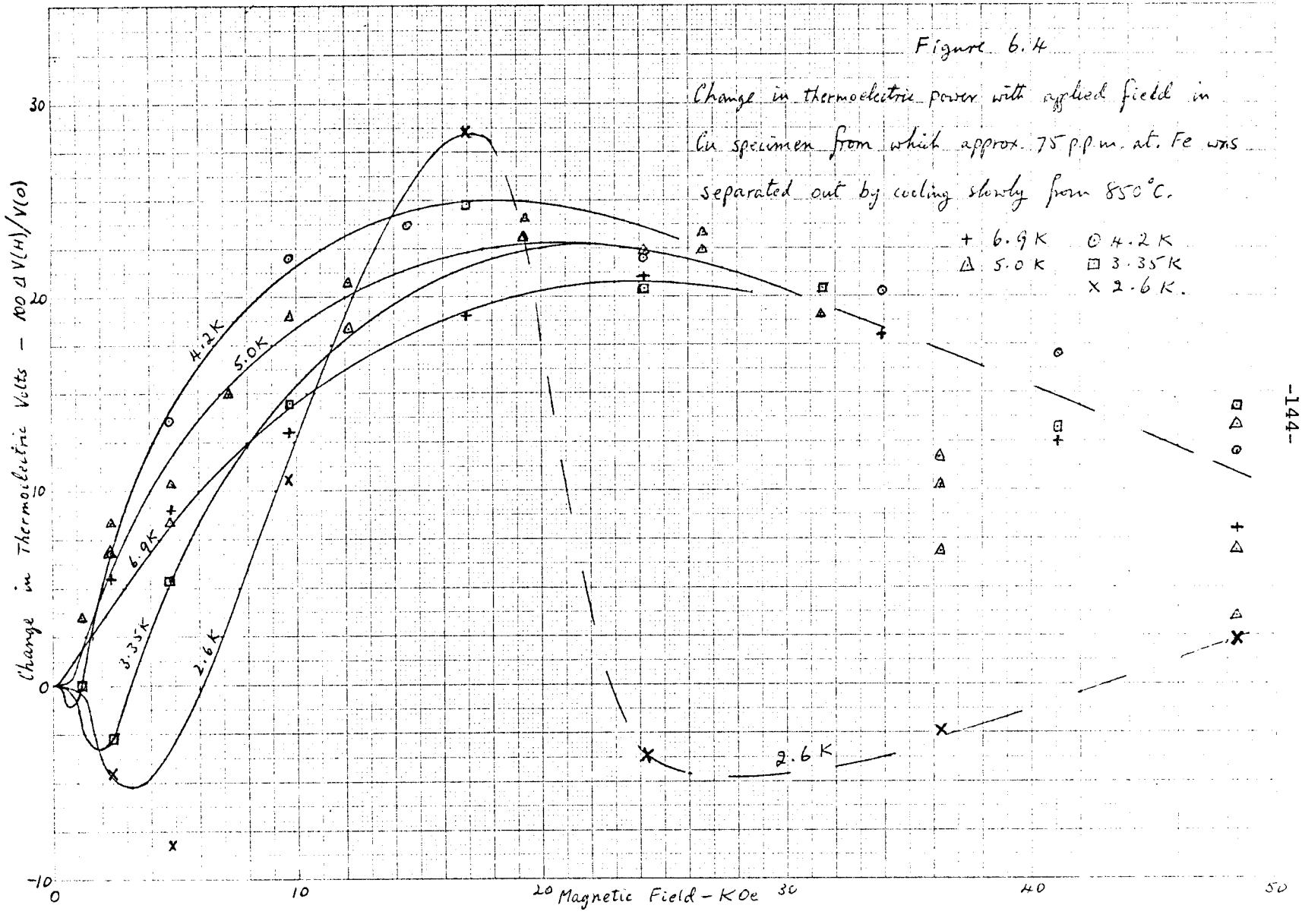

Figure 6.4

Change in thermoelectric power with applied field in Cu specimen from which approx. 75 p.p.m. at. Fe was separated out by cooling slowly from 850°C.

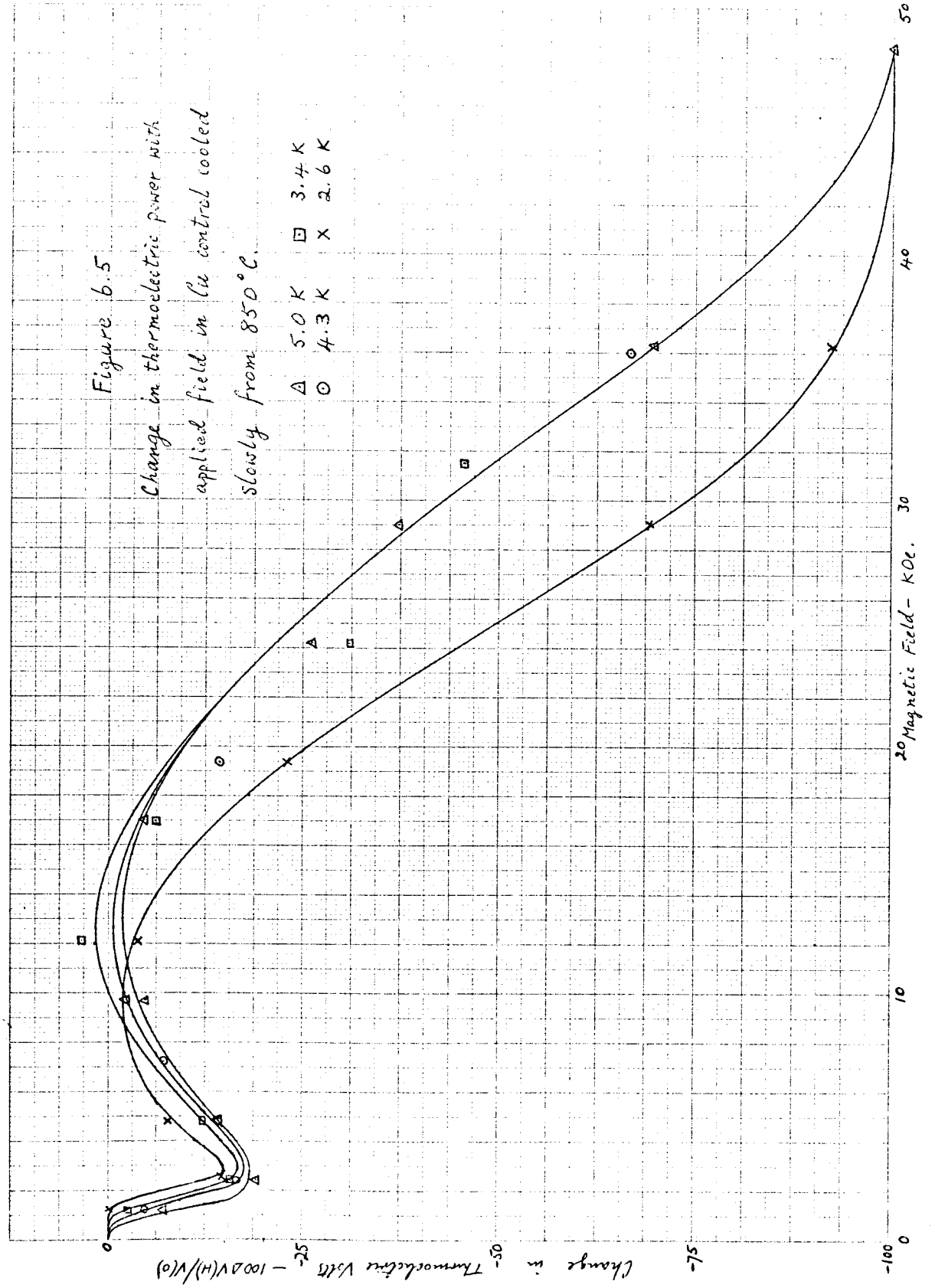

considerable similarity to those of our Au Fe samples reported in Chapter 4 and it appears that the initial sharp drops at low fields may be due to the same cause, namely, to a few p.p.m. Pb present in the Cu which was used to prepare our samples, and which separated out during the slow cooling from 850°C. Although the exact shape of the curves at low fields is uncertain, the measurement precision was sufficient to show that the sharp drop occurs at progressively lower field strength as the temperature is raised, and in fig. 6.4 can be seen to disappear altogether at about 7 K. Hansen (1958) gives little information on the solid solubility of Pb in Cu and states only that it is less than 0.09 at.% above 600°C.

We can estimate the quantity of Pb impurity which would produce the observed effects on the assumption, as in Au Fe, that finely separated Pb on going normal contributes to the electron scattering to about the same extent as dissolved Pb. We see in fig. 6.5 that the upper parts of the curves for the Cu control subtend to -20% at zero field. The residual resistance ratio found for this specimen was .00145, so that the increase in resistivity due to the anomaly was 0.6 n Ωcm. Norbury (1922) does not give the incremental resistivity due to Pb in Cu, but

for Sn in Cu, which would be the same, according to Norbury's rule, he gives 2.6 $\mu\Omega$cm/at.% and we see that the observed effects in the Cu control specimen could be due to about 2 p.p.m. atomic Pb.

It is interesting that the magnitude of the low field anomaly, observed in the sample to which Fe had been added (fig. 6.4) is much smaller than in the copper control. The curves in fig.6.4 appear to subtend to about -6% at zero field, indicating an increase in resistivity due to Pb going normal, of only 0.12 n Ω cm which is 1/5 of the value found for the Cu control. This has the obvious explanation that the presence of about 75 p.p.m. separated Fe provided a considerable area of Cu-Fe interface onto which the Pb could readily separate. On going normal, such Pb would make almost no additional contribution to the boundary scattering already existing between the separated Cu-Fe. An alternative explanation that some of the Pb dissolved in the separated Fe is unlikely, since Hansen states that the solid solubility of Pb in Fe is only $\sim 2.7 \times 10^{-4}$ at.% Pb at 1530°C. Further measurements on this specimen were made 8 months later, which showed that the magnitude of the anomaly had by then decreased still further: this is readily explainable on the basis of

further Pb migration to Cu- Fe boundaries.

The maxima in the curves which were observed at intermediate field strengths, appear at first sight to resemble the maxima observed in Au Fe alloys and to be due to some other magnetic impurity in the Cu. We called it impurity x above, but the specimens in this first set had a very low electron scattering, as shown by their residual resistance ratios, and therefore had low thermal resistance which was in parallel with the thermal resistance of the quartz rod on which the specimen was mounted. If the magnetic field affected the thermal resistance of the specimen it would change the measured thermoelectric voltage independently of any change that it might make to the thermoelectric power. Using the same formula for the thermal conductivity as used in Appendix A3, we can estimate the thermal resistance of these slowly cooled specimens to be about $10^4/T$, K/W, which is more than an order of magnitude less than the thermal resistance of the quartz rod, estimated to be about $2 \times 10^5/T$, K/W (as given in Appendix A.3). The stycast lo-K on which each Cu specimen was mounted was also in parallel with the quartz rod, but being a composite dielectric material its thermal resistance at liquid

He temperature was large compared to that of the copper specimen. Measurement of the thermal resistance across the specimen as mounted in an experiment gave a value of approximately $10^4/T$, K/W, and so confirmed that the thermal resistance of the specimen controlled the temperature drop across it.

Data given by Muto et al (1964) shows that pure copper has a positive magnetoresistance in both longitudinal and transverse fields and since the thermal resistance is directly proportional to electrical resistance at low temperatures where impurity scattering dominates, the thermal resistance will increase in a magnetic field in the same proportion as the electrical resistance. We can, therefore, apply suitable corrections to our experimental curves shown in figs. 6.4 and 6.5, using the data given by Muto et al. When this is done, and the low field anomalies are suitably removed, we obtain corrected magneto-thermopower data for both the Cu control and the specimen onto which 75Å Fe had been deposited, showing a monotonic decrease with applied field in substantial agreement with the trends seen in fig. 6.3. (The curves have not been redrawn as corrected because our measurement precision on these alloys was not sufficient to make them of real value).

It therefore seems that "impurity x" in the copper control responsible for its thermoelectric power was, in fact, Fe present to the extent of 0.06 p.p.m. atomic. The Fe content left in solid solution in the other specimen onto which 75 Å Fe had been deposited and then separated by slow cooling from 850°C was correspondingly 0.09 p.p.m. atomic Fe, as shown in Table 6.1.

SUMMARY

Our measurements of the thermoelectric power of Cu Fe alloys in applied magnetic fields up to 50 KOe and between 7K and 1.5K have not shown any increases with applied field, such as seen in Au Fe alloys and attributed to Fe-Fe interactions. This is in agreement with theoretical expectation of Rivier and Zuckerman, and others, as discussed in Chapter 5, that such interactions should be frozen out or screened out below T_K by the progressive formation of the Nagaoka bound state between the conduction electrons and the transition metal d electrons. Our magnetothermopower data do, nevertheless, show some concentration dependence which seems to indicate that some interaction effect still exists. Our results should show agreement with the theory of Weiner and Beal-Monod (1970), but the predicted temperature dependence does not appear to agree with our results. The effect of

magnetoresistance has been shown to be small, even at the low concentration of our alloys, contrary to the finding of MacDonald and Pearson (1957).

At zero field our S vs T data agrees well with results reported by Kjekshus and Pearson (1961).

CHAPTER 7

EXPERIMENTS ON Rh Fe and Au Ce ALLOYS

Rh Fe Alloys

Three samples of Rh wire were obtained from Engelhard Industries, one stated to be 99.99% pure Rh and two containing small amounts of Fe, and designated El alloy 18499, nominally .02 at.% Fe, and El alloy 18507, nominally .11 at.% Fe. In addition, samples of 99.99% pure Rh wire were obtained from Gallard-Schlessinger Company and from Koch-Light Laboratories.

All the samples, except the one obtained from Gallard-Schlessinger Company, were independently analysed by the Mineral Science Division, Department of Energy, Mines and Resources in Ottawa, and all were found to contain both Fe and Cu, as shown in Table 7.1. The two alloy samples from Engelhard were analysed for Fe by electron microprobe and the others by semiquantitative spectrochemical analysis. The electron microprobe analysis also showed the Fe to be uniformly distributed in the two El alloys within the error limits of the equipment, which was .02 at.%. The Fe concentrations in the three Engelhard samples were also

TABLE 7.1

DATA ON Rh Fe ALLOYS

Sample	Anneal	Residual Resistance Ratio		Concentrations at.% Fe		Concentrations at.% Cu	Thermoelectric Power S_m at 4.2K $\mu V/K$
		Measured	Fe	by slope of resistivity vs temperature plot	by electron microprobe	by semi-quantitative spectrochemical analysis	
Engelhard El alloy 18507	As received	.399	.0276	.25	.17	.03	.67
	1200°C	.162	"				
	725°C	.1244	"				1.76
Engelhard El alloy 18499	As received	.311	.0133	.12	.105	.06	
	1200°C	.0914	"				
	725°C	.0623	"				2.035
					by semi-quantitative Spectrochemical Analysis		
Engelhard 99.5% pure	As received	.04825	.0011	.010	.01	.03	
	1200°C	.0511	"				
	725°C	.02335	"				0.60
Gallard-Schlessinger.99.99% pure	As received	.0533					
	1200°C	.0331					
Koch-Light Labs. 99.99% pure	As received	.225	.0019		.02	.03	
	1200°C	.00857					

determined by the measurement of their resistivities as a function of temperature over the range from about 4K to 1.5K. The Fe concentrations are given by the slopes of the resistivity vs. temperature plots using data given by Coles (1964). These determinations are considered to be more accurate than the others and are also shown in Table 7.1.

Table 7.1 also includes the residual resistance ratios of all the samples; these were measured both as received and after annealing. The portions of these ratios due to Fe are also given, computed from the measured concentrations using Coles (1964) data. All the samples as received were quite springy and the residual resistance ratio measurements indicated that they contained large numbers of crystal lattice defects. The samples were therefore annealed and, since Rh metal was known to work harden very rapidly at room temperature, care was taken to handle them as little as possible afterwards. An annealing temperature of 1200^{o}C was used initially because this was given as the annealing temperature for Rh by Smithells (1967). According, however, to van Antwerpen (1965), defects are quickly and effectively annealed out at 725^{o}C and this temperature was therefore used later for the three Engelhard specimens whose thermo-

electric powers were studied. In both cases the specimens were cooled slowly after anneal by switching off the oven and leaving them to cool inside.

The variation of the measured thermoelectric power S_m with temperature is shown in fig. 7.1 for the three Engelhard specimens annealed at 725°C and for one of them, E1 alloy 18507 as received. These curves show a maximum for $|S_m|$ in the vicinity of 3K, which contrasts with the experimental results reported by Coles (1964) and Nagasawa (1968), neither of whom observed a peak above 1K. The values of S_m at 4.2K are listed in Table 7.1 and it can be seen by comparing these for E1 alloy 18507, obtained before and after anneal, with the corresponding measured values of the residual resistance ratio, that they do not conform to the Nordheim-Gorter rule, equation (3.1). This is on the assumptions that only the Fe contributes to S_m and that the characteristic thermoelectric power due to the Fe is not a function of concentration.

The variation of the thermoelectric powers with applied field are shown in figs. 7.2 to 7.5. These show a small change for E1 alloy 18507 due to annealing which could be an effect of magnetoresistance. Apart from this, it is noted that the temperature dependence of $\Delta S(H)/S(o)$ does not scale as H/T, and comparisons between the three alloys show only a small concentration dependence.

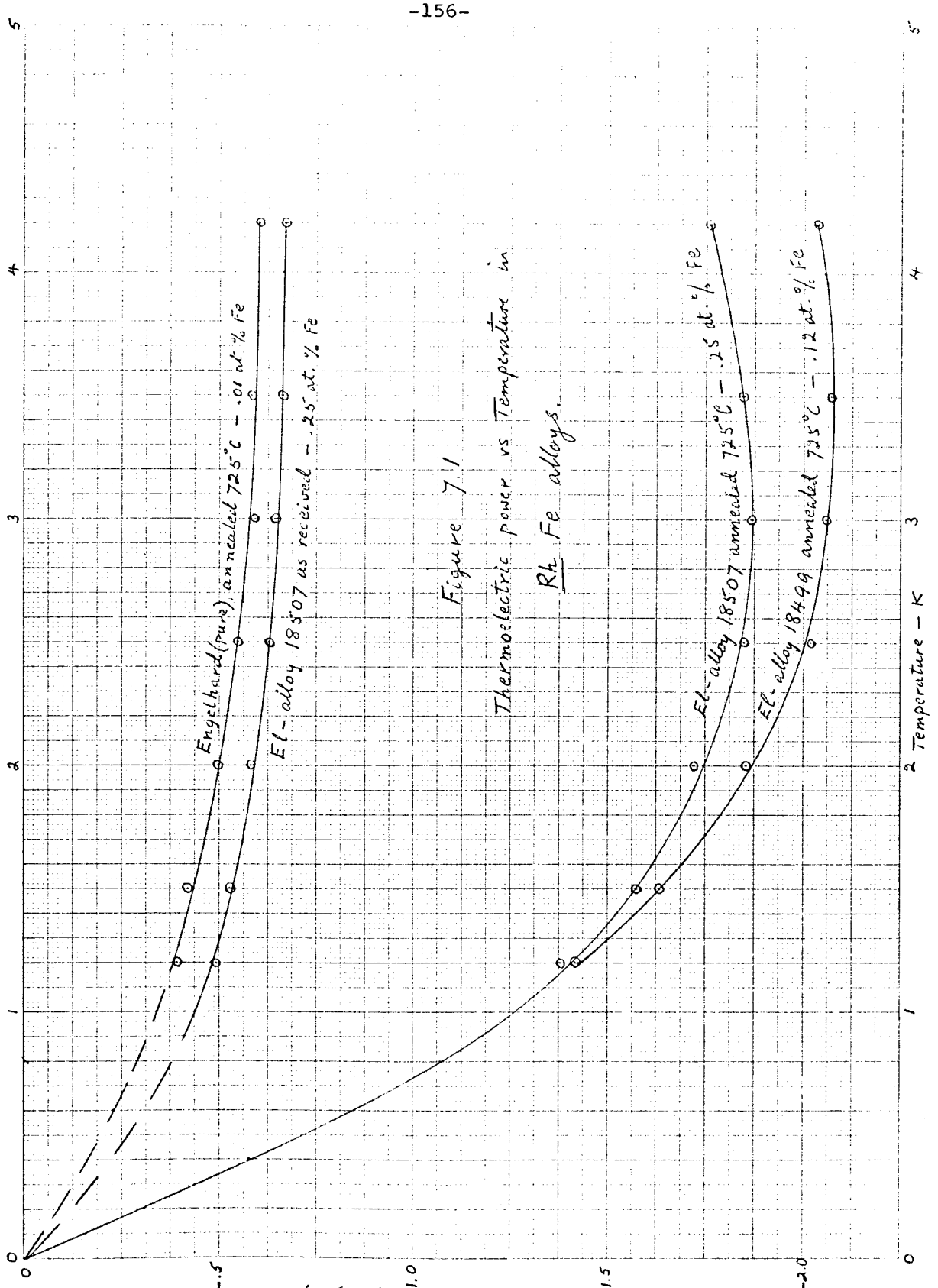

Figure 71
Thermoelectric power vs Temperature in Rh Fe alloys.

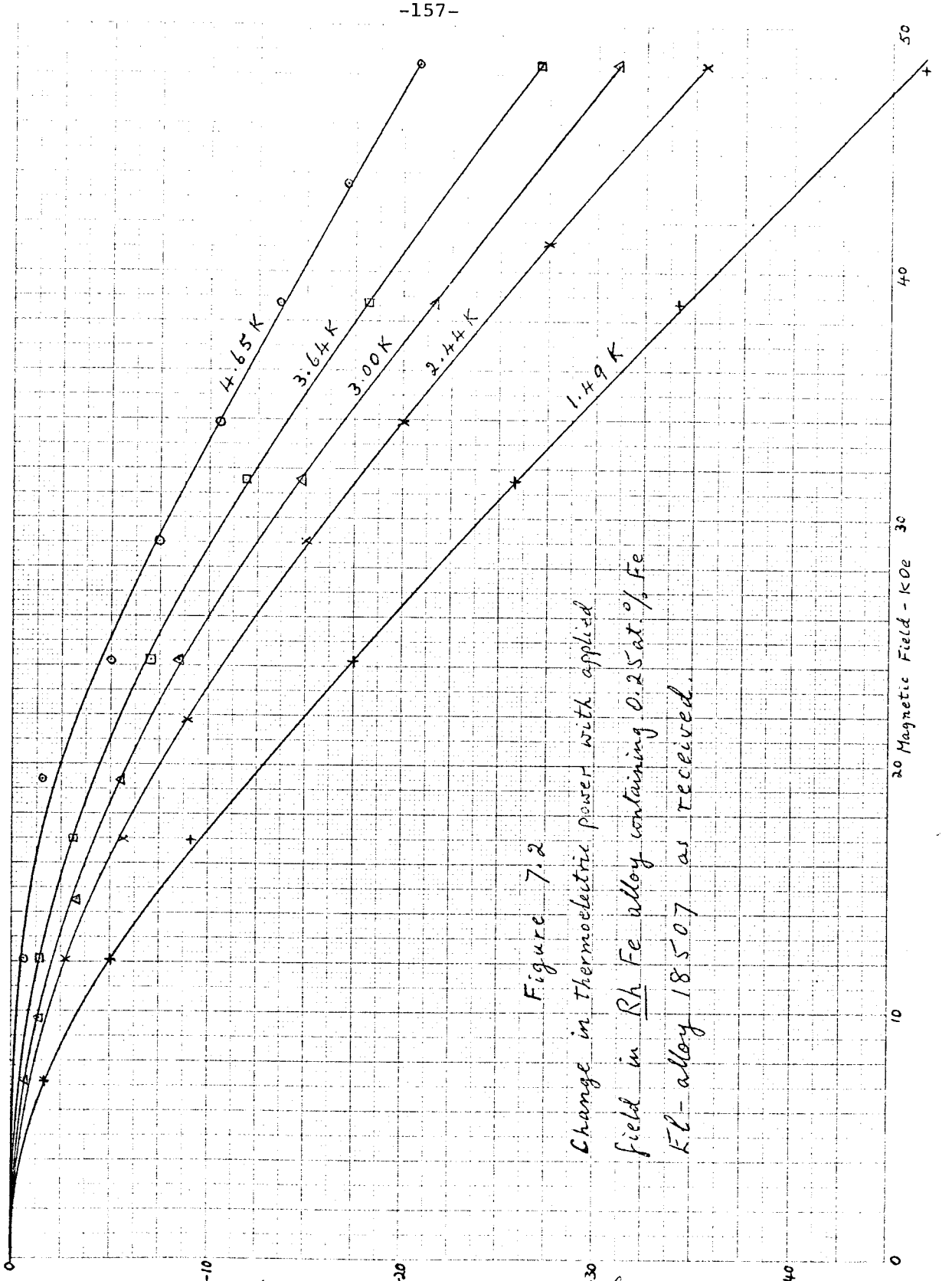

Figure 7.2
Change in thermoelectric power with applied field in Rh Fe alloy containing 0.25 at % Fe
Fe - alloy 18507 as received.

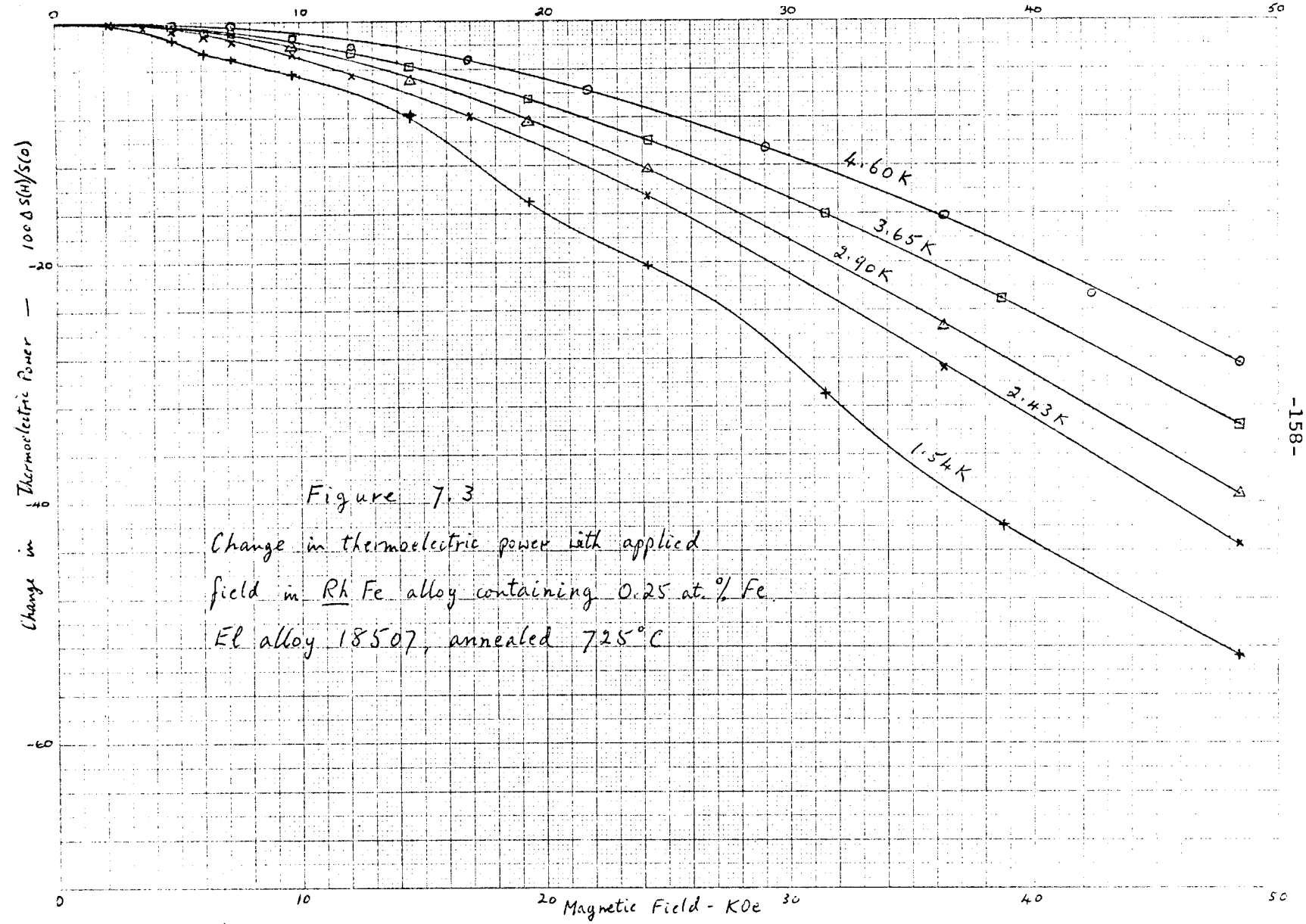

Figure 7.3

Change in thermoelectric power with applied field in Rh Fe alloy containing 0.25 at.% Fe

El alloy 18507, annealed 725°C

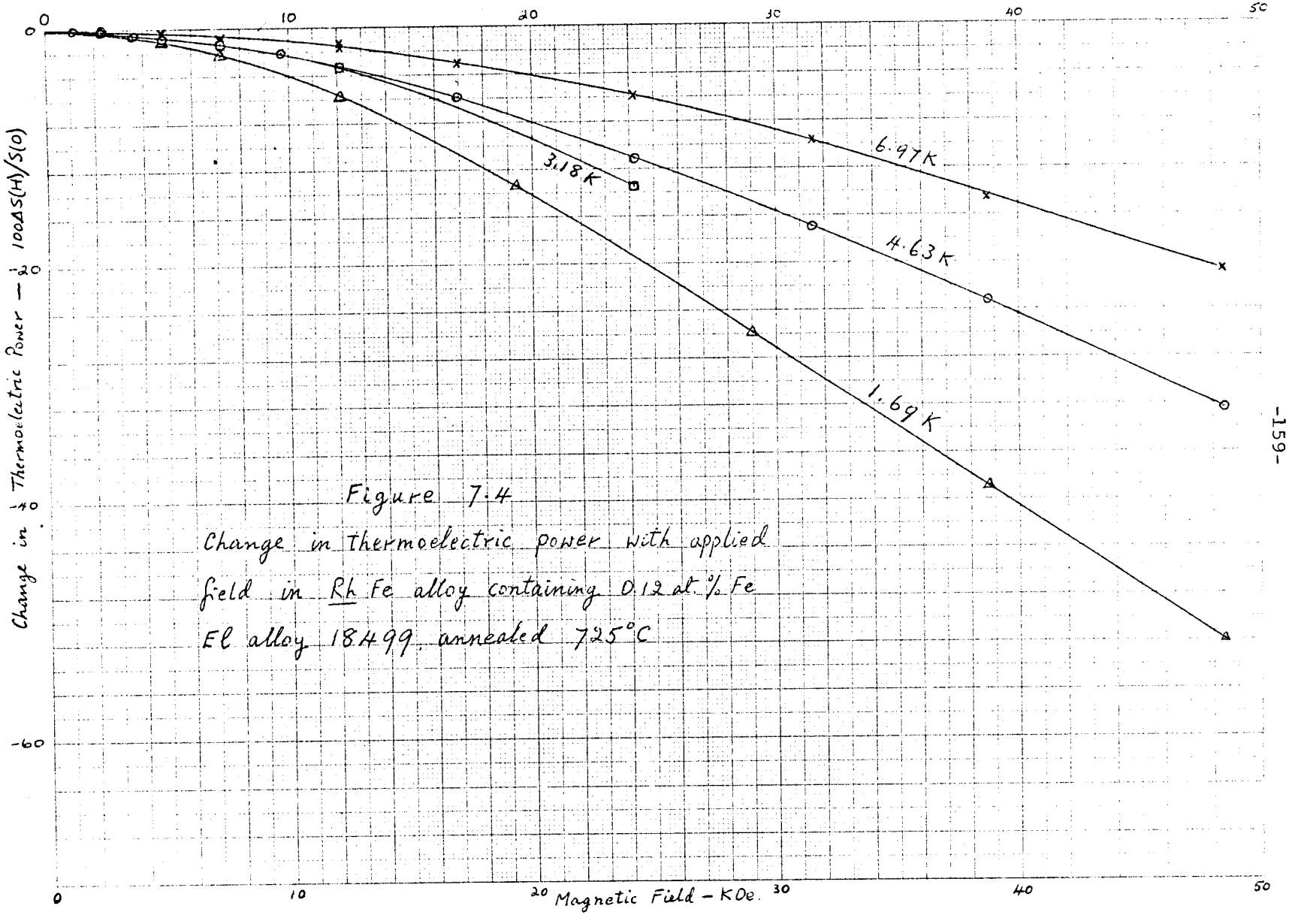

Figure 7.4

Change in Thermoelectric power with applied field in Rh Fe alloy containing 0.12 at.% Fe

El alloy 18499, annealed 725°C

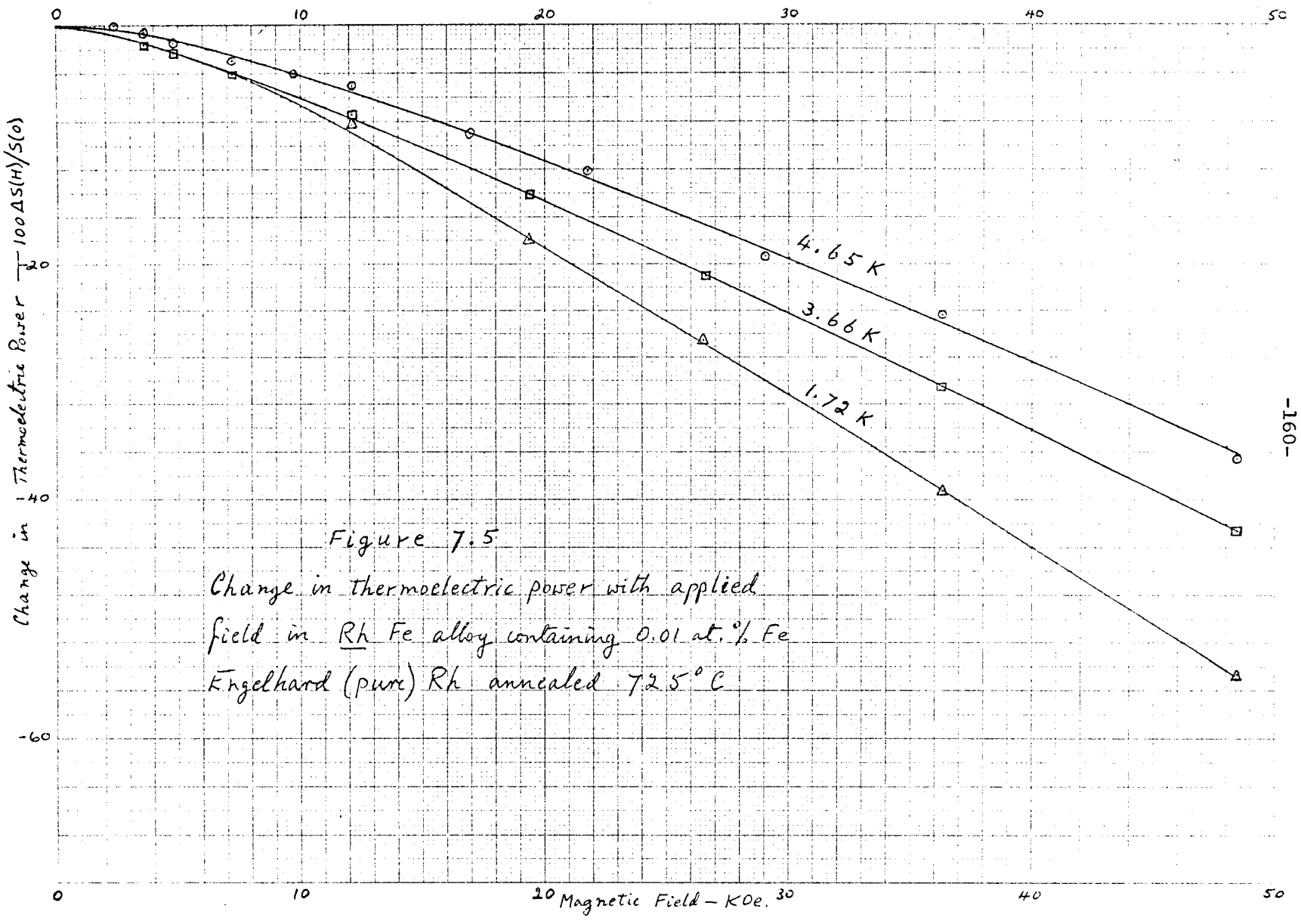

Figure 7.5

Change in thermoelectric power with applied field in Rh Fe alloy containing 0.01 at.% Fe
Engelhard (pure) Rh annealed 725°C

Au Ce Alloys

Specimens were prepared by first treating Cominco 99.9999% pure Au wire .01 cm. diameter with Cl_2 gas, as described in Chapter 3, for long enough to ensure that their Fe contents would be less than 0.1 p.p.m. atomic Fe. Cerium was then deposited on the wire by vacuum evaporation at $<10^{-7}$ torr. The intention was then to diffuse the Ce into the Au at a temperature of about 850°C in vacuum, but repeated attempts both in a reducing atmosphere and in 10^{-7} torr appeared to be largely unsuccessful. Most of the Ce appeared to remain on the surface of the wire, where it could be seen as a surface discolouration, and the residual resistance ratios increased little from the value for the pure Au, as shown in Table 7.2. Rider et al (1965) have shown that the solid solubility of Ce in Au is only about 0.2 at.% at its maximum near 800°C. Details of the sample preparations are given in Table 7.2.

Both samples ACe and BCe were analysed spectrographically by P. Tymchuk of the Analytical Section, Division of Applied Chemistry, National Research Council in Ottawa, with the following results:

TABLE 7.2

DATA ON Au Ce ALLOYS

Sample	Residual Resistance Ratio $(\rho_r/\rho)_{20}$	Measured Thermoelectric Power S_m at 4.2K $\mu V/K$
Cominco Au treated 3 hrs.H_2,43 hrs.Cl_2 at 800°C .094 at.% Ce deposited and diffused in oven for 1/4 hr. H_2, 18 hrs. vacuum at 800°C	.00135	
Sample A Ce		
Cominco Au treated 24 hrs. CO, 21½ hrs. Cl_2 at 800°C .0235 at.% Ce deposited and diffused in evaporator for 1/2 hr. at est. 750°C and in oven for 20 hrs. at 750°C after H_2 flush	.00244	3.19
Cominco Au treated 23 hrs. H_2, 23 hrs. Cl_2 at 750°C 10 min. in evaporator in vacuum at est. 750°C	.00133	
Cominco Au treated 23 hrs. H_2, 23 hrs. Cl_2 at 750°C 10 min. in evaporator in vacuum at est. 750°C .105 at.% Ce deposited and diffused in evaporator for 6 hrs. at est. 700°C	.00176	
Sample B Ce		
Cominco Au treated 23 hrs. H_2, 23 hrs. Cl_2 at 750°C 10 min. in evaporator in vacuum at est. 750°C .105 at.% Ce deposited and diffused in evaporator for 6 hrs. at est. 750 to 800°C	.00231	2.83

Impurity	Sample ACe p.p.m. atomic	Sample BCe p.p.m. atomic
Fe	0.81	1.9
Sn	0.63	.18
Mn	.07	.14
Si	.42	.28
Ce	350	None visible, <35, if any

They were asked to dissolve off surface Ce before analysis because sample ACe was known to have received about 235 p.p.m. on the surface and sample BCe about 1000 p.p.m. The amount of Ce found in sample ACe is not compatible with this and with our resistivity and thermoelectric power data, and it is thought that the Ce on this sample may have acquired an oxide coating, perhaps during the oven treatment at 750^{o}C, which would resist dissolution. It is thought that the Fe must have been present as impurity in the Ce and been vacuum deposited along with it. Unlike the Ce, this Fe would, of course, readily diffuse into the Au.

The results of thermoelectric power measurement vs temperature are given in fig. 7.6 and show thermoelectric powers of about the same magnitude as reported by Gainon et al (1967) for Ce in Au, but the Fe impurity contents shown by the analysis to be 0.81 p.p.m. atomic and 1.9 p.p.m. atomic

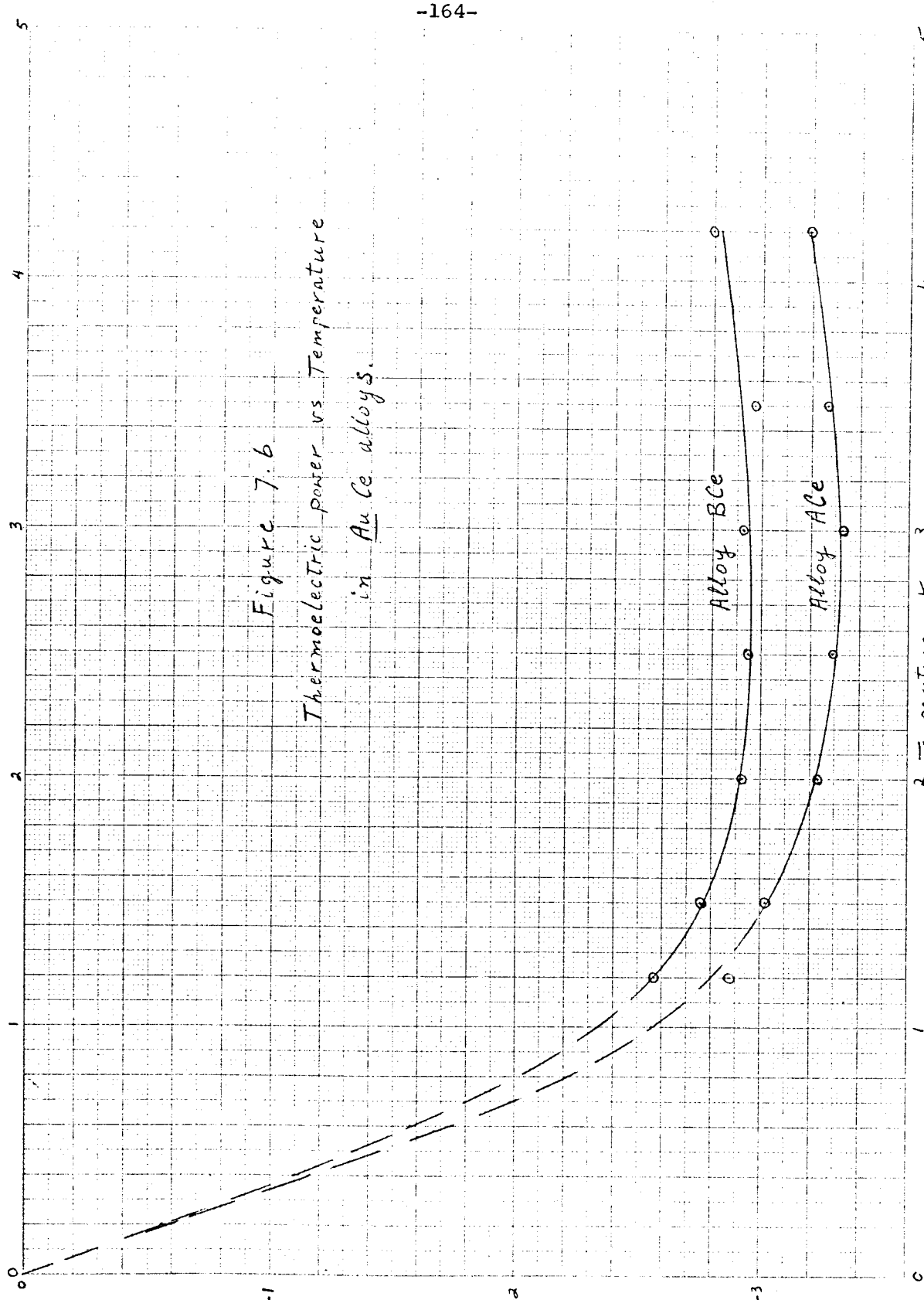
HEWLETT-PACKARD/MOSELEY DIVISION
9270-1023
FOR USE ON AUTOGRAF RECORDERS
10 UNITS/DIVISION
Figure 7.6
Thermoelectric power vs Temperature
in Au Ce alloys.
Alloy BCe
Alloy ACe
Thermoelectric Power — μV/K
Temperature — K
0
1
2
3
4
5
-1
-2
-3

in samples ACe and BCe respectively are sufficient, with the observed residual resistance ratios, to give thermoelectric powers of the same magnitude. The shape of the curves, however, does not agree with those for Fe in Au, as both samples ACe and BCe show pronounced maxima between 2.5K and 3K. The curves in fig. 7.7 and 7.8 showing the change in the observed thermoelectric voltage due to an applied magnetic field are curiously almost identical with the curves of fig. 4.5 for the 0.54 p.p.m. atomic Fe in Au alloy before making any adjustments for the low field anomaly. It is possible that one or two p.p.m. Pb may have been deposited from the Ce along with the Fe and the Sn, which were seen in the spectrographic analysis.

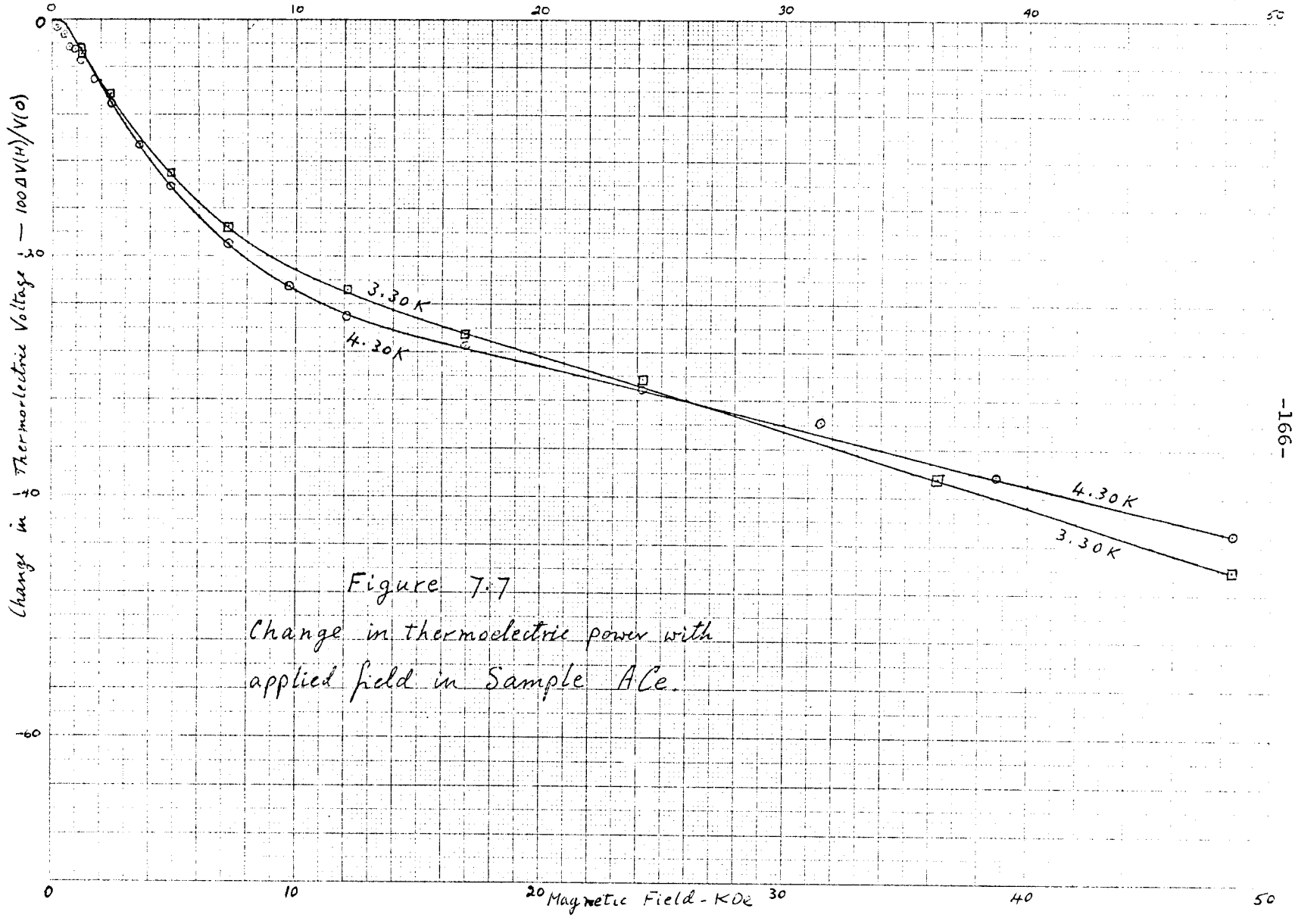

Figure 7.7

Change in thermoelectric power with applied field in Sample ACe.

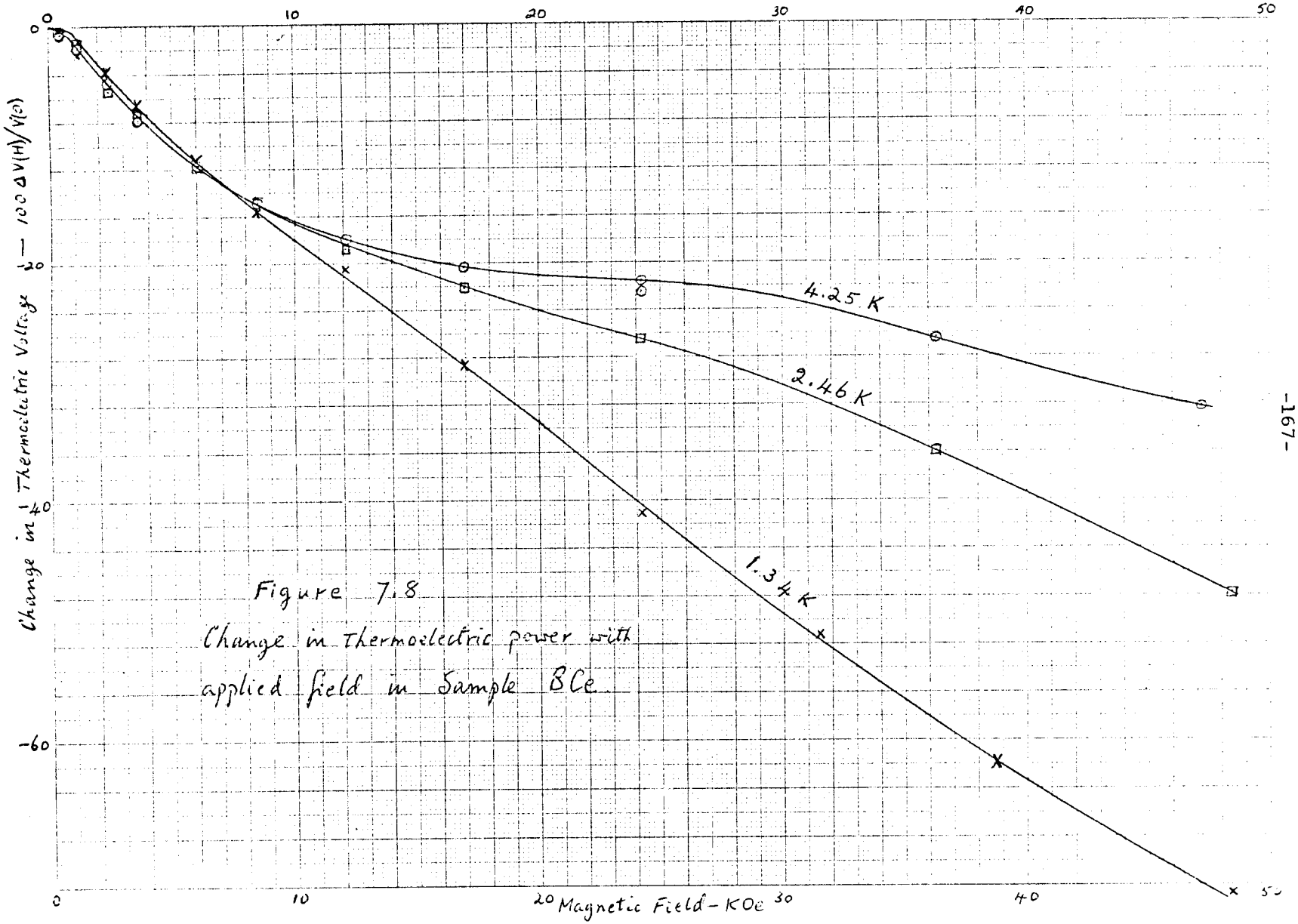

Figure 7.8
Change in thermoelectric power with applied field in Sample 8Ce

CONCLUSIONS

1. The increase in thermoelectric power due to an applied magnetic field which is found in dilute alloys of Fe in Au and in some other alloys of transition elements in noble metals, is evidence of long-range interaction between isolated magnetic atoms which extends to at least 30 or 40 lattice spacings, with large internal fields existing at the magnetic atom sites. This interaction occurs through the intermediary action of the conduction electrons of the host noble metal, but only at a low enough temperature that it is not broken up by the lattice vibrational energy. We can look at it this way: the interaction is dependent on a conduction electron being scattered successively by two impurity atoms, and this requires that the electrons are not too strongly scattered by phonons. If we denote the energy of the interaction between impurity atoms by W, the interaction will then only be significant when W/kT is not small. Experimentally, it appears that this condition only exists below about 20K.

At the same time, there is a second interaction, which is the one considered by Rivier and Zuckerman (1968). This is between the conduction electrons and individual impurity

spins and if we denote its energy by U, a bound state, often referred to as the Nagaoka bound state, will exist when U/kT is large; when $U/kT \sim 1$ the condition, described by Rivier and Zuckerman, of continual formation and breakdown of this state will exist. Thus, $U \simeq kT_K$ where T_K is the Kondo temperature. This interaction effectively competes with the impurity-impurity interaction W, so that if $U > W$ the impurity-impurity interaction will not occur, or will be weakened. On the other hand, because the interaction U with individual impurity spins is relatively short-range, as compared to the impurity-impurity interaction W, it would seem that the U interaction could occur, provided $T \lesssim T_K$ even when $U < W$, and that in forming, it would act to screen out the long-range impurity-impurity interaction. This would seem to mean that the energy W of the long-range impurity-impurity interaction is decreased by this screening.

The result of these two separate interactions, involving the conduction electron spins, is that the impurity-impurity interaction will only be strong enough to produce an increase in thermoelectric power with applied field when both $W/kT > \sim 1$ and $U/kT < \sim 1$, except that if W is appreciably greater than U so that a strong impurity-impurity interaction exists over a range of $T > T_K$, it will

persist below T_K for $U/kT > 1$, but be progressively screened out as T is decreased. Thus, the increase in thermoelectric power with applied field is not observed in dilute alloys of Fe in Cu for which $T_K \approx 18K$, because there is no temperature range within which the long-range interaction is neither screened out by the bound state, nor broken up by lattice energy. It seems, in fact, that in Cu Fe alloys, W and U are about equal so that a weak long-range impurity-impurity interaction does exist, which is sufficient to give a concentration dependence to the magnetothermopower. The increase in thermoelectric power with applied field has been observed in Au Fe and Au Mn and will probably be seen in Au Cr, Ag Mn, Cu Mn and Cu Cr alloys, for all of which $T_K < 2K$ and in which Mössbauer experiments have shown that large internal fields exist.

2. A simple interaction between pairs of Fe atoms with a single valued internal field at the Fe atom sites is intuitively too simple, but no satisfactory theory for a field distribution has yet been proposed. A probability field distribution proposed by Klein is not capable of explaining the experimental results either of Mössbauer experiments or of the effects of applied magnetic fields on the thermoelectric powers of dilute alloys; in particular, it yields too high probabilities for low and zero

field. Its apparent success in explaining specific heat results is perhaps because these are less sensitive to the details of the field distribution. The fact that a single valued pair model gives predictions which are close to agreement with experimental results may, hopefully, give some guidance in seeking a theoretical solution to this problem of finding the proper field distribution function.

3. Analysis of the experimental results has demonstrated the need for extreme purity, particularly in the most dilute alloy specimens, and for having precise information on all residual impurities in the alloys. It has also demonstrated the need for extreme care in specimen handling and heat treatment, in which each alloy has its own peculiar metallurgical requirements. Methods of preparing and of purifying specimens in the form of wires, requiring the minimum of subsequent handling, by what may be described as diffusion chemistry, has proved to be successful.

4. The change in the measured thermoelectric power of Au Fe and Cu Fe alloys due to what is believed to be a superconducting transition in Pb present to the extent of a few parts per million, appears to support the theory

that electron scattering at normal/superconducting boundaries does not add to the electrical resistivity of the alloy. This theory predicts that electrons are reflected as holes from such boundaries. Further work is needed to verify this conclusion. Magneto-resistance measurements and examination of the alloy specimens by electron microscope are obvious suggestions. These could be followed by preparation and testing of Au Pb Fe alloys of various composition.

APPENDIX 1

DESIGN OF QUARTZ ROD HEATER COILS h_1 AND h_2

Each of the heaters h_1 and h_2 was formed using 1 meter of .001 inch diameter insulated manganin wire, giving a total resistance of about 1000 ohms. This was double wound, starting near the free ends so that the two halves twisted together as they were wound on to give a non-inductive coil. The whole coil was cemented together and in place, using Eastman 910, which proved to be a good low temperature cement. This cement is a low viscosity liquid whose speed of setting increases as the thickness of its layer decreases; in bulk it may be stored for months; in a layer of the order of a micron thick it sets in a fraction of a second. Capillary action, combined with its low viscosity, causes it to spread out rapidly between surfaces to be joined. The good low temperature behaviour doubtless results from the extreme thinness of the bonding layer.

The supply circuit for the heaters, which is shown included in fig. 2-7, was designed so that the input power $P = IV = I^2R$, where I is the current through the heater of resistance R and V is the voltage developed across it, would

be independent of small changes in R. This was done by including a series resistance R_o which, with the effective source impedance of the potentiometer r, would equal the resistance R of the heater. With the values chosen, the error in P would not exceed 0.1% for a 6.5% change in R at any setting of the potentiometer r. This made it unnecessary to measure P independently for both heaters and gave reasonable confidence that P would not change, and hence that ΔT would remain constant within acceptable limits, during experiments involving the application of magnetic fields, when magnetoresistance effects in h_1 could be expected to occur. For manganin in a field of 50 KOe, $\Delta R/R$ is only about 4% (Kopp, private communication).

APPENDIX 2

HEAT LEAKS TO QUARTZ ROD AND THERMOCOUPLE CONTACTS

a. Heat Leak by Radiation see fig. A2-1

Net heat dQ absorbed by element dx of radiation shield at temperature T from can C at liquid helium bath temperature T_1 is

$$dQ = A.2\ \pi r(T_1^4 - T^4)\ dx \lesssim A.2\ \pi r(T_1^4 - T_o^4)\,dx$$

therefore heat flow Q(x) along the can at x is given by

$$Q(x) = \int_x^{x_1} dQ \lesssim 2\ \pi rA(T_1^4 - T_o^4)\ (x_1 - x)$$

If the thermal resistance of unit area of the Wood's metal joint is ρ cm^2 K/W and $S = 2\pi r'\ell$ is the area soldered where r is the radius of the can at the soldered joint and ℓ is the length in the x direction over which the soldered joint extends, then the temperature drop across this joint due to the heat flow Q(o) is

$$\delta T(o) = \frac{Q(o)\rho}{S} \lessapprox \frac{2\ \pi rA(T_1^4 - T_o^4)x_1\rho}{2\pi\ r'\ell} = \frac{r}{r'}\ \frac{A\rho}{\ell}\ (T_1^4 - T_o^4)x_1$$

The heat flow also produced a temperature gradient dT/dx along the can given by

$$\frac{dT}{dx} = -\frac{Q(x)}{2\pi rtK} \lessapprox -\frac{A}{tK}(T_1^4 - T_o^4)\ (x_1 - x)$$

where K is the thermal conductivity of copper. The can at

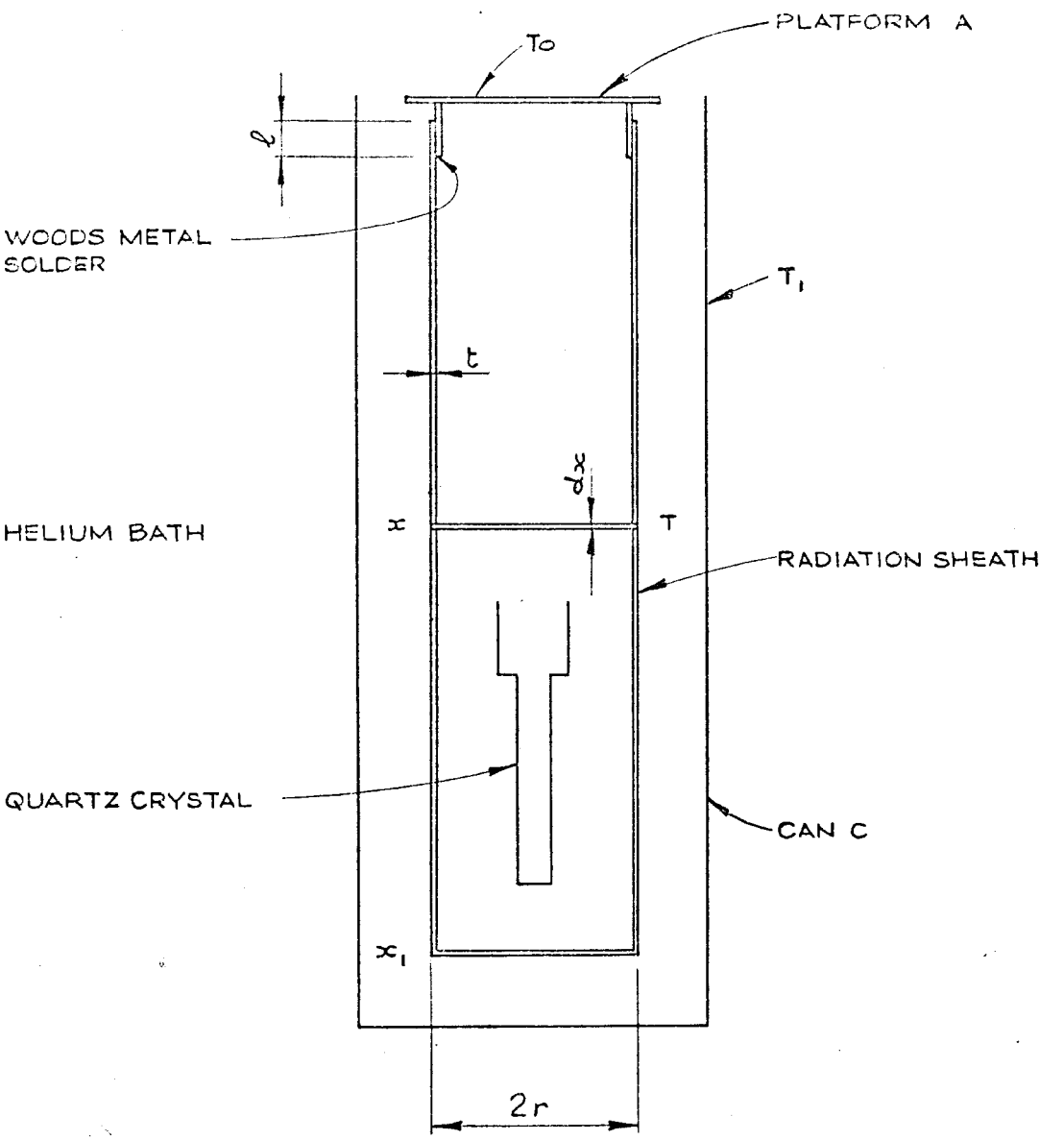

DIAGRAM OF RADIATION SHIELD
FOR CALCULATION OF HEAT LEAK
BY RADIATION TO QUARTZ ROD

FIGURE A2-1

x is therefore hotter than the can at the soldered joint at x=o by $\delta T(x)$ where

$$\delta T(x) = \int_o^x \frac{dT}{dx}\, dx \leq \frac{A}{tK} (T_1^4 - T_o^4)(x_1 x - \tfrac{1}{2}x^2)$$

The radiation shield at x is therefore hotter than the platform A by an amount δT given by

$$\delta T = \delta T(o) + \delta T(x) \leq \frac{rA\rho}{r'\ell} (T_1^4 - T_o^4) x_1 + \frac{A}{tK} (T_1^4 - T_o^4)(x_1 x - \tfrac{1}{2}x^2)$$

This is a maximum at $x = x_1$ giving

$$\delta T_{max} < A(T_1^4 - T_o^4) \left\{ \frac{r\rho x_1}{r'\ell} + \frac{x_1^2}{2tK} \right\}$$

Inserting values t = .05 cm, K = 2 W/cmK (for electrolytic tough pitch copper), x_1 = 17.5 cm, ρ = 800 cm^2K/W, ℓ = 0.5 cm, r = .953 cm, r′ = 2.70 cm, T_1 = 4.2K and assuming the minimum value for T_o = 1.2K and the maximum possible value of A for a perfect black body, $A = 5.68 \times 10^{-12}$, we find δT_{max} <20 micro K and clearly any heat leak from the shield can not cause a temperature error at e_2 greater than this.

b. Heat Leak Along Thermocouple Wires. see fig.A2-2

Temperature of a thermocouple wire at its thermal anchor is $T_o + \Delta T$ where

$$\Delta T = (T_1 - T_o) \frac{R_1}{R_1 + R_2}$$

in which R_1 is the thermal resistance of the anchor and R_2

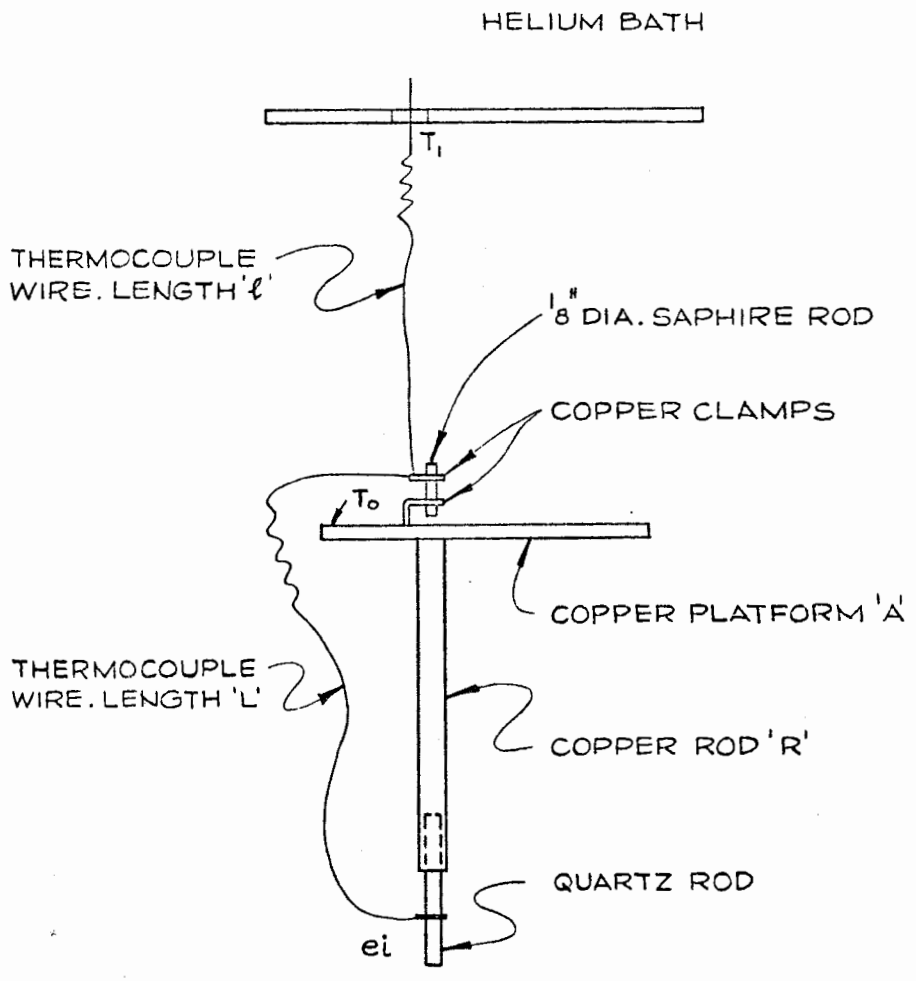

DIAGRAM OF THERMAL ANCHORS
FOR CALCULATION OF HEAT LEAKS
ALONG THERMOCOUPLE LEADS
FIGURE A2-2

is the thermal resistance of the thermocouple wire between the He bath at temperature T_1 and the anchor.

The maximum value of ΔT will occur at the minimum T_o which, in our experiment, was 1.2K.

For Au-Fe wire Berman et al (1964) give the thermal conductivity at 4K as 0.4W/cm K and at 1K as 0.1 W/cm K, the diameter of our Au-Fe wires was .008 cm. and the length between the He bath and the anchor was approximately 10 cm.

$$\therefore R_2 \simeq 7.4 \times 10^5 \text{ K/W} \quad \text{when } T_o = 1.2\text{K}.$$

For Supercon wires with .001 inch copper cladding on .005 inch diameter superconducting core and assuming a mean thermal conductivity for the copper of 2.7 W/cm K

$$R_2 \simeq 3.0 \times 10^4 \text{ K/W}$$

For the thermal anchors consisting of a 1/8 inch diameter sapphire rod held in copper clamps, Brock (1965) gives the thermal resistance at 1.2K as about 1200 K/W. This is principally the contact resistance between the sapphire and the copper. We improved the contacts by rubbing Indium on to the surface of the sapphire. Neeper and Dillinger (1964) measured the resistance of Indium-sapphire junctions between 1.1 K and 2.1 K and, expressing their results as conductivity per square cm. K_a, they

fitted the relation

$$K_a = \frac{T^{2.85}}{28} \quad W/cm^2\ K$$

For our anchors this gives a thermal contact resistance of 35 K/W for each copper clamp at 1.2K. Under these conditions the thermal resistance of the sapphire becomes important and for sapphire, Brock (1965) gives a thermal conductivity at 1.2K of 45 mW.cm K. With 1/4 inch maximum spacing between the clamps, this gives a thermal resistance of 180 K/W and therefore a total resistance R_1 per anchor of 250 K/W. This is in reasonable agreement with results obtained by Brock on an Indium vice which he used to clamp a silicon rod.

The predicted values of the temperature difference ΔT across the anchors which will be a maximum when T_o = 1.2K are:

$$\Delta T \lesssim 25 \text{ mK for the supercon anchors}$$

$$\lesssim 1 \text{ mK for the Au-Fe anchors.}$$

The resulting error at the quartz rod contact e_2 will be less than this, depending on the relative thermal resistances of the wires leading down from the anchors and the resistance of the quartz rod, including its contacts.

From the thermal anchors to the contact e_1 the wire lengths L were about 25 cm and each of the supercon wires

had the copper cladding removed over a length of more than one cm. Radhakrishna and Nielsen (1963) give the thermal conductivity at 1.2K of Niobium containing 0.2 at.% Zirconium as 2.2 mW/cm K and with 2.0 at.% Zr as 1.9 mW/cm K. The core of the supercon wire was Niobium with 25 at.% Zr and it is therefore reasonable to assume that its thermal conductivity is not greater than 2 mW/cm K. The thermal resistance of the supercon wires was therefore $\geq 4 \times 10^6$ K/W. The thermal resistance of 25 cm. of the Au-Fe wire was also $\simeq 4 \times 10^6$ K/W at 1.2K.

The contacts e_i were made as described by Huntley (1963) using 12 strands of copper wire wrapped around the quartz rod, twisted to tighten and glued in place. Measurements made by Huntley indicate a thermal resistance between these contacts and the quartz rod of approximately 1600 K/W. The thermal conductivity of the quartz rod was measured and found to be the same as reported by Brock (1965), who gives a value 0.4 mW/cm K at a temperature of 1.2K and increasing roughly in proportion to the temperature. The cross sectional area of the quartz rod used in the earlier experiments was .035 cm^2 and the length from e_2 to the copper rod R (at x = o) was 1.925 cm. Thus its thermal resistance at 1.2K between e_2

and the copper rod was 1.4×10^5 K/W. The quartz rod used in the later experiments and in the final check calibration had a cross section area .20 cm^2 and length from e_2 to the copper rod of 1.79 cm; its thermal resistance at 1.2K was therefore $.224 \times 10^5$ K/W.

The quartz rod was inserted into the copper rod R to a depth of 1.5 inches, as shown in fig. A2-3. The gap between the quartz and the copper was nowhere greater than .003 inch and was filled completely with Araldite, care being taken to ensure that all air was excluded so that there were no empty gaps; this was done by first filling the hole in the rod R with Araldite, then heating it to reduce the Araldite viscosity before pushing in the quartz rod. The thermal resistance between the quartz rod at x = o and the copper rod R consists of contact resistance between the layers and the resistance of the Araldite layer and of the part of the quartz rod inserted into the copper. It may be computed as follows:

Heat -dQ flowing out from element of quartz rod dx at x is a function of the contact resistance ρ_1 between the quartz and the Araldite, the thickness t of the Araldite layer and its thermal conductivity K_a and the contact resistance ρ_2 between the Araldite and the copper; it is related to the

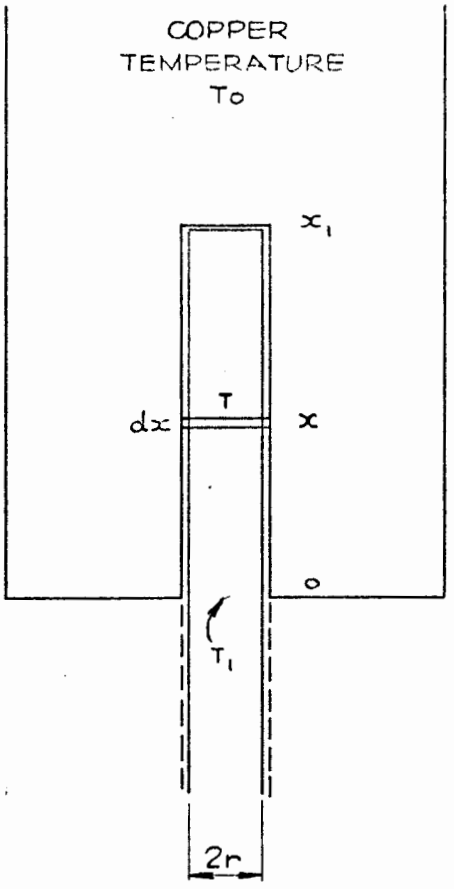

DIAGRAM OF QUARTZ ROD~
COPPER ROD JUNCTION
FOR CALCULATION OF THERMAL RESISTANCE

FIGURE A2-3

temperatures through the layer by:

$$T - T' = -\frac{\rho_1}{2\pi r}\frac{dQ}{dx}$$

$$T' - T_o' = -\frac{t}{2\pi r\, Ka}\frac{dQ}{dx}$$

$$T_o' - T_o = -\frac{\rho_2}{2\pi r}\frac{dQ}{dx}$$

where T is the temperature of the quartz at x

T' " " " " " Araldite at x adjacent to the quartz

T_o' " " " " " Araldite at x adjacent to the copper

T_o is the temperature of the copper.

$$\therefore T - T_o = -\frac{t/K_a + \rho_1 + \rho_2}{2\pi r}\frac{dQ}{dx}$$

Heat flow Q(x) along the quartz rod at x having thermal conductivity K_q is

$$Q(x) = -\pi r^2 Kq \frac{dT}{dx}$$

$$\therefore \frac{dQ}{dx} = -\pi r^2 Kq \frac{d^2T}{dx^2} - \frac{2\pi r}{t/K_a + \rho_1 + \rho_2}(T - T_o)$$

This can be solved to give

$$T - T_o = (T_1 - T_o)e^{-\alpha x} \quad \text{where } \alpha = \sqrt{\frac{2}{rKq(t/K_a + \rho_1 + \rho_2)}}$$

therefore the thermal resistance between the quarts rod at x = o and the copper rod is $\frac{T_1 - T_o}{Q(o)} = \frac{1}{\pi r}\sqrt{\frac{t + (\rho_1 + \rho_2)Ka}{2\ r\ Ka\ Kq}}$

This calculation has been simplified, using one dimensional heat flow equations by assuming no radial temperature gradient inside the quartz. In view of the low thermal conductivity of quartz, this is clearly not correct but the resulting error in the computed thermal resistance should not be too great, provided the length of the quartz rod inserted into the copper is large compared to its radius.

Huntley (1963) gives experimental values obtained with sapphire and ruby rods 0.25 cm diameter: he found thermal resistances of about 1000 K/W at 1.2K. Applying this to the above formula we find $\rho_1 + \rho_2 = 1760$ cm^{2}K/W so that for any reasonable values of t and Ka their ratio t/Ka can be neglected in comparison to the contact resistances $\rho_1 + \rho_2$ and the formula simplifies to

$$\frac{T_1 - T_o}{Q(o)} = \frac{1}{\pi r}\sqrt{\frac{\rho_1 + \rho_2}{2\ r\ Kq}} = \text{junction resistance.}$$

For the smaller diameter quartz rod r = .10 cm, Kq = .0004 W/mK at 1.2K, the formula gives a junction resistance of 15,000 K/W. For the larger diameter rod, r = .25 cm and the junction resistance is 3800 K/W.

The maximum error in the temperature at e_2 which is due to heat leaks along the thermocouple wires connecting to e_1

and e_2 when T_o = 1.2K is thus approximately

$$2 \times \frac{25 \times 1.5 \times 10^5}{4 \times 10^6} = 1.9 \text{ mK}$$

for the small diameter quartz rod and approximately 0.3 mK for the larger rod.

In an attempt to detect a difference experimentally, the Au-Fe secondary reference wire was re-calibrated when connected between the copper post L on the platform A and the He bath, and this was compared with the previous calibration with the wire connected between e_2 and the He bath. No error could be detected attributable to this cause.

c. Heat Leaks along Manganin Heater Wires

The wires leading to the heaters h_1 and h_2 were 40 a.w.g. manganin and each lead was tightly wrapped twice around the gas thermometer bulb G and glued in place with Eastman 910. Thermal resistance of 10 cm. of 40 a.w.g. manganin wire between the He bath and the gas thermometer is approximately 10^7 K/W, assuming a thermal conductivity for manganin of .006 W/cm K.

Compared to this, the thermal resistance between the gas thermometer bulb and the two turns of the manganin wire wound around it is only about 100 K/W: this is computed for a gas thermometer bulb diameter of 2.54 cm, wire radius .005 cm.

mean spacing between wire and bulb .003 cm and thermal conductivity of the glue of .4 mW/cm K.

These resistances indicate that the heater leads are only a few micro-K above the temperature of the gas thermometer when not being used to supply heat and could make no detectable contribution to any calibration error.

APPENDIX A3

THERMAL RESISTANCES OF Au-Fe SPECIMENS AND THERMAL DIFFUSION TIMES

At low temperatures, where the scattering of electrons in metals is dominated by impurity scattering, the thermal conductivity K_a is proportional to the temperature T and is given by

$$K_a = \frac{L\,T}{\rho_r}$$

where L is the Lorentz constant = 2.45×10^{-8} W ohm/K^2 and ρ_r is the residual electrical resistivity.

For the Au-Fe alloy containing nominally .03 at.% Fe with residual resistance ratio $(\rho_r/\rho)_{20} = 0.125$, as given in table 3.1, this gives $K_a = .089\ T$, in reasonable agreement with the experimental results reported by Berman et al (1964). Using this formula for the other Au-Fe alloys, with the resistance ratios given in table 3.1, we obtain the thermal resistances R_a for the other alloy specimens. These are tabulated below. The thermal resistances of the appropriate quartz rods on which they were mounted between contacts e_1 and e_3 are tabulated for comparison, together with the specimen thermal diffusion times τ, calculated using the formula $\tau = \frac{c\ell_a^2}{K_a}$

where C is the specific heat of the alloy and l_a the length of the specimen. Since we do not need to know the thermal diffusion times with great accuracy, the lattice specific heat C_v may be calculated using the Debye expression which, for $T \leq \theta_D/20$ can be written

$$C_v = 464.5\left(\frac{T}{\theta_D}\right)^3 \text{calories/gram atom K}$$

where θ_D is the Debye characteristic temperature, which for gold is 185 K. At 4.2K, this gives C_v =.0172 calories/gram atom K. The electronic specific heat $C_e = \gamma T$ is small compared to this being given as 1.8×10^{-4} (see Daunt, 1955, Chapter XI).

In the tabulation below, the values of τ are given, calculated for 4.2K. At lower temperatures the values of will be smaller because C_v is proportional to T^3, whereas K_a is proportional only to T.

Specimen	Thermal Resistance of Quartz Rod, R_s K/W	Thermal Resistance of Alloy specimen R_a K/W	Thermal Diffusion Time in Specimen at 4.2K Seconds
Au+230 ppm at.Fe	$2.3 \times 10^5/T$	$10^7/T$	46
Au+ 43 ppm at.Fe	$2.2 \times 10^5/T$	$1.5 \times 10^6/T$	7
Au+0.54 " at.Fe	"	$1.5 \times 10^5/T$	0.7
Au+<16 " at.Fe	"	$1.3 \times 10^5/T$	0.6

It can be seen that, for the two most dilute alloys, their thermal resistance is of the same order as that of the quartz.

APPENDIX A4

SOLDERS IN HIGH MAGNETIC FIELDS

It is important that any materials used in the measuring circuits at liquid helium temperatures which are located in the vicinity of the magnet should not pass through a superconducting transition at any combination of field and temperature occurring during the experiments. This principle applies to both the electrical and thermal circuits since both electrical and thermal resistances change abruptly on passing through the transition.

Special solders have therefore to be used at all the thermojunctions and at all points in the direct path of the heat flow from the crystal to the helium pot P. At the crystal contacts e_i which are located in the maximum field, a special solder composed of Bi and Cd may be used, which does not become superconducting within the temperature range covered by these experiments. (See Cochran et al, 1956, also Fassnacht et al, 1967). This solder is a eutectic mixture with a melting point of $140.5^{\circ}C$ and consists of

Bismuth	61.4% by weight
Cadmium	38.6% by weight.

This solder was also used at the thermal anchors located on the platform A and at any joints in the copper rod R. It has the disadvantage that it has to be kept within a very narrow temperature range during use, because if the temperature is raised appreciably above the melting point of the eutectic, one of the constituents oxidises and the solder composition changes; this is observed as a surface blackening and, of course, a progressive rise in the temperature at which the solder melts.

At the helium bath thermojunctions, located at the top of the vacuum can C, which never go below a temperature of about 4K, pure Indium metal could be used as a solder and was preferable to the Bi-Cd solder because it was easier to use.

APPENDIX A5

LIQUID HELIUM LEVEL GAUGE

A foamed polystyrene dewar with a copper liner was used for liquid nitrogen, surrounding the helium dewar, and it was therefore not possible to see the level of the liquid helium. Attempts were accordingly made to construct a superconducting level gauge which would give a panel meter readout of the liquid helium level.

The design first tried was a double open spiral of Nb-Zr superconductor wound down and back along a 1/16 inch diameter stainless steel rod with insulating layers of shrinkable teflon tubing. The total resistance just above the superconducting transition temperature was about 50 ohms. This gauge was calibrated by inserting it to known depths in a helium storage dewar and appeared capable of reading to an accuracy of better than 1 cm.

This gauge was installed in the helium dewar and was found to operate quite satisfactorily under equilibrium conditions, but when the dewar was being filled it was found to be completely useless because the helium boil-off was then sufficiently rapid to fill the whole dewar above the liquid with gas at, or only slightly above 4.2K, so

that the whole Nb-Zr wire went superconducting.

A second design was therefore tried, using Ta wire in place of the Nb-Zr, and was found to operate satisfactorily during the filling operation. Under equilibrium conditions, however, the resistance of the Ta wire changed drastically because, unlike the Nb-Zr, the pure Ta metal had a large temperature coefficient of resistance. This second design was retained because it was during filling that the liquid helium depth information was most needed. As the helium slowly evaporated during subsequent operation of the system, the depth could be checked periodically by dipping with a stainless steel tube in a conventional manner.

It would seem that a combination of two gauges, one of Ta and one of Nb-Zr, could be quite convenient and useful.

APPENDIX A6

MEASUREMENT OF RESIDUAL RESISTANCE RATIOS AND CALCULATION OF BULK RESISTANCE RATIO

The Tinsley potentiometer was used to measure the resistance at room temperature and at liquid helium temperature and hence the resistance ratio $(\rho_r/\rho)_{20} = \rho_{4.2}/(\rho_{293} - \rho_{4.2})$ of all the alloys which were investigated. This was done by comparison with a standard 1 ohm resistor and using the four wire method, with the current supply which is shown included in Fig. 2.6.

For some of the gold specimens it was important not to use solder, or to contaminate the specimens in any way, because we wished to give them further Cl_2 or heat treatment after measurement. A special holder was therefore constructed to provide purely mechanical contacts, as illustrated in fig. A6.1. After assembly, with a specimen laid across the four gold contact wires, this unit was firmly wrapped with Teflon tape.

One or more of the four contacts sometimes failed on cooling, but if they held on precooling in liquid N_2, they rarely opened up on transferring into liquid helium.

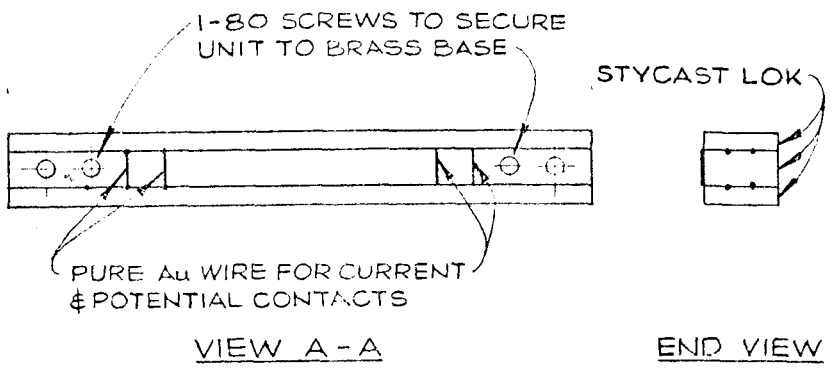

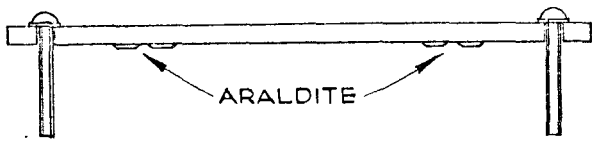

CLAMPING PLATE

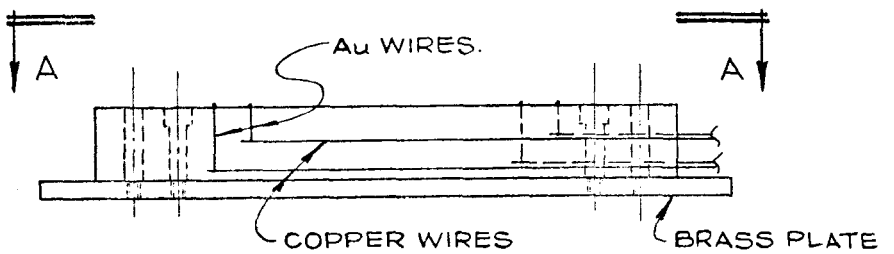

ELEVATION
CONNECTION BLOCK

SPECIMEN HOLDER FOR MEASUREMENT OF RESIDUAL RESISTANCE RATIO
FIGURE A6-1

Bulk Resistance Ratio

Because the specimens measured were in the form of small diameter wires, some of the residual resistivities contained an appreciable contribution from boundary scattering. Sondheimer (1952) gives the theoretical relationship between the measured and bulk resistivities for a wire of radius "a" as

$$\frac{\rho_r}{\rho_{or}} = \frac{(\rho_r/\rho)_{20}}{(\rho_{or}/\rho)_{20}} = \frac{1}{1 - \frac{12}{\pi}\int_0^1 (1-t^2)^{1/2} S_4(Kt)\,dt}$$

where

$$S_4(u) = \int_1^\infty e^{-ux}(x^2-1)^{1/2} x^{-4}\,dx$$

and K is the ratio of the wire diameter to the electron mean free path λ in the metal

$$K = \frac{a}{\lambda} = a\left(\frac{\sigma_{or}}{\lambda}\right)\left(\frac{\rho_{or}}{\rho}\right)_{20}\cdot\rho$$

where σ_{or} is the bulk residual conductivity of gold = $1/\rho_{or}$

Chambers (1952) gives an experimental value for the ratio of the bulk conductivity to the electron mean free path in gold as $\frac{\sigma_{or}}{\lambda} = 8.4 \pm 0.4 \times 10^{10}$ 1/ohm cm^2.

Sondheimer evaluated his integrals for a wide range of K values and gives a tabulation of resistivity ratio ρ_r/ρ_{or} From this we have plotted $(\rho_{or}/\rho)_{20}$ versus $(\rho_r/\rho)_{20}$ in figure A6.2 for both a = .004 cm and for a = .005 cm.

Figure A6.2
Measured vs bulk residual resistance ratios
of Au wires of diameter "a".

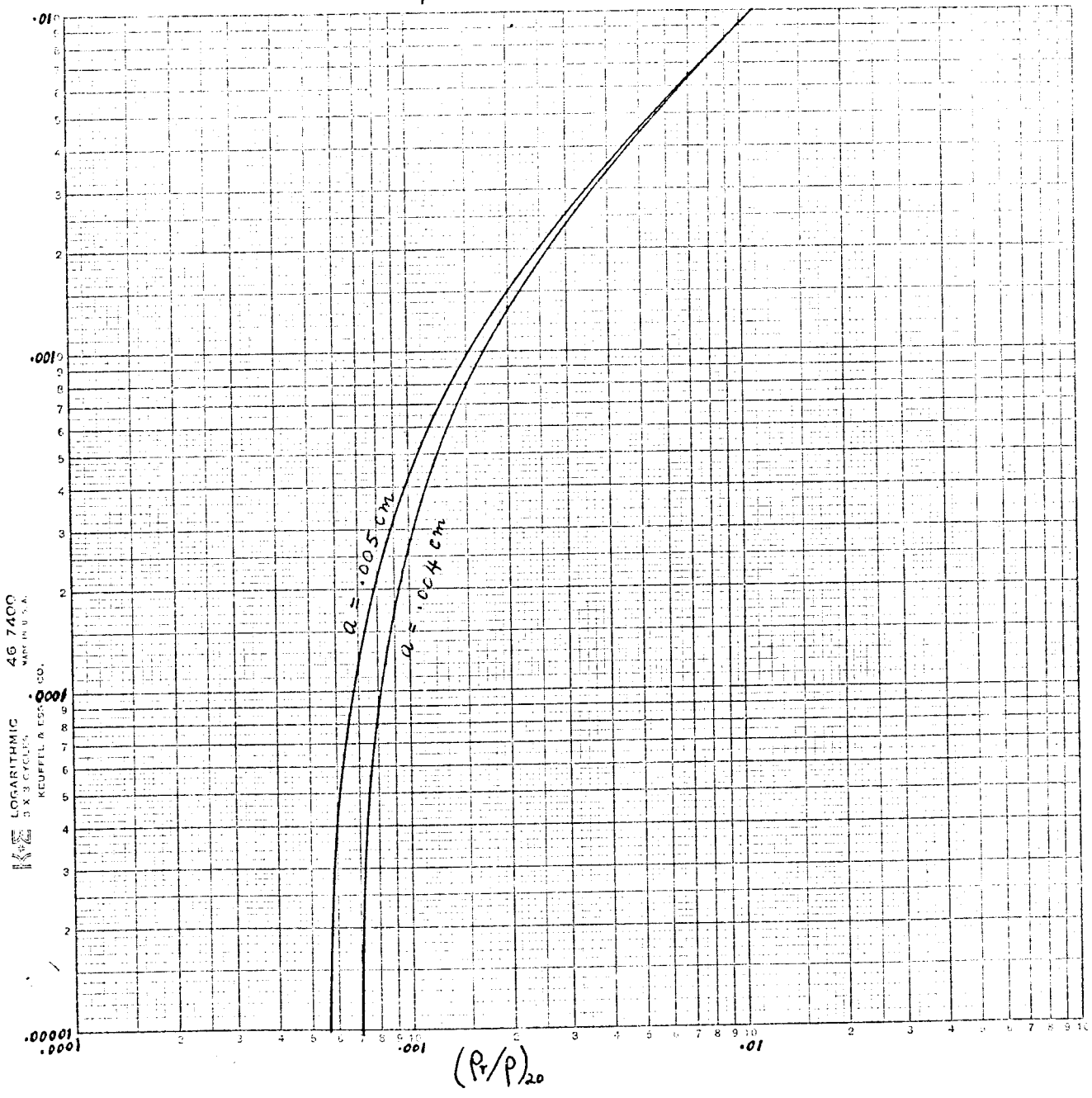

This graph was then used to obtain the bulk ratios given in table 3.1

APPENDIX A-7

RESIDUAL RESISTANCE RATIO DUE TO OTHER IMPURITIES IN Au Fe ALLOYS

The Au-Fe alloy wire used in the experiments had the nominal specification, as supplied by Johnson-Matthey, of being spectroscopically pure Au, plus .03 at.% Fe.

Analysis by P. Tymchuk, Analytical Section, Division of Applied Chemistry, National Research Council, Ottawa, showed that it contained (see table 3.2):

250 p.p.m. atomic Fe

100 to 130 p.p.m. atomic Sn

10 to 20 p.p.m. atomic Pb

7 p.p.m. atomic Si

MacDonald et al (1962) have shown that the incremental residual resistance ratio per atomic % Sn in Au is 1.365, giving an incremental residual resistivity of 3.0 $\mu\Omega$cm/at.% Sn.

Norbury (1922) showed that the incremental resistivities due to Pb and Sn in Au are about equal, in accord with Norbury's rule, since Sn and Pb are in the same group in the periodic table.

Based on this data, the residual resistance ratio due to Sn and Pb impurities in our wire as received from Johnson-Matthey would be .0178 $\pm$ .0022. This is used in table 3.1.

Analysis of a wire sample which had been treated with Cl_2 for 25 hours at 850°C showed (see table 3.2) that the Sn and Pb impurities had been removed, as well as the Fe, and for such samples no allowance has to be made for these impurities in table 3.1. This analysis showed also that the Si impurity content was unchanged. Any contribution to the residual resistance ratio due to Si was therefore present in all the samples and so is included in table 3.1, with the effects of crystal lattice defects.

It is interesting to note that, according to Norbury's rule, Si should have the same incremental resistance ratio as Sn and Pb. According to this, 7 p.p.m. atomic Si would have a ratio of .00095, equal to the bulk value found for the most highly purified samples of the Johnson-Matthey wire after being cooled slowly from 850°C.

The problem remains to estimate the amount of Sn and Pb impurities in the other treated samples, which will depend on the rate of removal of the Sn and Pb by the Cl_2 treatment. It is expected that this will be diffusion-limited, for the same reasons as for Fe. Both stannous and stannic chlorides boil below 850°C. Lead chloride boils at 950°C and must have appreciable vapour pressure at 850°C. Unfortunately, there is no data in the literature on the diffusion rates of

Sn and Pb in Au, but Jost (1960) gives data for Sn in Cu and in Ag, which are chemically similar metals to Au, and for these the diffusion constants D are:-

5.6 at.% Sn in Cu at 850°C, $D=3.9 \times 10^{-9}$ cm^2/sec

conc. 0 at.% Sn in Cu at 850°C, $D=1 \times 10^{-9}$ to 2×10^{-9} cm^2/sec

2 at.% Sn in Ag at 850°C, $D=4.9 \times 10^{-9}$ cm^2/sec.

If these diffusion rates can be taken as a guide, they indicate that the diffusion of Sn in Au is at least two to four times faster than Fe in Au. Corroborative data are supplied by the only non-magnetic impurities for which diffusion data in both Cu and Au are available. These are Pt and Pd, for which the rates in Cu and Au are equal within 10% and are about the same as for Sn.

On the basis of this limited information, the Cl_2 treated samples would all contain less than 1 p.p.m. atomic Sn and its contribution to their residual resistance ratios can be neglected. This has been assumed in compiling table 3.1. Perhaps the best support for this assumption lies in the consistent interpretation it yields for the thermoelectric power data.

There is no information available in the literature which could enable us to estimate the diffusion rate of Pb

in Au. Hansen (1958), however, states that Pb has zero solubility in Au below 500°C, so that an alloy cooled slowly from 850°C would contain no Pb in solution. Again, therefore, we have assumed in table 3.1 that Pb will make no contribution to the residual resistance ratios of any of the samples which were cooled slowly.

REFERENCES

Abrikosov, A.A. (1965) Physics 2, 5

Bean, C.P., Doyle, M.V. and Pincus, A.G. (1962)
Phys.Rev.Letters 9, 93

Berman, R. and Huntley, D.J. (1963) Cryogenics 3, 70

Berman, R., Brock, J.C.F. and Huntley, D.J. (1963)
Phys. Letters 3, 310

Berman, R., Brock, J.C.F., and Huntley, D.J. (1964)
Cryogenics 4, 233

Berman, R., Kopp, J., Slack, G.A. and Walker, C.T. (1968)
Phys. Letters 27A, 464

Borelius, G., Keesom, W.H., Johansson, C.H. and Linde, J.O.
(1930)
Proc. Acad.Sci.Amsterdam 33,32

Borelius, G., Keesom, W.H., Johansson, C.H. and Linde,J.O.
(1932)
Proc. Acad.Sci.Amsterdam 35,15,25

Borg,R.J., Booth, R. and Violet, C.E. (1963)
Phys. Rev. Letters 11, 469

Brock, J.C.F. (1965) Thesis, Oxford

Brock, J.C.F. and Huntley, D.J. (1968) Can.J. Phys. 46, 2231

Chambers, R.G. (1952) Proc. Roy. Soc. A215, 481

Cochran, J.F., Mapother, D.E., and Mould, R.E. (1956)
Phys. Rev. 103, 1657

Coles, B.R. (1964) Phys. Letters 8, 243

Daunt, J.G. (1955) Progr. in Low Temp.Phys. North Holland, Amsterdam

Daybell, M.D. and Steyert, W.A. (1968) Rev.Mod.Phys. 40, 380

Daybell, M.D. and Steyert, W.A. (1968b) Phys.Rev. 167, 536

Daybell, M.D., Pratt, W.P. and Steyert,W.A. (1969) Phys.Rev. Letters 22, 401

DuChatenier, F.S. and Miedema, A.R. (1966) Physica A32, 403

Fassnacht, R.E., and Dillinger, J.R. (1967) J.Appl.Phys. 38, 3667

Fischer, K.H. (1968)Proc. 11th Conf.Low Temp.Phys. (St. Andrews)

Foiles, C.L. (1968) Phys.Rev. 169, 471

Franck, J.P. and Martin, D.L. (1961) Can.J. Phys. 39, 1320

Gainon, D., Donzé, P. and Sierro, J. (1967) Solid State Commun. 5, 151

Gold, A.V., MacDonald, D.K.C., Pearson, W.B. and Templeton, I.M. (1960) Phil. Mag. 5, 765

Gonser, U., Grant, R.W., Meecham, C.J., Muir, A.H. Jnr. and Wiedersich, H. (1965) J. Appl. Phys. 36, 2124

Hansen, M. (1958) Constitution of Binary Alloys, McGraw Hill, N.Y.

Henry, W.E., (1963) Phys. Rev. Letters 11, 468

Huntley, D.J. (1963) Thesis, Oxford

Huntley, D.J. and Walker, C.W.E. (1969) Can.J. Phys. 47, 805

Jost, W. (1960) Diffusion in Solids, Liquids and Gases. Academic Press, N.Y.

Kjekshus, A. and Pearson, W.B. (1962) Can. J. Phys. 40, 98

Klein, M.W. and Brout, R. (1963) Phys.Rev. 132, 2412

Klein, M.W. (1964) Phys. Rev. 136, A1156

Kondo, J. (1964) Progr. Theor. Phys. 32, 37

Kondo, J. (1965) Progr. Theor. Phys. 34, 372

Kopp, J. (1969) Thesis, Oxford

Kubaschewski, O, and Ebert, H. (1944) Z. Elechtrochem.50,138

Loram, J.W., Ford, P.J. and Whall, T.E. (1970)
J. Phys. Chem. Solids, 31, 763

MacDonald, D.K.C., and Pearson, W.B. (1957)
Proc. Roy. Soc. A241, 257

MacDonald, D.K.C., Pearson, W.B., and Templeton, I.M. (1962)
Proc. Roy. Soc. A266, 161

Maki, K. (1969) Progr. Theor. Phys. 41, 586

Margenau, H. and Watson, W. (1936) Rev. Mod. Phys. 8, 22

Marshall, W. (1960) Phys. Rev. 118, 1519

Marshall, W., Cranshaw, T.E., Johnson, C.E. and
Ridout, M.S. (1964)
Rev. Mod. Phys. 36, 199

Monod, P. (1967) Phys. Rev. Letters 19, 1113

Montgomery, D.B. (1963) Rep. Progr. Phys. 26, 69

Muto, Y. Noto, K., and Hedgcock, F.T. (1964)
Can.J. Phys. 42, 15

Nagaoka, Y (1965) Phys. Rev. 138, A1112

Nagaoka, Y (1965) Physics 2, 39

Nagasawa, H. (1968) J. Phys. Soc. Japan 25, 691

Neeper, D.A. and Dillinger, J.R. (1964) Phys.Rev.135,A1028

Norbury, A.L. (1922) Trans. Faraday Soc. 16, 570

Nordheim, L. and Gorter, C.J. (1935) Physica 2, 383

Overhauser, A.W. (1959) Phys. Rev. Letters 3, 414

Overhauser, A.W. (1960) J. Phys. Chem. Solids 13, 71

Overhauser, A.W. (1963) J. Appl. Phys. 34, 1019

Pearson, W.B. andTempleton, I.M. (1961) Can. J. Phys. 39,1084

Radhakrishna, P. and Nielsen, M (1963) Phys. Letters 6, 36

Rider, P.E., Gschneidner, K.A. Jr. and McMasters, O.D. (1965) Trans. Met. Soc. AIME, 233, 1488

Rivier, N. and Zuckerman, M.J. (1968) Phys. Rev. Letters 21, 904

Rohrer, H. (1969) J. Appl. Phys. 40, 1472

Ruderman, M.A. and Kittel, C. (1954) Phys. Rev. 96, 99

Smithells, C.J. (1967) Metals Reference Book, Vol.III, Butterworth, London

Sondheimer, E.H. (1952) Advanc. Phys. 1, 1

Suhl, H (1965) Phys. Rev. 138, A515

Suhl, H and Wong, D (1967) Physics 3, 17

Templeton, I.M., and MacDonald, D.K.C. (1961)
Proc. Conf. on High Magnetic
Fields, (Boston)

Tinkham, M. (1958) Phys. Rev. 110, 26

Tymchuk, P., Russell, D.S and Berman, S.S. (1965)
Spectrochim. Acta 21, 205

Tymchuk, P., Desaulniers, J.A.H., Russell, D.S. and
Berman, S.S. (1967)
Appl. Spectry. 21, 15

van Antwerpen, F. (1965) Physica 31, 1777

van den Berg, G.J. (1964) Progr. Low Temp. Phys. 4, 194

Walker, C.W.E. (1970) Can. J. Phys. 48, 378

Walker, E.J. (1959) Rev. Sci. Instr. 30, 834

Weiner, R.A. and Béal-Monod, M.T. (1970) Phys. Rev. B2, 2675

Window, B (1967) Phys. Letters 24A, 659

Window, B. (1967b) Phys. Letters 25A, 144

Window, B. (1969) Proc. Phys. Soc. 2C, 2380

Window, B. and Johnson,C.E. (1969) Phys.Letters 29A, 703

Worobey, W. Lindenfeld, P. and Serin, B. (1965)
Phys. Letters 16, 15

Yosida, K. (1957) Phys. Rev. 106, 893

Ziman, J.M. (1964) Principles of the Theory of Solids,
University Press, Cambridge.